SOFT BIOCOMPATIBLE POLYAMPHOLYTE HYDROGELS FOR TISSUE ENGINEERING APPLICATIONS

by

MINKLE JAIN

Submitted to

Japan Advanced Institute of Science and Technology

In partial fulfilment of the requirements

for the degree of

Doctor of Philosophy

Supervisor: Associate Prof. Dr. Kazuaki Matsumura

School of Materials Science

Japan Advanced Institute of Science and Technology

March 2016

Referee-in-chief: **Associate Professor Dr. Kazuaki Matsumura**
Japan Advanced Institute of Science and Technology

Referees: **Professor Dr. Masayuki Yamaguchi**
Japan Advanced Institute of Science and Technology
Professor Dr. Kohki Ebitani
Japan Advanced Institute of Science and Technology
Associate Professor Dr. Tatsuo Kaneko
Japan Advanced Institute of Science and Technology
Associate Professor Dr. Satoshi Fujita
University of Fukui

Soft Biocompatible Polyampholyte Hydrogels For Tissue Engineering Applications

Minkle Jain

Kazuaki Matsumura Laboratory, School of Materials Science, JAIST

Introduction

Regenerative medicine and human tissue engineering are the two newly developed fields in medicine. Tissue engineering has emerged from the field of biomaterials and involves the combination of scaffolds, cells and biologically active compounds in functional tissues. The wider goal of regenerative medicine is to restore the normal function of the body tissues, which can be successfully achieved by repairing or replacing dysfunctional tissues. Hydrogels are attractive substitutes for tissue engineering as they meet many of these requirements such as resemblance to natural extracellular matrix (ECM), ability to absorb large quantities of water, improving biocompatibility over bulk polymers. Due to the immense importance of hydrogels in the field of tissue engineering, in my doctoral research I developed various kinds of hydrogels based on polyampholytes. Previously in my group, cryoprotective property of poly-L-lysine based polyampholyte was elucidated. In my research, I developed new polymer-based cryoprotectants and also employed these polyampholytes as one of the components in the fabrication of hydrogels. Hydrogels were prepared by chemical and physical cross-linking. Each hydrogel so developed have very unique applications in the field of tissue engineering.

Results and Discussion

Firstly in **chapter 2**, I developed cryoprotective hydrogels based on dextran polyampholyte. Hydrogel was fabricated using Cu-free Click chemistry. Cu-free Click cross-linking made this system a good candidate for injectable hydrogels. Hydrogels with cryoprotective property are very essential in the current scenario for the preservation of 2D or 3D tissue engineered constructs.

In next **chapter 3**, I developed thixotropic hydrogel based on poly-L-lysine polyampholyte and laponite. It is a very simple and effective method to fabricate injectable hydrogel using physical cross-linking. My major target was to

cryopreserve the cells using polyampholyte and formulates it into hydrogel (using laponite as cross-linker) after thawing without washing out cryoprotectant. These kinds of hydrogels are very important for tissue engineering applications, as firstly it eliminates the need of cell harvestment and cell maintenance and secondly, due to its thixotropic nature, it is very useful as an injectable hydrogel. Thixotropic nature of the hydrogel prevented the unnecessary loss of the effective biomaterials to the unaffected areas after injection.

After the development of this type of hydrogel, in **chapter 4**, I introduced chemical cross-linking in this system using 4-arm polyethylene glycol amine as a cross-linker. This led to the development of hydrogel with tuneable mechanical properties. Mechanical stiffness of the substrate plays a crucial role in regenerative medicine and tissue engineering. Substrate stiffness decides the fate of cell differentiation. The hydrogels so developed with varied mechanical properties can have potent applications.

The last material, which I developed in **chapter 5**, is based on dextran hydrogel, which incorporates the nano-assemblies. This hydrogel shows controlled codelivery of hydrophobic drug and growth factors. It is very useful for topical wound healing applications.

Conclusion

In conclusion, I believe I was able to successfully fabricate different hydrogels with various unique applications using polyampholytes. Besides their cryoprotective property, in my study I was able to utilize their behavior of charge tuneability for the development of hydrogels by the incorporation of laponite as a cross-linker. Due to the presence of charge on both the components, numerous combinations were obtained. To my knowledge, no such work has been reported before which describes the interaction of polyampholyte with laponite. The beautiful interaction of the two by changing various parameters has opened up new avenues in the field of tissue engineering. These systems can be potentially useful in the fields of stem cell based therapies (where substrate stiffness plays crucial role in cell differentiation), pH-triggered cell delivery, drug delivery applications, etc.

Keywords: Polyampholyte, hydrogels, laponite, cryopreservation, thixotropic.

TABLE OF CONTENTS

CHAPTER 1 1

GENERAL INTRODUCTION 1

1.1 What is tissue engineering? 2

1.2 Stem cells 2

1.3 Hydrogels 3
1.3.1 Synthetic hydrogels 4
1.3.2 Nanocomposite Hydrogels 8

1.4 Cryopreservation 11
1.4.1 Fate of cells at ultra-low temperature 12
1.4.2 Biophysical aspects of ice formation 13
1.4.3 Correlation between cryoinjury and the two phenomena occurring during freezing 14
1.4.4 Cooling Rates 14
1.4.5 Cryoprotective additives 16
1.4.6 History of CPAs 16
1.4.7 Problems associated with current CPAs 17
1.4.8 Polyampholytes as newer low toxic CPAs 17
1.4.9 Synthetic polyampholytes: an approach towards solving the mystery behind the mechanism of cryoprotection by polyampholytes 18
1.4.10 Cell encapsulation and cryoprotective hydrogels 19
1.4.11 Vitrification 20

1.5 OBJECTIVE OF THESIS 22

1.5 REFERENCES 24

CHAPTER 2 29

HYDROGELATION OF DEXTRAN-BASED POLYAMPHOLYTES WITH CRYOPROTECTIVE PROPERTIES *VIA* CLICK CHEMISTRY 29

2.1 Introduction 29

2.1.2 What are polyampholytes? 31

2.1.3 Swelling behavior of polyampholytes 32

2.2.2 Experiments 33
2.2.3 Azide-amino-dextran preparation 33
2.2.4 Polyampholyte preparation 34
2.2.5 Preparation of alkyne-substituted dextran 34
2.2.5 Hydrogel Preparation 35
2.2.6 Fluorescein isothiocyanate (FITC) labeling of Dex-PLL-PA 35
2.2.7 Nuclear magnetic resonance (NMR) spectroscopy 35
2.2.8 Scanning electron microscope observation 35
2.2.9 Cell Culture 35

2.2.10 Cryopreservation with azide-Dex-PA 36
2.2.11 Cryopreservation with azide-Dex-PA 36
2.2.12 Rheological characterization of hydrogels 37

2.3 Results and discussion 37
2.3.1 Synthesis of azide-substituted polyampholyte (PA) and its cryoprotective properties 37
2.3.2 Synthesis of alkyne-substituted dextran 43
45
2.3.3 Hydrogel formation via Cu-free click chemistry 45
2.3.4 Cryoprotective properties of the hydrogel 46
2.3.5 Rheological characterization of hydrogels 49

2.4 Conclusion 51

2.5 References 52

CHAPTER 3 55

THIXOTROPIC INJECTABLE HYDROGEL USING A POLYAMPHOLYTE AND NANOSILICATE PREPARED DIRECTLY AFTER CRYOPRESERVATION 55

3.1 Introduction 55

3.2 Nanocomposite synthesis 57
3.2.1 Polyampholyte preparation 57
3.2.2 Zeta potential measurement 58
3.2.3 Nanocomposite formulation 58
3.2.4 X-ray diffraction (XRD) measurements 59
3.2.5 ATR-FTIR 59
3.2.6 Rheological analysis 59
3.2.7 Cryopreservation protocol and determination of cell survival 59
3.2.8 Cell adhesion and viability 60

3.3. Results and discussion 61
3.3.1 Preparation of polyampholytes and their cryoprotective properties 61
3.3.2 Nanocomposite formulation 64
3.3.3 Characterization of the nanocomposite 65
3.3.4 Dynamic mechanical analysis 67
3.3.5 Cell adhesion and viability 74

3.4 Conclusion 76

3.5 References 76

CHAPTER 4 80

POLYAMPHOLYTE- AND NANOSILICATE-BASED SOFT BIO-NANOCOMPOSITES WITH TAILORABLE MECHANICAL AND CELL ADHESION PROPERTIES 80

4.1 Introduction 80

4.2 Hydrogel and nanocomposite synthesis 82
4.2.2 Polyampholyte synthesis 82
4.2.3 Preparation of PEG-based hydrogel 83

4.2.4 Nanocomposite formation 84
4.2.5 Swelling and degradation studies 84
4.2.6 Rheology study 85
4.2.7 Cell studies 85

4.3 Results and discussion 86
4.3.1 Preparation of the polyampholyte 86
4.3.2 Hydrogel and nanocomposite preparation 86
4.3.3 Swelling and degradation study 88
4.3.4 Mechanical properties 90
4.3.5 Cell culture study 93

4.4 Conclusion 94

4.5 References 95

CHAPTER 5 98

SELF-ASSEMBLED NANOGEL INCORPORATED DEXTRAN AND POLY-L-LYSINE BASED HYDROGELS WITH CONTROLLED DRUG RELEASE PROPERTIES 98

5.1 Introduction 98

5.2 Materials and Methods 104
5.2.2 Dextran aldehyde preparation using periodate oxidation 104
5.2.3 Succination of ε-poly-L-lysine 105
5.2.4 Synthesis of alkyl chain grafted dextran 106
5.2.5 Preparation of self-assembled AmB loaded nanoparticles 106
5.2.6 In vitro release study of AmB from Dex-DDSA nanoparticles 107
5.2.7 Preparation of Dex-ald/ PLL SA hydrogel 107
5.2.8 bFGF release from hydrogels 108
5.2.9 Rheological measurements of hydrogels 108

5.3 Results and discussion 109
5.3.1 Dextran aldehyde preparation using periodate oxidation 109
5.3.2 Succination of ε-poly-L-lysine 110
5.3.3 Synthesis of alkyl chain grafted dextran 110
5.3.4 Preparation of self-assembled AmB loaded nanoparticles 112
5.3.5 In vitro release of AmB from Dex-DDSA nanoparticles 114
114
5.3.6 Preparation of Dex-ald/ PLL SA hydrogel 114
5.3.8 bFGF release from hydrogels 115
5.3.8 Rheological measurements of hydrogels 116

5.4 Conclusion 120

5.5 References 120

CHAPTER 6 124

CONCLUSION 124

ACHIEVEMENTS 127

ACKNOWLEDGEMENT **128**

Chapter 1

General Introduction

Regenerative medicine and human tissue engineering are the two newly developed fields in medicine. Tissue engineering has emerged from the field of biomaterials and involves the combination of scaffolds, cells and biologically active compounds in functional tissues. Failure and death of specialized cell functions in the body causes aging, injuries and diseases. With the better understanding of how diseases are developed in the body or how stem cells are controlled, it is easy to find newer and better ways to treat the diseases of patients. The wider goal of regenerative medicine is to restore the normal function of the body tissues, which can be successfully achieved by repairing or replacing dysfunctional tissues. In the pursuit of the development of regenerative medicine plethora of advances has been made in the field of science, technology, health care and medicine. Focus point of researchers is to gather knowledge about the functioning of different biological processes and then application of this for example in designing and development of methods to repair malfunctioning tissues or developing tools to accelerate drug discovery or to understand the root causes of diseases such as Parkinson's or sclerosis for the better treatment and many more. Usually organ repair is confused with organ regeneration. It was clearly explained by Yannas "An organ repair is the restoration of interrupted functions by scar tissue synthesis but it does not involve reconstruction of normal tissue" (1). But regeneration is the generation of missing organ mass at original site. It is revamping the original structure and function. Basically target of regenerative medicine is to repair the functionalities that have been lost but sometimes it can also help in treating congenital abnormalities too. It is the interplay of clinical application and research. The main focus is to repair, replace or regenerate organs, tissues, and cells in order to reconstruct impaired functions that might have occurred due to aging, disease, defects or trauma (2). Regenerative medicine is the combination of tissue engineering and stem cells technology.

1.1 What is tissue engineering?

Dr. WT Green in 1970 a paediatric orthopaedic surgeon at Boston's Children's Hospital has done first attempt in this field, where he carried out various experiments to generate new cartilage in nude mice. However experiments were not successful but he concluded that with the help of biomaterial science it would be possible to regenerate the complete tissue by cell seeding onto smart engineered scaffold (3). The term tissue engineering was coined in the workshop conducted at the Granlibakken Resort, Lake Tahoe, California, in February 1988 and UCLA symposium in 1992 (4). It is fastly growing as a potent solution to organ and tissue failures. These issues can be tackled by implanting natural, synthetic or semisynthetic imitates into the body that resembles the desired functionality or grow into the required one. Basic building block of the body is cell. Usually these cells secrete and generate their own support structure, which is extracellular matrix (ECM). ECM not only supports the cells but also act as relay station to various signaling molecules. If these processes somehow can be mimicked then it is easy to treat damaged tissues or to create new ones. This can successfully be achieved by better understandings of how cell organize themselves to tissues and to new organs or how they interact with their local environment. The other possibility of developing new tissue is by using an existing scaffold. Cells are stripped from donor organ and then they are cultured on various substrates under physiological conditions to formulate tissue engineered constructs for implantation. This technique does not require the anti-rejection drugs after implantation as the construct has been developed from the patient`s own cells.

1.2 Stem cells

Stem cells are the cells with two peculiar properties one is the ability of self-renewal that give rise to other stem cells and other is the ability to differentiate into other lineages under appropriate conditions. They are of two types:

- Embryonic Stem cells (ESCs)
- Non- embryonic Stem cells

Embryonic Stem cells

They are pluripotent cells and have the ability to differentiate into various types of germ layers. Gail Martin first described these cells in 1981 (5). Inner cell mass (ICM) give birth to pluripotent ESCs. During embryogenesis ICM develops into two types of layers one is epiblast and other is hypoblast. Yolk sac is being developed by hypoblast whereas three layers of embryo namely ectoderm, mesoderm and endoderm is derived from epiblast differentiation. These layers have the potential to develop into any tissue Fig.1-1 (6). Discovery of stem cells is an important milestone in science and can have strong impact on health care as compared to the discovery of antibiotics and anesthesia.

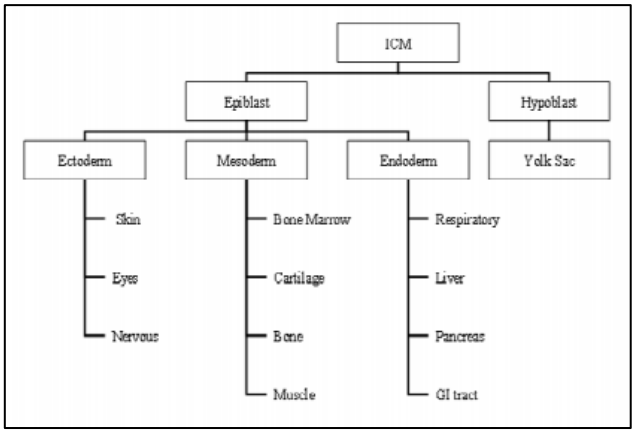

Figure 1-1 Pluripotent potential of embryonic cells[6]

Non-Embryonic Stem cells

They are the cells, which have lost pluripotent ability. They can be obtained from various sources such as amniotic fluid, umbilical cord tissue and bone marrow.

1.3 Hydrogels

Hydrogels are attractive substitutes for tissue engineering as they meet many of these requirements such as resemblance to natural extracellular matrix (ECM), ability to absorb large quantities of water, improving biocompatibility over bulk polymers. Hydrogels are hydrophilic polymer networks (7, 8) with a 3D configuration, making them promising candidates for implantable biomaterials applications. Injectable hydrogels can be implanted into various target sites in patients in a minimally invasive manner (9) with little prior knowledge of the

defect site geometry. Thus, hydrogels are attractive biomaterials for clinical applications (10).

Classification of hydrogels (11)

- On the basis of source material
  Natural and synthetic
- On the nature of Cross-linking
  Covalent or physical
- On the nature of network
  Homopolymer, copolymer, interpenetrating and double network
- On the basis of pores
  Homogeneous, microporus, macroporus
- On the basis of fete in organisms
  Degradable or non-degradable.

First hydrogel was prepared in 1953 Drahoslav Lim by copolymerization of 2-hydroxyethyl methacrylate (HEMA) with ethylene dimethacrylate (EDMA) (12). Earlier hydrogels were developed for various medical applications such as restoration of detached retina (13), augmenting vocal cords (14), prevention of scar after surgery (15) etc.

1.3.1 Synthetic hydrogels

- **Hydrogel preparation by Cross-linking polymerization**

Monomer possessing at least one polymerizable double bond copolymerizes with Cross-linking agent having at least two double bond is favorably used for hydrogel formulation Fig.1-2 (11).

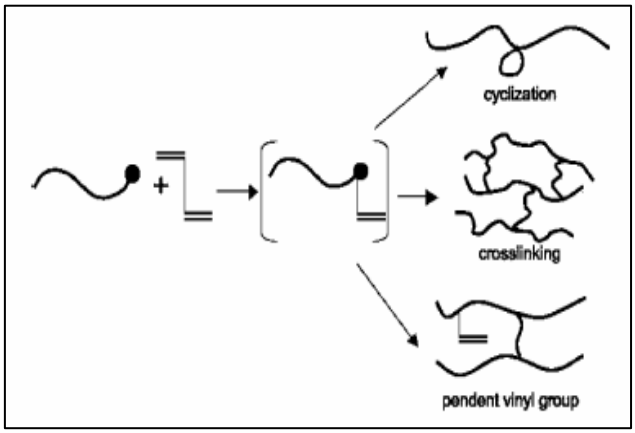

Figure 1-2 Possible reaction of vinyl group in cross-linking copolymerization[11]

- **Hydrogel preparation by Cross-linking of polymer precursor**

It may be possible that sometimes linear or branched polymers contain reactive or functional end groups that can be cross-linked using low molecular weight Cross-linking agents for example shown in Fig. 1-3 (16). In the given reaction scheme polymer precursor is a copolymer of N-methacryloylglycylglycine p-nitrophenyl ester with N,N-dimethylacrylamide, N-tert-butylacrylamide, and acrylic acid. Cross-linking agent is N,N-(ω-aminocaproyl)-4,4-diaminoazobenzene. Cross-linking occurs by the reaction of p-nitrophenyl ester groups of polymer precursor with amino groups of the Cross-linking agent. Cross-linking conditions are manipulated to minimize side reactions and increasing efficiency.

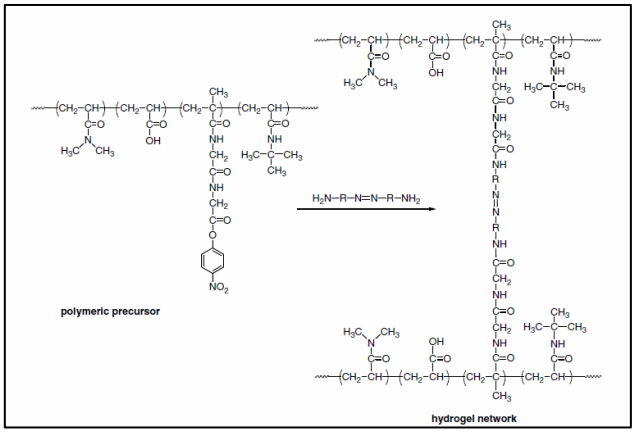

Figure 1-3 Cross-linking produced by polymer precursor with a low-molecular-weight Cross-linking agent[16]

Interpenetrating Polymeric Networks (IPNs)

IPNs are innovative and promising materials for drug delivery applications (17). They consist of interlocked networks of two independently cross-linked polymeric systems (18). The term IPN was coined by Millar (19). Usually their preparation is carried out by mixing monomers or polymer solution before Cross-linking is carried out as shown in Fig. 1-4 (20). It consists of two networks that can be formulated either simultaneously or sequentially depending on the conditions of Cross-linking adopted for the reaction (21, 22).

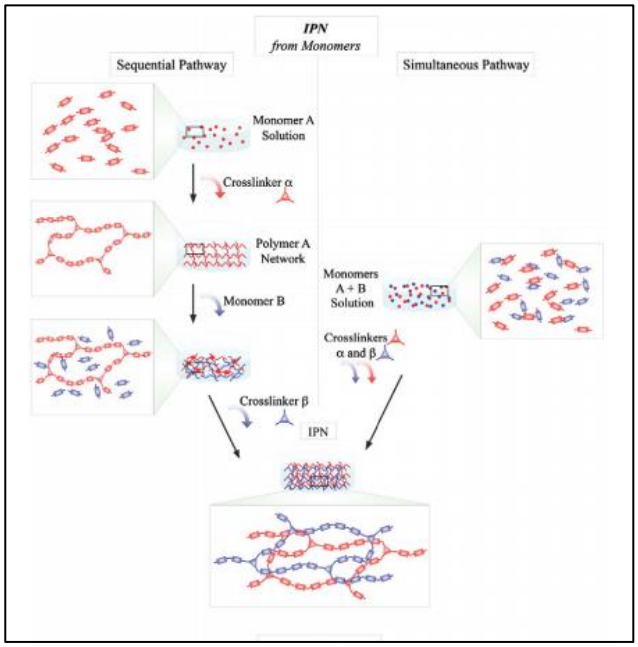

Figure 1-4 Schematic representation of the semi-IPN and IPN formation. Polymer A and Polymer B are generic polymers (such as linear, comb or grafted)[20]

Unique point is the combination of desirable properties of the individual components constituting IPN that give rise to new system with better properties. Sometimes synergistic effect of properties can also be obtained (23, 24). Several IPNs have been formed by the combination of natural and synthetic polymers that have better rheological properties, which are similar to natural occurring tissues thus making them promising candidate for tissue engineering applications.

- **Physically cross-linked Hydrogels**

Plethora of advances has been made in the field of physically cross-linked hydrogels. The root cause behind this is the toxicity of chemical cross-linkers and they also disrupt the integrity of proteins and cells encapsulated in the hydrogels. So there is a need to remove these cross-linkers from gels before they can be used as implants. Different strategies have been utilized for their formulation, which will be discussed briefly in the following section.

a) Gel formation by ionic interaction

Many polymers forms gel in the presence of ions. The major advantage of using this approach is that biodegradation can take place easily as soon as it is placed in extracellular fluid as ionic species present in the fluid competes with gel components for binding thus, leading to the breakdown of network. Interactions

can take place between two polymers possessing opposite charges or between a polymer and small molecule Fig. 1-5 (25). For example alginate a polysaccharide with mannuronic and glucuronic acid residues can be form gel in the presence of calcium ions (26). Gelling conditions are easy and gelation can be carried out at room temperature at physiological pH. Interesting point is for the formation of gels by ionic interaction it does not always require the presence of ionic groups in the polymer. One such example is the hydrogel formation by Dextran, which lacks any ionic group in the presence of potassium ions (27).

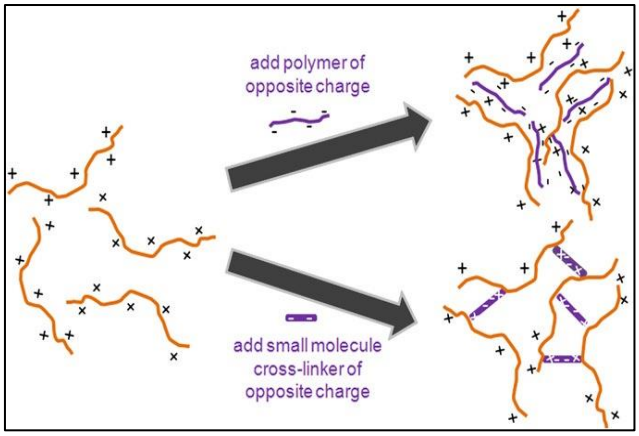

Figure 1-5 Mechanisms of in situ physical gelation based on charge interactions with an oppositely charged polymer or an oppositely charged small molecule cross-linker[25]

b) Gel formation by Hydrogen bonding

Most commonly these hydrogels are prepared by using homopolymers or by using mixture of two or more polymers. Poly (vinyl alcohol) (PVA) is a water soluble polymer. Its aqueous solution forms gels at room temperature however it is not so mechanically strong. But once this polymer is subjected to freeze thaw cycles it forms strong and elastic gel (28). This can be explained on the grounds that PVA crystallites are formed in the solution, which acts as physical Cross-linking sites in the solution (29). When mixture of polymers is used then rheological synergism is observed which means that polymer blends behave like gel like as compared to individual polymer (30). This is a result of hydrogen bonding interactions that takes place between the polymer chains due to their specific geometries Fig. 1-6 (31).

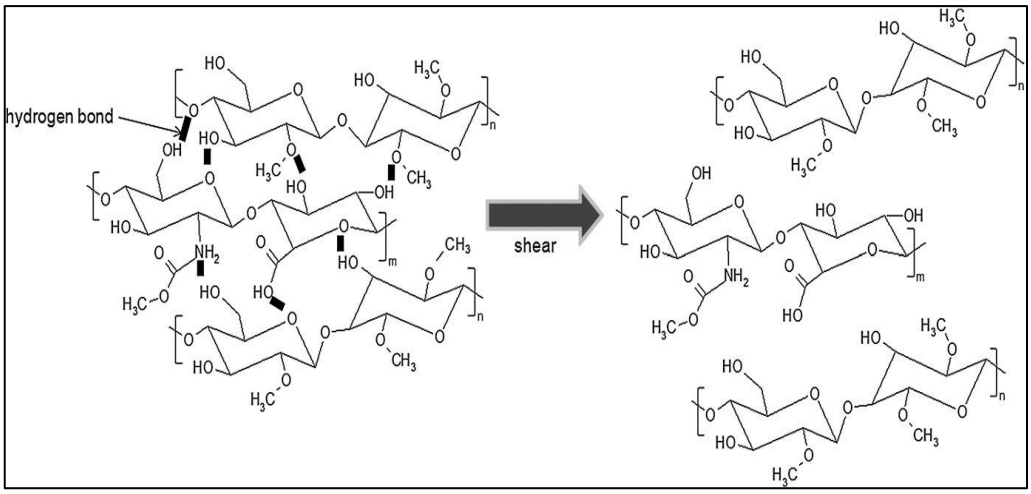

Figure 1-6 In situ physical gelation via hydrogen bonding interactions between geometrically compatible biopolymers (methylcellulose and hyaluronic acid)[31]

Gel formation by Hydrophobic interaction

Polymers with hydrophobic domains can form gels by reverse thermal gelation in aqueous environment. Polymers, which possess hydrophobic domains, are known as gelators. These gelators can be coupled to polymers containing hydrophilic domains after polymerization or by direct synthesis of polymer amphiphile. They are soluble in water at low temperatures but when temperature is increased hydrophobic domains aggregate to minimize the area in contact with bulk water. Temperature of gelation depends on many factors such as concentration of polymer, length of the hydrophobic block (25). Such kind of hydrogel formation is shown in Fig. 1-7 (25).

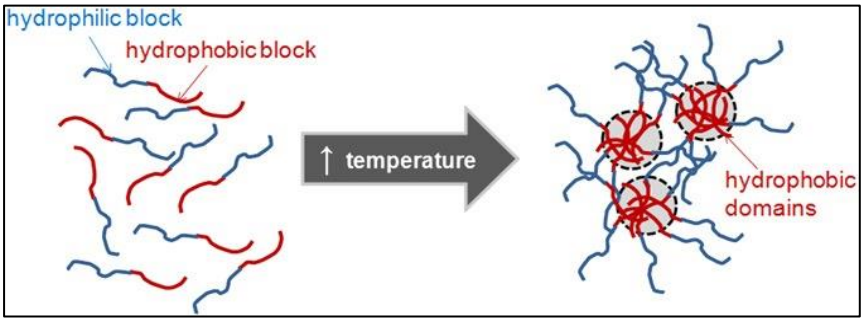

Figure 1-7 Mechanism of in situ physical gelation driven by hydrophobic interactions[25]

1.3.2 Nanocomposite Hydrogels

Since past few decades nanotechnology has revolutionized the scientific world. Nanocomposite hydrogels has overcome the challenges associated with the

current systems available for tissue engineering applications. Nanocomposite hydrogels are the molecular networks, which are physically, or covalently cross-linked with the nanoparticles. Various nanoparticles from inorganic and ceramic particles (silica, hydroxyapatite, calcium phosphate), metal oxides nanoparticles (gold, silver, iron oxides), carbon based nanomaterials (single wall carbon nanotubes) to polymeric nanoparticles (cyclodextrins, hyperbranched polymers) have been used for this purpose Fig. 1-8 (32).

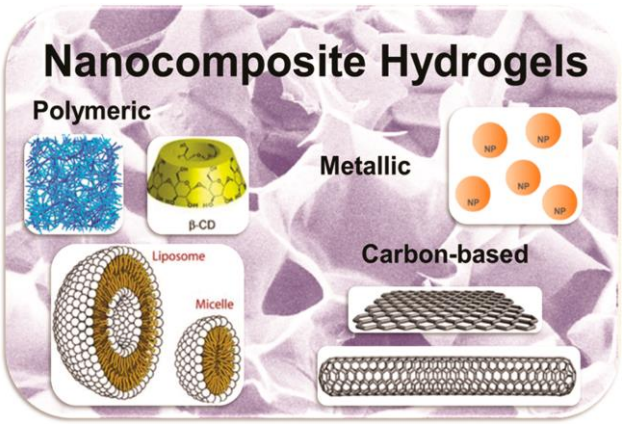

Figure 1-8 Nanoparticles such as carbon-based nanomaterials, polymeric nanoparticles, and metallic nanoparticles are combined with the polymeric network to create reinforced nanocomposite hydrogels[32]

Incorporation of these materials modulates the physical and chemical properties of hydrogels. This field is gaining interest because introduction of nanoparticles imparts properties to the hydrogels which can never be obtained by only polymeric systems. Various examples from the literature can be taken where incorporation of nanoparticles has enhanced the stimuli responsiveness in the hydrogels. Transdermal patches are in great demand these days and are better than oral delivery and injections as it eliminates the phobia and pain associated with injections. But low permeability of the release products by the skin is restriction on these materials. This can be overcome by formulation of nanocomposite for example Giri et al. (33) fabricated a composite made of guar gum and multi walled carbon nanotubes (MWCNTs) for the release of sodium diclofenac as transdermal system. Incorporation MWCNTs enhance the mechanical stability, drug retention efficiency and drug loading capacity of the composite. Addition of synthetic silicate particles also known as nanoclay modulates the rheological response of the hydrogels. It leads to the formation of

nanocomposites with enhanced mechanical properties (34, 35). Synthetic silicates are a novel class of nanomaterials with a high degree of anisotropy and functionality; these materials interact with biological entities in a manner that is entirely different from their respective 3D micro and macro counterparts because of their high surface to volume ratio (36, 37). Synthetic silicates strongly interact with polymeric networks, resulting in the formation of physically cross-linked networks and significantly increased mechanical stiffness (35, 38, 39). The exfoliated hydrogels containing silicate and polymer result in the formation of highly organized structures. Incorporation of the silicate nanoparticles within a polymer network yields strong bioactive characteristics, facilitating their potential use in a variety of musculoskeletal tissue engineering applications (40-42).

Graphene has also drawn great interests as the incorporation of Graphene leads to better electron mobility, mechanical stability and thermal conductivity to hydrogels (43).

Introduction magnetic nanoparticles in the hydrogels modulate the self-healing property of the gels. Usually during the implantation of the hydrogels, they face stress that leads to the development of crack and fissures in it thus hampering the functionality of the gel. In order to solve this problem self-healing hydrogels are good solution which have the ability to regain their original structure after the application of stress (44). Wei`s group has prepared carboxy modified Fe_3O_4 nanoparticles into chitosan-PEG hydrogels which renders magnetic and self-healing property to the nanocomposite (45).

Conventional hydrogels are hydrophilic polymer network but to deliver hydrophobic drugs using them is almost impossible. In this regard nanocomposite hydrogels can possibly solve the problem. Polymeric nanoparticles such as micelles, microspheres, liposomes and cyclodextrins when introduced in the hydrogels not only manipulates the mechanical property of the gel but also can be used for the delivery of hydrophobic drugs. For example Nagahama et al. developed co-delivery system, which is injectable in nature and composed of self-assembly of copolymer micelles, clay nanodisks (CNDs), and doxorubicin (DOX). Cyclodextrins (CDs) widely been used for the delivery of drugs which have poor water solubility. It incorporates drug in its hydrophobic core thus helpful in

capturing as well as release of drug (46). There is a pressing need for the development of hybrid systems, which are multiple stimuli sensitive rather to single one. For example in the cancer therapy targeted drug delivery is very much required. In the vicinity of cancer cells higher temperature and low pH is there as compared to other cells. So formulation of the systems which have dual responsiveness will be desirable. Multifunctional core-shell nanogels have been developed by Wu et al. Fig. 1-9 (47). These nanogels are capable of doing simultaneous optical temperature sensing, tumor targeting and combined chemical and photothermal treatment. In this system thermo sensitive PEG based nanogel is shell and Ag-Au as core and hyaluronic acid chains as targeting ligands (47).

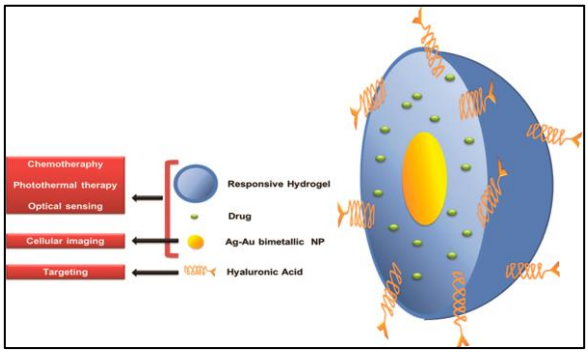

Figure1-9 Schematic illustration of multifunctional core-shell nanogel[47]

1.4 Cryopreservation

Nature governs whether the biological material will decay or die. The structure and function of living organelles and cells can change and be lost with time, which is matter of concern for the researchers studying these systems. Several attempts have been made to stop the biological clock since ancient times, which was successfully achieved by controlling temperature and water content.

Refrigeration is one of the everyday life processes that have been extensively used because it provides us means for slowing the rate of deterioration of perishable goods. Removal of water from various biological materials paves another way for arresting biological degradation, which initiates again by water addition.

The pioneering work in this field was conducted in 1949 by Polge and coworkers, who stored fowl semen in a freezer by adding glycerol as cryoprotectant (48). Afterwards, many successful experiments were carried out, such as cryopreservation of bull spermatozoa (49), plant cultures (50), plant callus (51), and human embryos for in vitro fertilization programs (52).

The application of low-temperature preservation to living organisms has revolutionized areas of biotechnology such as plant and animal breeding. The most interesting feature of cryopreservation is that both prokaryotic and eukaryotic cells can be cryopreserved at temperatures down to −200°C, which is a remarkable milestone for structural and molecular biologists. The most important ingredient required to achieve this goal is a cryoprotectant (CPA).

In the context of tissue cultures, simple preservation techniques like refrigeration cause limited shell life, high risk of contamination, and genetic drift. Therefore, cryopreservation has become indispensable in biological, medical, and agricultural research fields, and in the clinical practice of reproductive medicine. In the era of microbial contaminations, natural disasters, or alteration of genetic expressions in the latter generations, cryopreservation of sperm and embryos helps to maintain a backup of the microorganisms proliferating on animals, thus saving significant space and resources that could be used to better manage the microorganisms currently used for research. Moreover, it is an important tool to preserve strains that are not currently being used but could have potent applications in the future.

1.4.1 Fate of cells at ultra-low temperature

How can a man who's warm understand one who's freezing? Alexander Solzhenistyn.

Life is a complex process that happens in water. When temperature is below −0.6°C, biological water under isotonic conditions becomes thermodynamically unstable and tends to be in the crystalline state. Since biological systems are almost entirely made of water, the water-ice phase transition in these systems is a subject of great interests for cryopreservation. In particular, what are the effects of extremely low temperatures on cells?

1.4.2 Biophysical aspects of ice formation

When biological systems are cooled to temperatures below the equilibrium melting point, ice begins to form in the extracellular medium. This extracellular ice plays an important role in the cryopreservation process because it alters the chemical environment of the cells, exerts mechanical constraints, and leads to the development of ice inside the cells (53). The formation of extracellular ice has synergistic effect on the unfrozen fraction composition in the extracellular solution. Dropping temperature leads to the increase in the solute concentration in the extracellular solution, which is a driving force for the diffusion of solutes into and water flux out of the cell. At low temperature, the plasma membrane, which is more permeable to water than to the solute, behaves like a semi-permeable membrane in time scale of cryopreservation (54). Cells respond to this by releasing water via osmosis and undergo dehydration during freezing, the kinetic model of which was first given by Mazur (55).

Solidification of the external medium can cause cell deformation because the ice matrix surrounding the cell acts as a mechanical constraint. During freezing, this mechanical force squeezes the cells into the channels of unfrozen liquid between ice crystals. Rapatz et al. (56) have directly measured the width of the unfrozen liquid channels between ice crystals, and observed that channels diameters decrease with temperature, and the cells present in the channels get deformed as the channel width reaches the cell dimensions.

Besides these two processes, another effect of extracellular ice onto cells is the initiation of ice formation inside the cells. It has been experimentally proven that extracellular ice catalyzes the intracellular ice formation (57, 58). Toner et al. (57) proposed that ice formed inside the cells by nucleation on intracellular catalytic sites.

Since the cytoplasmic supercooling and diffusion constant of intracellular water depend on the instantaneous properties of the intracellular solution, the dynamics of ice formation inside the cells are highly affected by the corresponding dehydration process (53). The fate of the cellular water during cryopreservation depends on the relative magnitudes of water transport and rate of nucleation. When cells are cooled slowly, the rate of water coming out of the cells is relatively fast, thus preventing intracellular ice formation and favoring cell

dehydration. At rapid cooling rates, exosmosis of water is slow in comparison of intracellular water being supercooled, thus resulting in intracellular ice formation.

1.4.3 Correlation between cryoinjury and the two phenomena occurring during freezing

Injury occurring because of intracellular ice formation during rapid cooling is believed to be due to mechanical forces (59). Possible sites of injury are the plasma membrane (60) and the membrane of intracellular organelles (61).

Cell dehydration during slow cooling is also a source of cell damage (62). Lovelock (63) reported that hypertonic solutions cause denaturation of lipoproteins, which leads to hemolysis in red blood cells (RBC). Other theories proposed cell shrinkage as a response towards highly concentrated extracellular solution.

The two approaches used for cryopreservation are slow-rate freezing and vitrification. The core objective of the two methods is to minimize cryoinjury, intracellular ice formation, and dehydration.

Slow-rate freezing involves the pre-equilibration of cells in cryoprotectant solutions followed by slow cooling at the rate required for the particular type of cell being used. However, during the whole process, care must be taken to prevent intracellular ice formation. This complete process requires special equipment and takes 3–6 h to complete.

Vitrification is the conversion of liquid into glass. In this approach, an attempt is made to prevent ice formation throughout the entire sample. This process avoids the damaging effects of intra- and extracellular ice formation.

1.4.4 Cooling Rates

There are various factors affecting the efficiency of cryopreservation. One of the principal factors is the rate of freezing, which should be optimum. The relation between cell survival and cooling rate shows an inverted U-shaped curve Fig. 1-10 (55). Each system has an optimum cooling rate, the efficiency of which is greatly affected by whether the rate of cooling is too fast or too slow (64, 65). When the rate of cooling is very slow, there is minimal intracellular ice formation, which implies high degree of cell dehydration. On the other hand, at very high cooling rates, rapid water flow through the membrane can result in rough

pressure distribution across the membrane (66) in sudden change in size and shape of the membrane (67).

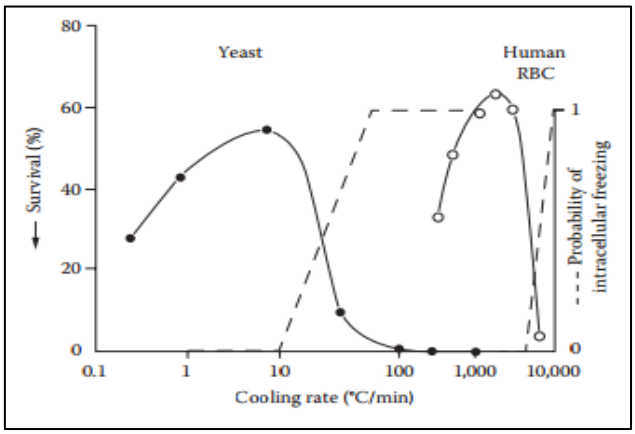

Figure 1-10 Plot of the survival percent versus the cooling rate for different cell types of cells [55]

Slow Cooling

When cells are frozen/cooled at slow rate (controlled rate), formation of extracellular ice takes place first, followed by a differential water gradient across the cell membrane, which results in the movement of intracellular water to the outside. This has an important cryoprotective effect because it reduces the amount of water available to form ice. This process reduces the amount of water inside the cells, which could potentially form ice, thereby protecting the cells. Intracellular ice formation is very lethal for cells and is the most important cause for cell death during cryopreservation. As the system is further cooled down, no further crystallization of ice is observed due to a tremendous increase in the viscosity of the unfrozen fraction (solutes), which turns into an amorphous solid lacking any ice crystals. On the other hand, slow cooling results in the increase of the solution effect, which can be damaging to the cells. The amount and rate at which water is lost from the inside of the cells depends on cell permeability; tolerance towards fast cooling is better for more permeable cells than for less permeable cells (62, 68). Interestingly, there is interplay between ice crystal formation and solution effects on cell damage.

Generally, a cooling rate of 1°C/min is preferred. However, there are exceptions to this requirement such as for yeast (69, 70), liver (71), and higher plant cells (72), which shrink or become plasmolyzed when the rate of cooling is 1°C/min, but

when the rate is increased to about 200°C/min or more, these cells remain in their normal state. In the case of yeast, shrinkage is the result of water loss and not of solutes loss (73, 74); therefore, in these cells, water content is an estimate of the volume of the cell. However, faster cooling rates render the cells unable to maintain equilibrium with the extracellular solution due to the inability of water to leave the cells, which causes intracellular ice formation to preserve the equilibrium Fig. 1-11 (55).

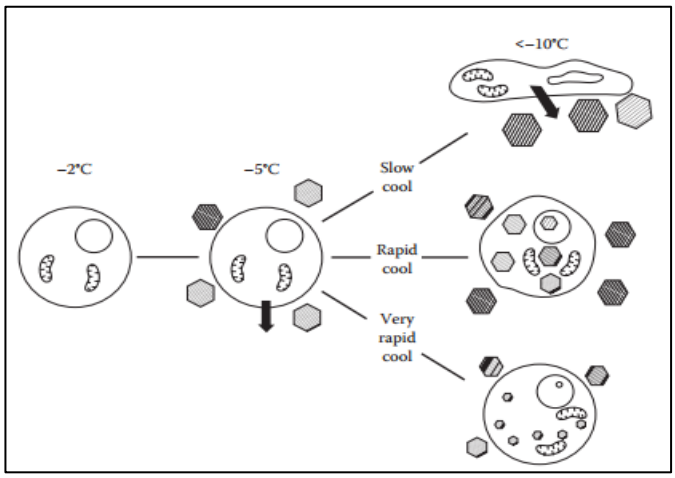

Figure 1-11 Schematics of the physical events occurring in cells during freezing [55]

1.4.5 Cryoprotective additives

CPAs are additives provided to cells before freezing to enhance post-thaw survival (53, 75).

CPA can be divided into two different groups (76, 77):

1. Low-molecular-weight CPAs such as glycerol, ethylene (propylene) glycol, dimethyl sulfoxide (DMSO), which can penetrate the cell membrane.

2. Non cell membrane-penetrating CPAs that can usually do not enter inside the cells, like polymers such as polyvinyl propyliodone, hydroxyl ethyl starch (HES), and various sugars.

1.4.6 History of CPAs

Ever since the discovery of the role of glycerol in cryopreservation by Polge et al. in 1949, the use of CPAs has become common practice. Lovelock (78) later found that the protective property shown by glycerol is due to its non-toxicity, high solubility in aqueous electrolyte solutions, and its ability to permeate living cells.

However, he found that glycerol is impermeable to bovine red blood cells and proposed DMSO as an alternative solute with greater permeability to living cells and exerting protective action against the freezing damage to human and bovine red blood cells. This CPA gained considerable attention globally and was mentioned as miracle compound. In the same period, Garzon (79) and Knorp (80) independently proposed HES as a cryoprotectant for erythrocytes (81). Thereafter, HES continued to be used as the CPA for RBCs (78-82), granulocytes (83), cultured hamster cells (84), and pancreatic islets (85, 86).

1.4.7 Problems associated with current CPAs

The cryoprotective properties of glycerol are relatively weak and DMSO, which is considered the most effective CPA, shows high cytotoxicity (87) and disturbs the differentiation of neuron-like cells (88), cardiac myocytes (89), and granulocytes (90). When DMSO is used at low concentration, it can decrease the membrane thickness and induce temporary water pores, while, when it is used at higher concentrations, it causes the disintegration of the bilayer structure of the lipid membrane (91). Therefore, after thawing, it is necessary to remove it. In the current scenario, the most efficient cryopreservation technique, which is being used worldwide in cell banks, is 10% DMSO in the presence of fetal bovine serum (FBS). Importantly, it has been reported that post-thaw survival of cells decreases without the addition of FBS to the cryopreserving solution (92, 93). Indeed, it is the interplay between FBS and DMSO at the appropriate ratio that makes DMSO a potent cryoprotectant. However, the pit hole of this technique is that animal-derived proteins should be avoided for clinical usage due to high risk of infection. Therefore, these issues stimulated the development of new CPAs.

1.4.8 Polyampholytes as newer low toxic CPAs

In 2009, Matsumura et al. (94) developed polyampholytes based on poly-L-lysine with an appropriate ratio of amino and carboxyl groups as a new CPA (COOH-PLL) Fig. 1-12 a, which is a non-penetrating CPA and shows very low cytotoxicity. COOH-PLL shows high cryopreservation efficiency without the addition of any other CPAs. The authors reported that L929 cells were cryopreserved using 7.5% COOH-PLL as the sole CPA and in the absence of animal-derived proteins. Moreover, COOH-PLL shows high post-thaw survival efficiency when used at 7%

or more compared to 10% DMSO Fig. 1-12 b. In addition, compared to DMSO, cell attachment efficiency is higher with COOH-PLL than with 10% DMSO.

a) b)

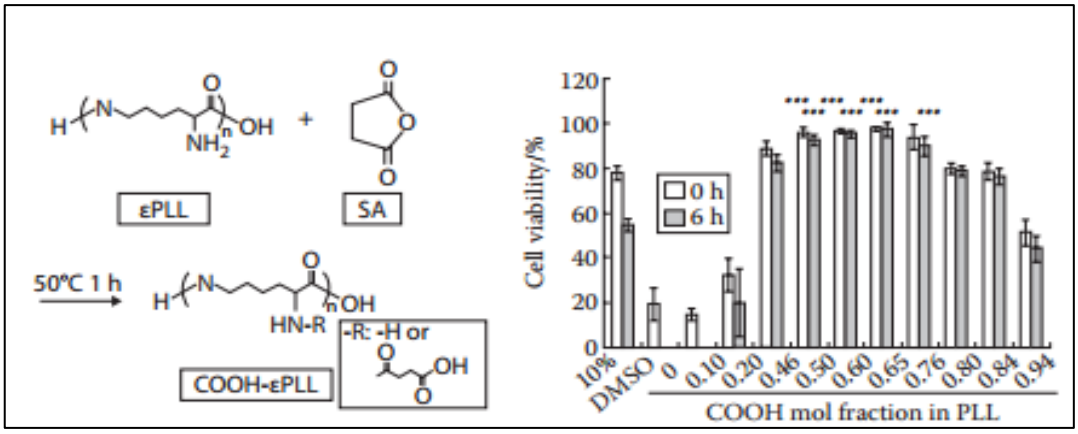

Figure 1-12 Cryoprotective property of carboxylated poly-l-lysine (PLL). (a) Schematic representation of the reaction of PLL succinylation. (b) L929 cells were cryopreserved using 10% DMSO and 7.5% (w/w) PLL at different ratios of COOH. Cell viability immediately (white bars), and 6 h (gray bars) after thawing at 37°C. Data are expressed as mean ± standard deviation (SD) for three independent experiments (n = 5). ***p < 0.001 vs. 10% DMSO for the corresponding time period (0 or 6 h)[94]

The development of this CPA opened the gateways towards new strategies of cryopreservation. Recently, Matsumura et al. (95) showed that the period of cryopreservation using COOH-PLL was not restricted to one week by successfully cryopreserving human bone marrow cells (hBMSCs) for up to 24 months. This result showed that this novel CPA did not alter the phenotypic characteristics and proliferative ability of the cells following thawing after cryopreservation for 24 months.

1.4.9 Synthetic polyampholytes: an approach towards solving the mystery behind the mechanism of cryoprotection by polyampholytes

Using reversible addition-fragmentation chain transfer (RAFT), Rajan et al. (96) synthesized polyampholytes, which exhibit cryoprotective properties and show relationship between their cryoprotective properties and cell membrane protection. The authors reported on a copolymer synthesized at 1:1 ratio of methacrylic acid (MAA) to 2-(dimethylamino)ethyl methacrylate (DMAEMA), which showed the highest cell viability compared to copolymers synthesized at

2:3 and 3:2 ratios. In order to elucidate the cryoprotection mechanism, the authors introduced different hydrophobic and hydrophilic moieties in the polymer. They found that the cell viability after cryopreservation with hydrophilic and hydrophobic polyampholyte solutions at the same polymer concentration (10%) was higher in the case of hydrophobic polymer. They also varied the molecular weight of the polymers through RAFT polymerization and found that the protective properties of these CPAs were related to water absorption, which depends on the molecular weight of the compound. Thus, careful control of the molecular weight using RAFT polymerization may be an effective tool for the development of polyampholyte CPAs. The authors also found that synthetic CPAs protected the cell membrane during cryopreservation, which effect was enhanced by the introduction of hydrophobic moieties (96). However, the cryoprotection mechanism of theses CPAs is still not clear and needs to be further investigated in the future.

1.4.10 Cell encapsulation and cryoprotective hydrogels

Successful application of hydrogels in tissue engineering is due in part to the possibility of encapsulating cells without adversely affecting their viability. Most of the connective tissues in our body are composed of tissue-specific cells encapsulated within a specific extracellular matrix (ECM), which has a complex function-orientated structure (97).

Vrana et al. reported that a poly (vinyl alcohol) cryogel containing many Cross-linking points encapsulated vascular endothelial cells and smooth muscle cells through physical hydrogel formation via crystallization during freezing (98). In that report, the authors found that cells could be stored for the desired period using the cryogelation process, during which gelation proceeds after thawing occurs. When this cryogel is used to encapsulate cells in a freezing process, CPAs must be added to avoid freezing damage to the cells.

Since CPAs are generally cytotoxic (99, 100), they need to be removed after thawing. However, their complete removal from hydrogels is challenging. However, since hydrogels are the material of choice for various applications in regenerative medicine because of their unique properties like biocompatibility, flexible methods of synthesis, range of constituents, and desirable physical

characteristics, if hydrogels having cryoprotective properties could be developed, then the problem of CPAs removal would be solved. Moreover, tissue engineering applications in regenerative medicines could be successful if further advances could be made in low-temperature preservation.

1.4.11 Vitrification

The word vitrification originated from the Latin word vitreum, which means glass. Vitrification refers to the process of transformation of any substance into a glassy state, involves cooling at very fast rate, and causes enormous increase in viscosity. Rapid cooling leads to the formation of amorphous ice, i.e., water molecules lacking long-range order unlike in crystalline ice. As such, during the process of vitrification, water transforms directly to a glassy state, thereby preventing crystallization because the rate of freezing is so high that water molecules do not have time to form ice crystals. In vitrification, the viscosity of the intracellular fluid is elevated to such an extent that molecules get arrested and cease to behave as a liquid. By averting mechanical damage caused by ice crystals and resisting the change in salt concentration, vitrification prevents major damages to cells. Vitrification and freezing are not entirely different because the crystalline and vitreous phases often coexist. Indeed, during standard cryopreservation using controlled freezing of cells, a fragment of the system also undergoes vitrification.

Although vitrification studies had been performed since the 19th century when Tammann vitrified the molecules of carbon compounds in 1898 (101), one of the earliest studies on the use of vitrification in biological applications was carried out by Luyet in 1937, who is sometimes referred to as the founder of cryobiology. Luyet tried to vitrify living matter without the addition of any CPA and identified the prospective of attaining structurally immobile states for cryopreservation by rapid cooling (102).

Vitrification has been shown to provide effective preservation for a number of cells, including monocytes, ova, early embryos, and pancreatic islets (103-105).

Matsumura et al. (106) successfully vitrified human induced pluripotent (iPS) cells using COOH-PLL. The development of an efficient method to cryopreserve stem cells is very important because iPS cells enable the production of disease- and patient-specific pluripotent stem cells for cell therapy applications without

using human oocytes or embryos (107, 108). The authors developed a vitrification solution comprising ethylene glycol (EG) and sucrose as well as COOH-PLL, and found that this solution inhibited devitrification. Cells retained their pluripotency when frozen and warmed on a relatively large scale in cryovials. In addition, this vitrification solution does not require DMSO or serum proteins.

The process of vitrification involves exposure to very high concentration of CPA and subsequent cooling in liquid nitrogen. At the initial stage of conventional freezing, low concentration (15–20% w/v) of CPA is used because it will reach very high values once ice starts to grow at very low temperatures and most of the water is frozen. However, in the process of vitrification, the initial concentration of CPA is very high because there is no change in its value as the temperature is decreased; in fact, at very low temperatures the concentration remains the same because the glassy state is obtained without any ice formation. While thawing, the whole sequence of vitrification is reversed.

1.5 Objective of Thesis

In my doctoral research I developed various kinds of hydrogels based on polyampholytes. Previously in my group, cryoprotective property of poly-L-lysine based polyampholyte was elucidated. In my research, I developed new polymer based cryoprotectants and also employed these polyampholytes as one of the components in the fabrication of hydrogels. Hydrogels were prepared by chemical and physical cross-linking. Each hydrogel so developed have very unique applications in the field of tissue engineering.

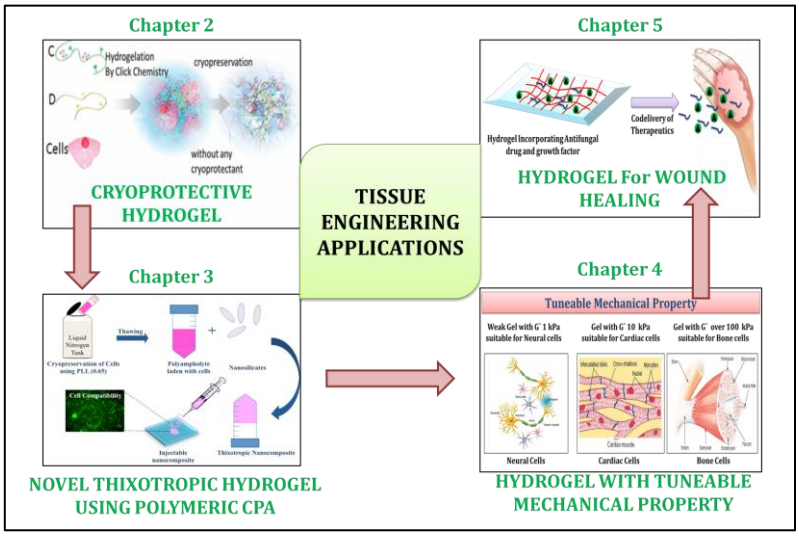

Figure 1-13 Objective of my doctoral research

In chapter 2, I developed cryoprotective hydrogels based on dextran polyampholyte. Hydrogel was fabricated using Cu-free Click chemistry. Cu-free Click cross-linking made this system a good candidate for injectable hydrogels. Hydrogels with cryoprotective property are very essential in the current scenario for the preservation of 2D or 3D tissue engineered constructs. In order to achieve this target, various complicated reaction schemes were followed.

In next chapter 3, I developed thixotropic hydrogel based on poly-L-lysine polyampholyte and laponite. It is a very simple and effective method to fabricate injectable hydrogel using physical cross-linking. My major target was to cryopreserve the cells using polyampholyte and formulates it into hydrogel (using laponite as cross-linker) after thawing without washing out cryoprotectant. This study clearly demonstrates that poly-L-lysine based polyampholyte can easily be converted to hydrogel without carrying out any chemical modifications. Charge

on the polymer and laponite resulted in the tuneability of mechanical property of the hydrogel. These kinds of hydrogels are very important for tissue engineering applications, as firstly it eliminates the need of cell harvestment and cell maintenance and secondly, due to its thixotropic nature, it is very useful as an injectable hydrogel. Thixotropic nature of the hydrogel prevented the unnecessary loss of the effective biomaterials to the unaffected areas after injection.

After the development of this type of hydrogel, in chapter 4, I introduced chemical cross-linking in this system using 4-arm polyethylene glycol amine as a cross-linker. This led to the development of hydrogel with tuneable mechanical properties. Mechanical stiffness of the substrate plays a crucial role in regenerative medicine and tissue engineering. Substrate stiffness decides the fate of cell differentiation. The hydrogels so developed with varied mechanical properties can have potent applications.

The last material which I developed in chapter 5 is based on dextran hydrogel, which incorporates the nano-assemblies. This hydrogel shows controlled codelivery of hydrophobic drug and growth factors. It is very useful for topical wound healing applications.

All of these materials are discussed in detail in my subsequent chapters.

1.5 References

1. Yannas IV: tissue and organ regeneration in adults. Springer publishing, 2007.
2. Greenwood HL, Thorsteinsdóttir H, Perry G, Renihan J, Singer PA, Daar AS. Int. J. Biotechnology, 2006, 8, 60–77.
3. Green WT. Clin Orthop Relat Res., 1977, 124, 237-250.
4. "Tissue Engineering. Selected Papers from the UCLA Symposium of Tissue Engineering. Keystone, Colorado, April 6-12, 1990", J Biomech Eng., 1991, 113, 111-207.
5. Martin GR. Proc. at. Acad. Sci. USA. 1981, 78, 7634-7638.
6. Bajada S, Mazakova I, Ashton BA, Richardson JB, Ashammakhi N. Stem Cells in Regenerative Medicine Topics in Tissue Engineering, Vol. 4. R Reis, & F Chiellini © 2008.
7. Martens P, Metters AT, Anseth KS, Bowman CN. J. Phys. Chem. B, 2001, 105, 5131-5138.
8. Lutolf MP, Hubbell JA. Nat. Biotechnol. 2005, 23, 47-55.
9. Jain M, Rajan R, Hyon SH, Matsumura K. Biomater. Sci., 2014, 2, 308-317.
10. Nguyen MK, Lee DS. Macromol. Biosci., 2010, 10, 563-579.
11. Kopecek J, Yang J. Polym Int., 2007, 56, 1078–1098.
12. Wichterle O, L´ım D. Nature, 1960, 185, 117.
13. K˘r´ıstek A, K¨onig B, Wichterle O, Klin Abl Augenheilk [inGerman], 1966, 149, 219.
14. Kresa Z, Rems J, Wichterle O. Arch Otholaryngol, 1973, 17, 360.
15. Hub´a˘cek J, Wichterle O, Kliment K, Hub´a˘cek J, Du˘sek J. C˘eskoslovenska´ otolaryngologie [in Czech], 1968, 17, 211.
16. Yeh PY, Kope˘ckov´a P, Kope˘cek J. J Polym Sci A: Polym Chem, 1994, 32, 1627.
17. Liu YU, Park MB. Biomaterials, 2009, 30, 196–207.
18. Gupta N, Srivastava AK. Polym Int., 2003, 35, 109.
19. Millar JR. J. Chem. Soc., 1960, 1311–1317
20. Matricardi P, Meo CD, Coviello T, Hennink WE, Alhaique F. Advanced Drug Delivery Reviews, 2013, 65, 1172–1187
21. Johnson JA, Turro NJ, Koberstein JT, Mark JE. Prog. Polym. Sci., 2010, 35 332–337.

22. Chikh L, Delhorbe V, Fichet O. J. Membr. Sci., 2011, 368, 1–17.
23. Robeson LM. Hanser Publishers, Munich, Hanser Gardner Publications, Cincinnati, 2007.
24. Weng L, Gouldstone A, Wu Y, Chen W. Biomaterials, 2008, 29, 2153–2163.
25. Hoare TR, Kohane DS. Polymer, 2008, 49, 1993-2007.
26. Gacesa P. Carbohydr. Polym., 1988, 8, 161–182.
27. Watanabe T, Ohtsuka A, Murase N, Barth P, Gersonde K. Magn. Reson. Med., 1996, 35, 697–705.
28. Yokoyama F, Masada I, Shimamura K, Ikawa T, Monobe K. Colloid Polym. Sci., 1986, 264, 595–601.
29. Hassan M, Peppas NA. Macromolecules, 2000, 33, 2472–2479.
30. Lapasin R, Pricl S. Cornwall, U.K.: Blackie Academic and Professional, 1995.
31. Gupta D, Tator CH, Shoichet MS. Biomaterials, 2006, 27, 2370-2379.
32. Merino S, Martın C, Kostarelos K, Prato M, Vazquez E. Acs Nano, 2015, 9, 4986-4967.
33. Giri A, Bhowmick M, Pal S, Bandyopadhyay A. Int. J. Biol. Macromol., 2011, 49, 885–893.
34. Haraguchi K, Curr. Opin. Solid State Mater. Sci., 2007, 11, 47-54.
35. Chang CW, Spreeuwel A, Zhang C, Varghese S. Soft Matter, 2010, 6, 5157–5164.
36. Xia Y. Nat. Mater., 2008, 7, 758-760.
37. Cingolani R. Nat. Nanotechnol., 2013, 8, 792-793.
38. Gaharwar AK, Schexnailder PJ, Kline BP, Schmidt G. Acta Biomater., 2011, 7, 568-577.
39. Gaharwar AK, Rivera CP, Wu CJ, Schmidt G. Acta Biomater., 2011, 7, 4139-4148.
40. Zreiqat H, Howlett C, Zannettino A, Evans P, Tanzil GS, Knabe C, Shakibaei M. J. Biomed. Mater. Res. A, 2002, 62, 175-184.
41. Carrow JK, Gaharwar AK. Macromol. Chem. Phys., 2015, 216, 248-264.
42. Krsko P, Libera M. Materials Today, 2005, 8, 36–44.
43. Liu HW, Hu SH, Chen YW, Chen SY. J. Mater. Chem. 2012, 22, 17311–17320.
44. Wei Z, Yang JH, Zhou J, Xu F, Zrínyi M, Dussault PH, Osada Y, Chen YM. Chem. Soc. Rev., 2014, 43, 8114–8131.

45. Zhang Y, Yang B, Zhang X, Xu L, Tao L, Li S, Wei Y. Chem. Commun., 2012, 48, 9305–9307.
46. Zhong D, Liu Z, Xie S, Zhang W, Zhang Y, Xue W. J. Appl. Polym. Sci., 2013, 129, 767–772.
47. Wu W, Shen J, Banerjee P, Zhou S. Biomaterials, 2010, 31, 7555–7566.
48. Polge C, Smith, AU, Parkes AS. Nature, 1949, 164, 666.
49. Smith AU, Polge C. Veterinary Record, 1950, 62, 115-117.
50. Latta R. Canadian Journal of Botany, 1971, 49, 1253-1254.
51. Bannier LJ, Steponkus PL. Hortscience 1972, 7, 411-414.
52. Cohen J, Simons R, Fehily CB. The Lancet, 1985, 325, 647.
53. Karlsson JO, Toner M. Biomaterials, 1996, 17, 243-256.
54. Lynch ME, Diller KR. Transactions of the ASME, 1981, 81, 229-232.
55. Mazur P. The journal of General Physiology, 1963, 47, 347-369.
56. Rapatz G, Menz LJ, Luyet BJ. Cryobiology, 1966, 3, 139-162.
57. Toner M. Advan Low-Temp Biol, 1993, 2, 1-51.
58. Mazur P. Annals of the New York Academy of Sciences, 1965,125, 658-676.
59. Mazur P. Cryobiology, 1977, 14, 251-272.
60. Fujikawa S. Cryobiology, 1980, 17, 351-362.
61. Mazur P. Cryobiology, 1966, 3, 214-315.
62. Mazur P, Leibo S, Chu EHY. Experimental Cell Research, 1972, 71, 345-355.
63. Lovelock E. Biochimica et Biophysica Acta., 1953, 10, 414-426.
64. Mazur P. In Proceedings of the Workshop on Preservation of Mouse Strains. 1976, 1-12.
65. Jacobs M, Glassman H, Parpart A. J. Cell. Comp. Physiol., 1935, 7, 197-225.
66. Woelders H, Matthijs A, Engel B. Cryobiology, 1997, 35, 93-105.
67. Muldrew K, McGann L. Biophysics, 1994, 166, 532-541.
68. Nei T, Araki T, Matsusaka T, Nei T. Ed. Freezing and Drying of Microorganisms. University of Tokyo Press, Tokyo, Japan, 1969, 3.
69. Nei T. Oxford, Blackwell Scientific Publications, edited by Parkes, A. and Smith, A., 1960, 78.
70. Mazur P. J. Bacteriol., 1961, 82, 662-672.
71. Meryman H, Platt W. NM 000 018.01.08,1955, 1, 13.
72. Asahina E. Contrib. Inst. Low Temp. Sci., Hokkaido Univ., 1956, 10, 83.

73. Mazur P. Biophysic J., 1963, 3, 323-353.
74. Mazur P, Leibo S, Farrant J, Chu E, Hanna M, Smith L. Wolstenholme GEW, O'Connor M, eds. The Frozen Cell. London: J and A Churchill, 1970, 69-88.
75. Lovelock E. Proceedings of the Royal Society Series B, 1957, 147, 427-433.
76. Karow A. Journal of Pharmacy and Pharmacology, 1969, 21, 209-223.
77. Stolzing A, Naaldijk Y, Fedorova V, Seethe S. Transfusion and Apheresis Science, 2012, 46, 137-147.
78. Lovelock E, Bishop MW. Nature, 1959, 183, 1349-1355.
79. Garzon AA, Cheng C, Lerner B, Lichtenstein S, Karlson KE. Journal of Trauma, 1967, 7, 757-766.
80. Knorpp CT, Merchant WR, Gikas PW, Spencer HH, Thompson NW. Science, 1967, 157, 1312-1313.
81. Lionetti F J, Hunt SM. Cryobiology, 1975, 12, 110-118.
82. Kim H, Tanaka S, Une S, Nakaichi M, Sumida S, Taura YA. Journal of Veterinary Medical Science, 2004, 66, 1543-1547.
83. Lionetti FJ, Hunt SM, Gore JM, Curby WA. Cryobiology, 1975, 12, 181-191.
84. Ashwood MJ, Warby C, Connor KW, Becker G. Cryobiology, 1972, 9, 441-449.
85. Kenmochi T, Asano T, Maruyama M. Cell Transplant, 2008, 17, 61-67.
86. Maruyama M, Kenmochi T, Sakamoto K, Arita S, Iwashita C, Kashiwabara H. Transplant Proceedings, 2004, 36, 1133-1134.
87. Fahy GM. Cryobiology, 1986, 123, 1-13.
88. Oh JE, Karlmark RK, Shin JH, Pollak A, Hengstschlager M, Lubec G. Amino Acids, 2006, 31, 289-298.
89. Young DA, Gavrilov S, Pennington CJ. Biochemical and Biophysical Research Communications, 2004, 322, 759-765.
90. Jiang G, Bi K, Tang T. International Immuno pharmacology, 2006, 6, 1204-1213.
91. Gurtovenko AA, AnwarJ. J. Phys. Chem. B, 2011, 111, 10453-10460.
92. Men H, Agca Y, Critser ES, Critser JK. Theriogenology, 2005, 64, 1340-1349.
93. Son JH, Kim KH, Nam YK, Park JK, Kim SK. Biotechnology Letters, 2004, 26, 829-833
94. Matsumura K, Hyon SH. Biomaterials, 2009, 30, 4842-4849.

95. Matsumura K, Hayashi F, Nagashima T, Hyon SH. Journal of Biomaterials science, Polymer Edition, 2013, 24, 1484-1497.
96. Rajan R, Jain M, Matsumura K. Journal of Biomaterials science, Polymer Edition, 2013, 24, 1767-1780.
97. Goh KL, Meakin JR, Aspden RM. J Theor Biol., 2007, 245, 305-311.
98. Vrana N, Matsumura K, Hyon SH. J. Tissue Engineer. Regen. Med., 2012, 6, 280-290.
99. Lowenthal R M, Park DS, Goldman JM, Hill RS, Whyte G, Th'ng KH. British journal of Haematology, 1976, 34, 105-117.
100. Douay L, Gorin NC, David R. Experimental Haematology, 1982, 10, 360-366.
101. Tammann G. Zeitschrift for Physikalische Chemie, 1898, 25, 441-479.
102. Luyet B. Biodynamica., 1937, 1, 1-14.
103. Takahashi T, Hirsh A, Erbe E, Bross J, Steere R, Williams R. Cryobiology, 1986, 23, 103-115.
104. Jutte N, Heyse P, Jansen H, Bruining G, Zeilmaker G. Cryobiology, 1987, 24, 292-302.
105. Leeuw A, Daas J, Kruip T, Rall W. Cryobiology, 1992, 32, 157-167.
106. Matsumura K, Bae J, Kim H, Hyon SH. Cryobiology, 2011, 63, 76-83.
107. Meng X, Shen J, Kawagoe S, Ohashi T, Brady R, Eto Y. Proc. Natl Acad. Sci. USA, 2010, 107, 7886-7891.
108. Park I, Arora N, Huo H. Cell, 2008, 134, 877-886.

Chapter 2

Hydrogelation of dextran-based polyampholytes with cryoprotective properties *via* click chemistry

2.1 Introduction

Hydrogels have been the material of choice for many applications in regenerative medicine because of their unique biocompatibility, flexible methods of synthesis, range of constituents, and desirable physical characteristics (1, 2). They can be used as scaffold materials for drug delivery vehicles, as engineered tissue replacements, and in a variety of other applications (3). For tissue engineering applications, injectable hydrogels are important tools because of their ability to homogeneously encapsulate the cells, their easily manipulated physical and chemical properties, and their ability to be administered in a minimally invasive manner (4–6). They are also potential substrates for tissue engineering, because drugs and cells can be readily integrated into the gelling matrix.

Cell encapsulation with such hydrogels provides cells with a three-dimensional environment that is similar to the in vivo conditions. Previously, we developed a poly(vinyl alcohol) cryogel with many Cross-linking points that encapsulated vascular endothelial cells and smooth muscle cells (7) through physical hydrogel formation *via* crystallization during freezing (8). In that report, we found that cells could be stored for the desired period using the cryogelation process, where gelation proceeds after thawing occurs. When this cryogel is used to encapsulate cells in a freezing process, cryoprotectants (CPAs) must be added to avoid freezing damage to the cells. “CPA” is the functionally derived term coined to describe “any additive that can be provided to cells before freezing that yields a higher post-thaw survival than can be obtained in its absence” (1, 9, 10). However, in general, CPAs are cytotoxic (11, 12) and need to be removed after thawing. It is likely to be difficult to completely remove CPAs from inside the

hydrogel. Therefore, if a hydrogel can be developed that itself has cryoprotective properties, the problem of the removal of CPAs could be solved.

In addition to these challenges, the success of tissue engineering applications in regenerative medicine requires further advances in low-temperature preservation. Storage of tissues and tissue engineering products is an important technique for the commercialization of tissue engineering (13–15). However, cryopreservation of regenerated tissues including cell sheets and cell constructs is not easy compared to the cryopreservation of cell suspensions, and conventional freezing methods destroy the membranous structures of cultured sheets during the freezing and thawing processes (16). Cryopreservation of cell-containing constructs is in high demand for tissue engineering applications such as producing "off-the-shelf" tissue-engineered products. A hydrogel that has cryoprotective properties could be a good alternative for the storage of tissue-engineered constructs or cell-based systems.

In spite of these problems, the application of cryopreservation to living cells and tissues has revolutionized the areas of biotechnology, plant and animal breeding programs, and modern medicine. Using this technique, cells from prokaryotic and eukaryotic organisms can be recovered from temperatures down to almost 200 °C below the freezing point of water. This has been made possible by the presence of CPAs, as mentioned above. Currently, 10% dimethyl sulphoxide (DMSO) solution is the most efficient CPA and is commonly used for cell preservation in cell banks worldwide (17, 18) in spite of its cytotoxicity and its effects on cell differentiation (19).

As an alternative to the use of cytotoxic CPAs, we have shown in our previous study that carboxylated poly-L-lysine (COOH-PLL), which is classified as a polyampholyte, yields excellent post-thaw survival efficiency (7, 20–23). Cryoprotective properties are generally found in polyampholytes, and the balance of positive and negative charges is very important (20, 24). However, the detailed mechanisms by which non-membrane- penetrating polymers can have good cryoprotective properties are still not clear. Nevertheless, we have shown that the polyampholytes were adsorbed on the cell membrane during freezing (23) and hypothesized that the mechanisms are related to the protection of the membrane from outside. The results of this previous report were the seeds from which we

conceived of the idea that a hydrogel that is formed with a polymeric CPA could itself have cryoprotective properties.

Among the natural polymers suitable for such a purpose is dextran, a hydrophilic, biocompatible, and nontoxic polysaccharide composed of linear α-1,6-linked D-glucopyranose residues. From a structural point of view, dextran has reactive hydroxyl groups that can be modified to introduce positive and negative charges and also to introduce functional groups with which to form an in situ hydrogel (25). Because dextran is naturally resistant to protein adsorption and cell adhesion, modification of its polymer backbone allows the development of a hydrogel with specific characteristics (26).

In this study, I attempted to make a polyampholyte based on dextran because of its ease of chemical modification, and showed that the dextran-based polyampholytes have good cryoprotective properties. I also intend to modify the dextran to develop a hydrogel forming dextran-based polyampholyte CPA as a building block for cell scaffolds with cryoprotective properties for tissue engineering applications. I have shown that hydrogels form from dextran substituted with azide and alkyne groups *via* Cu-free click chemistry (25) when there is an appropriate ratio of carboxyl and amino groups. These hydrogels yield excellent post-thaw survival rates of more than 90% of murine fibroblasts. This is the first report of successful cryopreservation of cells encapsulated in a hydrogel with its own cryoprotective properties, and such approaches could open new avenues for tissue engineering research and application of polymeric hydrogels.

2.1.2 What are polyampholytes?

Polyampholytes are special class of polymers in which cationic and anionic sites are randomly distributed along the polymer backbone (27, 28). In these polymers it may be possible that one charged species surmount the other or one of the charged species is dominant in narrow pH range. Typically polyampholyte carries net charge and this can be tuned with change in pH and ionic strength of the system under study. In this context they can behave either as polycationic or polyanionic species. In contrast polyzwitterions which are special subclass of polyampholytes bears same number of cationic and anionic groups within the same monomer unit that renders overall zero charge on them under neutral

conditions (29). Due to this charge neutrality they exhibit different properties from polyampholytes (30-33).

2.1.3 Swelling behavior of polyampholytes

Solution property of polyampholytes prepared either by random or block copolymers is different. Polyampholytes exhibit different isoelectric point (IEP) and swelling behavior depending on pH of the solution. Swelling is minimum at IEP as compared to low or high pH. This observation can be attributed to electrostatic interactions that exist between the charged subunits of polyampholyte. At IEP collapse of polyampholyte as there is a perfect balance between the positively and negatively charged subunits of polyampholyte. When pH of the solution is changed from the IEP, electrostatic repulsions between the charged subunits becomes prominent that leads to the expansion of polymer. The size and viscosity of polyampholyte solution depends on the type of subunits constituting the polyampholyte. This is also greatly affected by the concentration of salt in the system. It is observed that size and viscosity increases with the increase in the concentration of salt at or near IEP. This is known as antipolyectrolyte effect. This can be explained on the grounds that with the increase in the salt concentration shielding of electrostatic interactions takes place that exists among subunits (Fig. 2-1). The increase is observed until all the interactions are shielded (34-37).

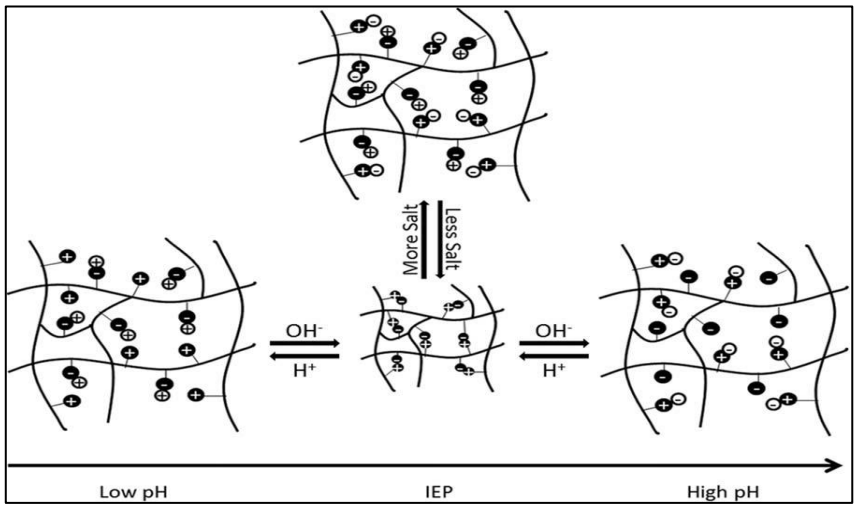

Figure 2-1 Schematic showing the impact that change in pH and salt concentration has on the electrostatic interactions in polyampholyte polymer systems[37]

2.2 Polyampholytes synthesis and their Cryoprotective properties

2.2.1 Materials

Dextran with a molar mass of 70 kDa (dextran, Mw = 70 kDa, Meito Sangyo Co., Ltd, Nagoya, Japan) was dried in vacuum oven at 50°C for 24 h before use. p-Pyrrolidinopyridine (PYP, Wako Pure Chemical Industries Ltd, Osaka, Japan) was recrystallized from distilled ethyl acetate and stored over a silica gel at 0°C. All reaction solvents were purified by distillation and stored over a 4A˚ molecular sieve. Standard solvent F consisted of 50% $HCONH_2$, 45% N,N-dimethylformamide, and 5% CH_2Cl_2 (v/v) (38).

2.2.2 Experiments

2.2.3 Azide-amino-dextran preparation

First, 3-azidopropanol and 3-azidopropyl carbonylimidazole (AP-CI) were synthesized following the procedure in the literature (39). 3-Chloropropanol (Wako, 5 mL, 5.66 g, 59.7 mmol), sodium azide (Tokyo Chemical Industry Co., Ltd (TCI), 7.83 g, 119 mol), and tetrabutylammonium hydrogen sulphate (TCI, 0.167 g) were dissolved in 20 mL of water and stirred at 80°C for 24 h, then stirred overnight at room temperature. The solution was extracted three times with 100 mL ether and dried over sodium sulphate. The ether was removed by rotary evaporation, and 3-azidopropanol was obtained as a liquid and purified by vacuum distillation (boiling point 62°C at 3–4 mbar). Next, mixing 13.77 g (84.93 mmol) of 1,1-carbonyldiimidazole (CDI) and 150 mL of ethyl acetate yielded a turbid suspension, to which 5.72 g (56.9 mmol) 3-azidopropanol was added drop-wise under vigorous stirring while the reaction mixture turned into a clear solution. After 2 h of reaction at room temperature, the solution was extracted three times with 150 mL of water. The organic layer was dried over magnesium sulphate. After the magnesium sulphate was filtered off, the solvent was evaporated by rotary evaporation and AP-CI was obtained as a liquid.

To synthesize the azide-amino-substituted dextran (azide- amino-Dex), first the azide substitution was performed using AP-CI and triethylamine (38). Dex (3 g)

and AP-CI (544 mg, 2.8 mmol) were dissolved in DMSO (33 mL) for 20 h at 50°C. After 20 h, the hydroxyl groups of azide-dextran (azide-Dex) were activated by CDI (0.27 g, 0.09 eq. per sugar unit) (Tokyo Chemical Industry Co., Ltd, Japan) for 2 h at 50°C. For this reaction, the required amount of ε-poly-L-lysine (PLL) (JNC Corporation, Tokyo, Japan) was added after activation, and the reaction was run for 36 h at 50 °C. Azide-amino-Dex was purified by dialysis (cutoff molecular weight: 14 kDa) against water for 48 h and then freeze-dried for 24 h. The amount of amino groups in the azide-amino-Dex was determined using the 2,4,6-trinitrobenzenesulfonate (TNBS) method (40). Briefly, 0.3 mL of 250 mg mL^{-1} sample solution, 1 mL of 1.0 mg mL^{-1} TNBS solution, and 2 mL of 40 mg mL^{-1} sodium bicarbonate aqueous solution containing 10 mg mL^{-1} sodium dodecyl sulphate (pH 9.0) were mixed and incubated at 37°C for 2 h. After the mixture was cooled at 25°C, the absorbance was measured at 335 nm using glycine as the standard sample.

2.2.4 Polyampholyte preparation

To synthesize the carboxylated azide-amino-dextran (azide-dextran polyampholyte, azide-Dex-PA), azide-amino-Dex and succinic anhydride (SA) (Wako) in 0%–90% mol ratios (SA/ NH_2-dextran amino groups) were mixed and reacted at 50°C for 3 h to convert the amino groups into carboxyl groups. The amount of amino groups that were converted into carboxyl groups was determined using the TNBS assay (20).

2.2.5 Preparation of alkyne-substituted dextran

Alkynes with different degrees of substitution (DSs) were prepared. To synthesize alkyne-substituted dextran, dibenzylcyclooctyne (DBCO) acid (Click Chemistry Tools, Scottsdale, AZ, USA) was used. In this reaction, CDI was first dissolved in solvent F, and then DBCO acid dissolved in solvent F was added and allowed to react at 25°C for 2 h. Subsequently, dextran and PYP dissolved in solvent F were added to the reaction mixture dropwise, and the reaction was run for 18 h. After the reaction was over, the product, DBCO-substituted dextran (DBCO-Dex), was purified by multiple precipitations using methanol (38).

2.2.5 Hydrogel Preparation

Hydrogels were formed when azide-Dex-PA and DBCO-Dex were dissolved in Dulbecco's modified Eagle's medium (DMEM; Sigma-Aldrich, St Louis, MO) without foetal bovine serum (FBS). For the preparation of different hydrogels, the desired amounts of azide-Dex-PA and DBCO-Dex were dissolved in the culture medium. The hydrogel began to form after the azide-Dex-PA and DBCO-Dex was mixed, depending upon the concentration of the two reactants. Hydrogel formation was evaluated using the test-tube-tilting method, where a test tube containing the gel was inverted.

2.2.6 Fluorescein isothiocyanate (FITC) labeling of Dex-PLL-PA

For fluorescent labeling, 10% Dex/DMSO solution was treated with FITC at a 1/100 molar ratio to Dex for 16 h at 50°C. The FITC-Dex was purified by dialysis (molecular weight cutoff, 10 kDa; Spectra/Por, Spectrum Laboratories, CA, USA) against water for 48 h. The amination and succination reactions were performed to obtain FITC-labeled Dex-PA. The interaction between the FITC-labeled Dex-PA and the L929 cells following cryopreservation was observed using confocal laser-scanning microscopy (FV1000-D; Olympus, Tokyo, Japan).

2.2.7 Nuclear magnetic resonance (NMR) spectroscopy

The ^{1}H-NMR (400 MHz) spectra of the synthesized chemicals were recorded at 25°C on a Bruker AVANCE III 400 spectrometer (Bruker BopSpin Inc., Switzerland) in $CDCl_2$ for AP- CI and D_2O for dextran derivatives.

2.2.8 Scanning electron microscope observation

Prior to scanning electron microscope observation, the freeze dried hydrogels were sputter-coated with gold for 240 s (E1030 Ion sputter). Then, images of the surface and interior of the hydrogel were recorded by a scanning electron microscope (Hitachi model 4200) at 15.0 kV.

2.2.9 Cell Culture

L929 cells (American Type Culture Collection, Manassas, VA, USA) were cultured in DMEM supplemented with 10% FBS. The cell culture was carried out at 37°C under 5% CO_2 in a humidified atmosphere. When the cells reached 80% confluence, they were removed by 0.25% (w/v) of trypsin containing 0.02%

(w/v) of ethylenediaminetetraacetic acid in phosphate-buffered saline without calcium and magnesium (PBS (-)) and seeded on a new tissue culture plate for the subculture.

2.2.10 Cryopreservation with azide-Dex-PA

Azide-Dex-PA cryopreservation solutions were prepared as follows. Azide-Dex-PA was dissolved in DMEM at a concentration of 7.5%–15% (w/w), and the pH was adjusted to 7.4 using HCl or NaOH. The osmotic pressure was adjusted by addition of 10% (w/w) NaCl aqueous solution using an Osmometer 5520 (Wescor, Inc., UT, USA). The L929 cells were counted and resuspended in 1 mL of azide-Dex-PA solution at a density of 1×10^6 cells/mL in 1.9 mL cryovials and stored in an -80°C freezer overnight. Individual vials were thawed at 37°C in a water bath with gentle shaking, and the thawed cells were diluted 10-fold in 4°C DMEM. After centrifugation, the supernatant was removed and the cells were resuspended in 5 mL of medium. All the cells were counted using a hemocytometer and a trypan blue staining method. The reported values are the ratios of living cells to total cell numbers.

2.2.11 Cryopreservation with azide-Dex-PA

Azide-Dex-PA was dissolved in 10%–12% (w/w) DMEM, and the pH was adjusted to 7.4 using HCl or NaOH. The osmotic pressure was adjusted by addition of 10% (w/w) NaCl aqueous solution to about 580 mOsm using an Osmometer. L929 cells were counted and resuspended in 1 mL of azide-Dex-PA solution at a density of 1×10^3 cells/0.1 mL in a 96-well plate, and to this was added DBCO-Dex dissolved in DMEM at the required concentration. After this, the hydrogel formation occurred within 4–5 min. This plate was stored in a −80°C freezer overnight without any other cryoprotectants. The 96-well plate was thawed after 1 day, and then the viability of the cells was determined using a live–dead assay kit (Life Technologies Corp., NY, USA). The reported values are the ratios of living cells to total cells. As a control, cells were encapsulated in a collagen hydrogel (Cell matrix Type I-A, Nitta Gelatin, Inc., Osaka, Japan), in a hydrogel formed by azide-Dex (non-ionic hydrogel), and in an azide-amino-Dex without any succination and cryopreserved in the same way as for the polyampholyte hydrogel.

2.2.12 Rheological characterization of hydrogels

Rheological measurements were conducted using a strain-controlled rheometer (TA Instruments Model TA AR2000ex). Cone-plate geometry with a cone diameter of 25 mm and an angle of 4° was employed. Hydrogels for the rheological studies were prepared in the same fashion as those for the cryoprotective studies. In each measurement, 250 μL of a mixed solution of azide-Dex-PA and DBCO-Dex was loaded onto the plate by a micropipette. The dynamic viscoelastic properties of the polymer solutions during hydrogelation were measured by oscillatory shear experiments performed at a fixed frequency of 1 Hz at room temperature.

2.2.13 Statistical analysis

All data are expressed as the mean ± standard deviation (SD). Measurements for post-thaw viability were collected with n = 5. All experiments were conducted in triplicate. Data among the different groups were compared using a one-way analysis of variance (ANOVA) with a post-hoc Tukey–Kramer test.

2.3 Results and discussion

2.3.1 Synthesis of azide-substituted polyampholyte (PA) and its cryoprotective properties

The NMR spectrum of 3-azidopropyl carbonylimidazole (AP-CI) is given in Fig. 2-2. Azide groups were introduced into the dextran by treatment with AP-CI (Scheme 1a), and dextran samples with different DSs of azide groups were synthesized.

The DS was calculated from the ^{1}H-NMR spectra (Fig. 2-3) using the following formula:

$$DS\ (\%) = ((I_{methylene} / 2) / (I_{anomeric\ proton}) \times 1.04) \times 100$$

Here, Imethylene and Ianomeric proton are the integrals of the methylene peaks of the introduced azide propanol located at 2.0 ppm and of the anomeric proton of dextran located at 4.9 ppm, respectively, and 1.04 is the correction factor for the average 4% of α-1,3 linkages in dextran (41, 42).

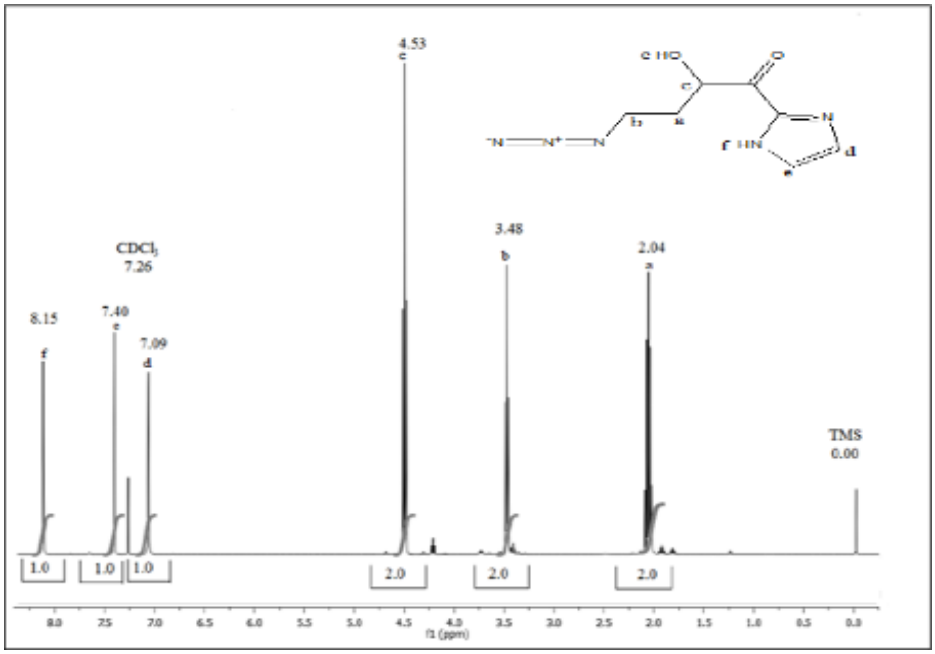

Figure 2-2 ^{1}H-NMR Spectrum of azide-CDI (AP-CI).

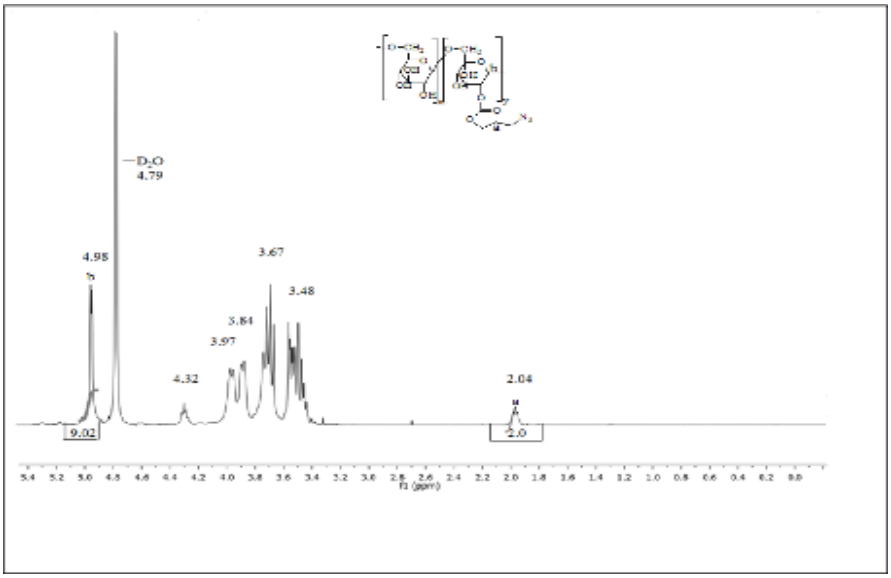

Figure 2-3 ^{1}H NMR spectrum of Dextran Azide (DS=10.65%).

Amino groups were introduced into dextran by treatment with PLL (Scheme 1b), and it was possible to control the NH_2 group introduction rates per sugar unit of azide-amino-Dex from 18% to 40%, as calculated by the TNBS assay. The amino groups were converted into carboxyl groups by treatment with SA (Scheme 1c). The ratio of carboxylation shown in parentheses, e.g., azide-Dex-PA (0.65), indicates that 65% of the amino groups introduced into dextran have been

converted into carboxyl groups by SA addition. The ratio of carboxylation was well controlled by the reaction with SA, and the values were proportional to amount of SA added.

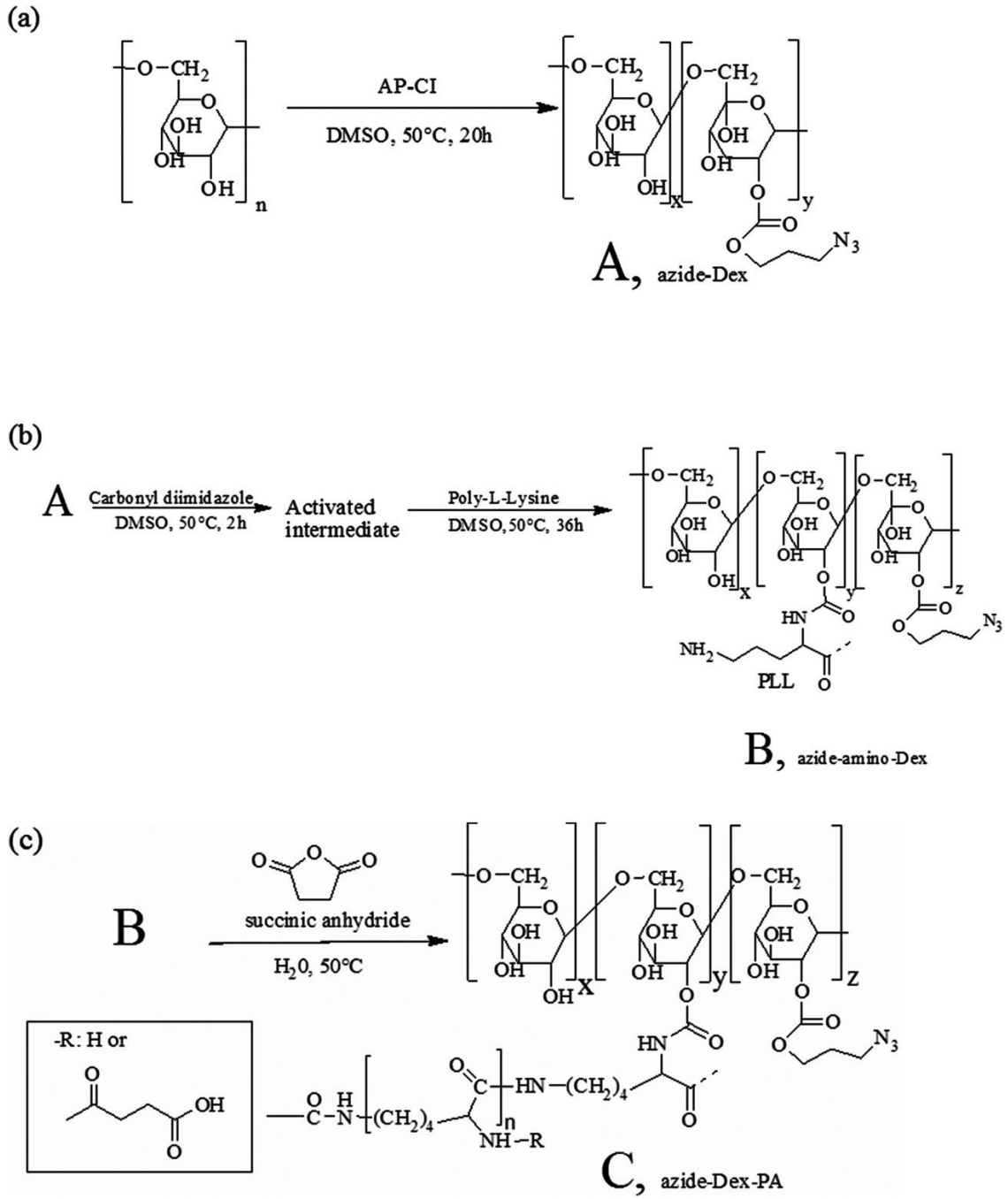

Scheme 1 Schematic representation of the synthesis of dextran polyampholyte (Dex-PA). (a) Substitution of azide in dextran. Dextran and 3-azidopropyl carbonylimidazole reacted to form dextran azopropyl carbonate (azide-Dex, A). (b) Amination of azide-dextran. A was activated with 1,1'-carbonyldiimidazole (CDI), and poly-L-lysine was grafted onto azide-Dex (azide-amino-Dex, B). (c) Succinylation of azide-amino-dextran. Succinic anhydride (SA) reacted with the azide-amino-Dex, yielding the carboxylated azide-amino-Dex (azide-Dex-PA, C).

The cell-cryoprotection properties of azide-Dex-PA depend on the polymer concentration, the amount of amino groups introduced into the dextran, the ratio of carboxylation, and the osmolarity of the solution. Fig. 2-4a shows the cell viabilities obtained immediately after thawing for solutions of azide-Dex-PA with 10% polymer concentrations and various COOH introduction ratios, with an osmotic pressure of 580 mOsm. The cell viability increased with the percentage of introduced carboxyl groups up to 69%. When L929 cells were preserved with 10% azide-Dex-PA with carboxylation ratios of 0.50, 0.54, 0.57, 0.62, 0.66, and 0.69, the viability after thawing was similar to that when 10% DMSO without FBS was used. This result shows that the PLL polyampholytes introduced into the dextran backbone with azide groups still have good cryoprotective properties like those of DMSO. When azide-Dex-PA (0.69) was used for cryopreservation with an osmotic pressure of 580 mOsm, concentrations of 10% resulted in highest viability (Fig. 2-4b). Fig. 2-4c shows the cell viabilities immediately after thawing for solutions of azide-Dex-PA (0.69) with 10% polymer concentrations and various NH_2 introduction ratios, with an osmotic pressure of 580 mOsm. In this figure, the calculated amount of NH_2 groups introduced via introduction of PLL is shown as the number of NH_2 groups for each dextran sugar unit. The cell viability obtained with 10% azide-Dex-PA (0.69) in which the NH_2 group introduction rate was 39.5% was significantly higher than that for the NH_2 introduction rate of 18.8%. The cell viability after cryopreservation tends to increase with increasing numbers of NH_2 groups introduced by the PLL. This indicates that a certain amount of charged groups is required to provide the cryoprotective function. I controlled the osmotic pressure of the 10% azide-Dex-PA (0.69) solutions to about 580 mOsm based on the results of a viability assay against the osmotic pressure of azide-Dex-PA(0.69). In this assay, azide-Dex-PA (0.69) solutions with osmotic pressures of

300–700 mOsm, which are higher than that of the living body, exhibited better cryopreservation properties (Fig. 2-4d) than those with lower pressures. It seems that the cells were dehydrated under relatively high osmotic pressures during cooling and thus avoided damage from intracellular freezing (43, 44). More than 90% viability was obtained after cryopreservation with 10% azide-Dex-PA (0.69) with 578 mOsm. These results agree well with our previous reports (20, 21),

which showed that polyampholytes could have cryoprotective properties for living cells.

a)

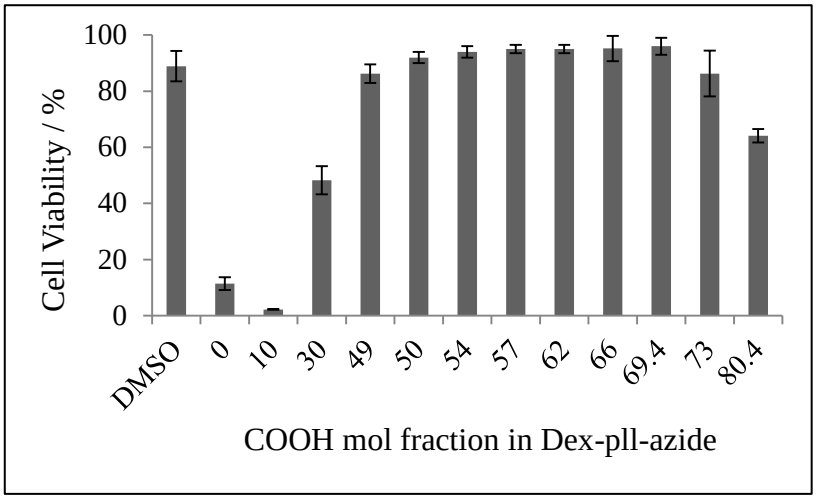

b)

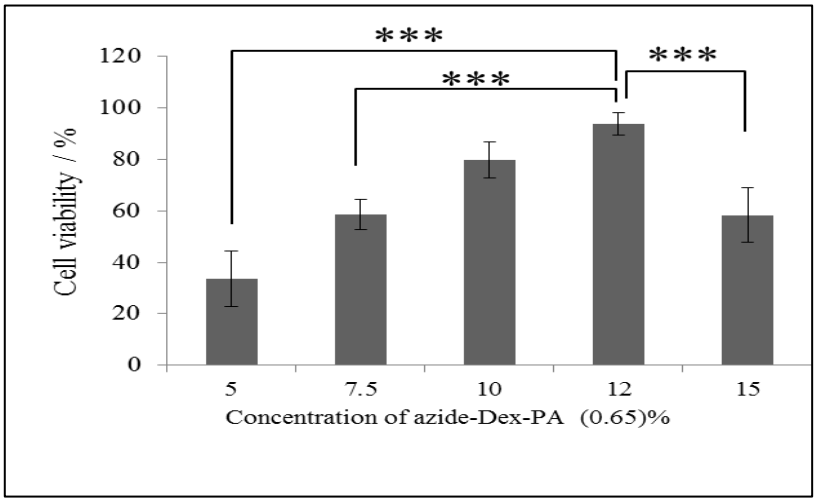

c)

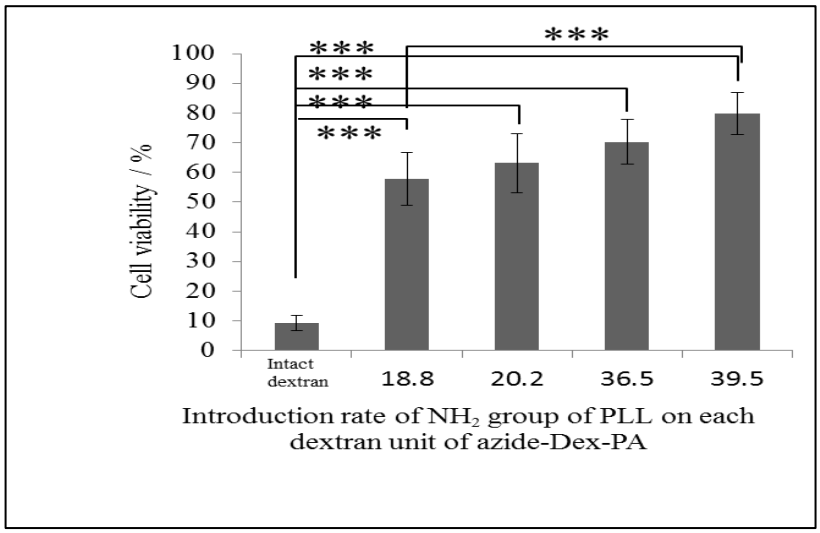

d)

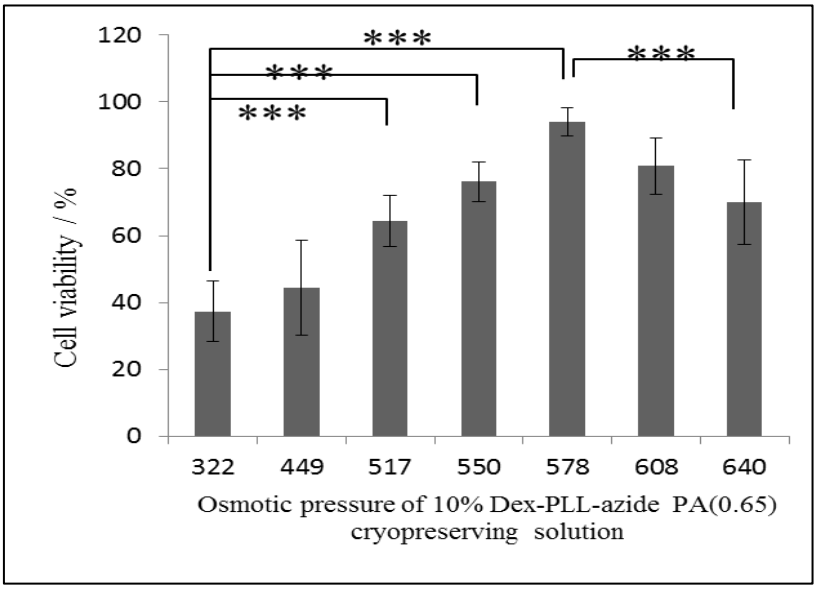

Figure 2-4 Cryoprotective properties of dextran polyampholytes (Dex-PAs). The viability of L929 cells cryopreserved with various azide-Dex-PAs as cryoprotectant agents (CPAs) was measured immediately after thawing. (a) L929 cells were cryopreserved with 10% DMSO and 12% (w/w) azide-Dex-PAs with different ratios of introduced COOH. (b) L929 cells were cryopreserved with various concentrations of azide-Dex-PA (0.65). (c) L929 cells were cryopreserved with 10% azide-Dex-PA (0.65) with various ratios of NH2 introduced by ε-poly-L-lysine (PLL). (d) L929 cells were cryopreserved with 10% Dex-PA (0.65) under various osmotic pressures. The osmotic pressures were adjusted with 10% (w/w) NaCl aqueous solution. Data are expressed as the mean ± SD. ***P < 0.001. ###P < 0.001 vs. 10% DMSO.

I and my collaborators have previously discussed the mechanisms leading to the cryoprotective properties of polyampholytes (23). To cryopreserve cells for long-term storage, intracellular ice formation has to be avoided. During freezing, the increasing osmotic pressure due to the concentrated, partially frozen extracellular solution dehydrates the cell. The speed and degree of dehydration both influence the cryoprotection. If polyampholytes, with their charged moieties, interact with salt molecules, which are ordinarily concentrated during freezing, the degree of dehydration could be controlled. An appropriate level of dehydration would therefore prevent intracellular ice formation. Although further investigation should be done, we proposed that polyampholytes act as

cryoprotective agents by protecting cells from stresses such as drastic changes in the soluble space size and osmotic pressure (23, 45). In this study, I confirmed that a high molecular weight (over 70 kDa) polyampholyte-based polysaccharide, namely, dextran with azide groups, also protected cells from freezing damage and that cryoprotection can be a property not only of polylysine derivatives but also of polyampholytes in general. The affinity of dextran-based polyampholytes for the cell surface during freezing was evaluated with a confocal laser microscope. After cryopreservation with 10% Dex-PA (0.69) labelled with FITC, adsorption of Dex-PA (0.69) onto the cells was observed. Dex-PA (0.69) molecules appeared to be adsorbed onto the cell membrane immediately after thawing (Fig. 2-5). As shown in Fig. 2-5, penetration of Dex-PA was prevented by the high molecular weight and high charge density. FITC labelling does not affect the cryoprotective properties of Dex-PA or the cell membrane interactions because of the low molar ratio of FITC. This polymer adsorbed to the cell surface during freezing, which may have then protected the cell membrane in the same way as COOH-PLL (23). Although the mechanisms by which the cell membrane is protected during freezing need to be investigated in future research, I aimed to develop a hydrogel with its own cryoprotective properties by taking advantage of this extracellular cell protection.

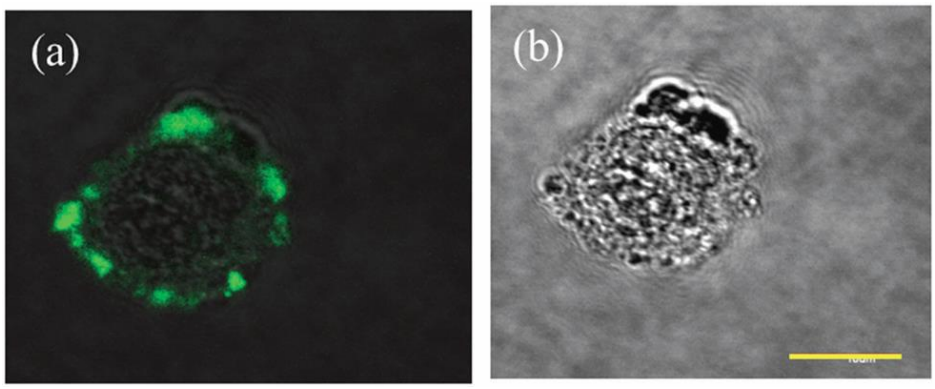

Figure 2-5 Confocal microscopic images of L929 cells cryopreserved with FITC-labelled Dex-PA (0.65) taken immediately after thawing. (a) Dark and (b) bright fields at the same point. The bar is 100 μm.

2.3.2 Synthesis of alkyne-substituted dextran

Hydrogels derived from Cu-free processes have many potential applications in tissue engineering. For example, they can be used in controlled drug delivery

systems and in 3D cell culturing (46). Hydrogels developed using Cu-free click chemistry also shed light on the possibility of cytotoxicity due to Cu. For this purpose, DBCO acid was introduced into the dextran as an alkyne substituent, as shown in Scheme 2, to synthesize dextran samples with different DSs of alkynes (Table 1).

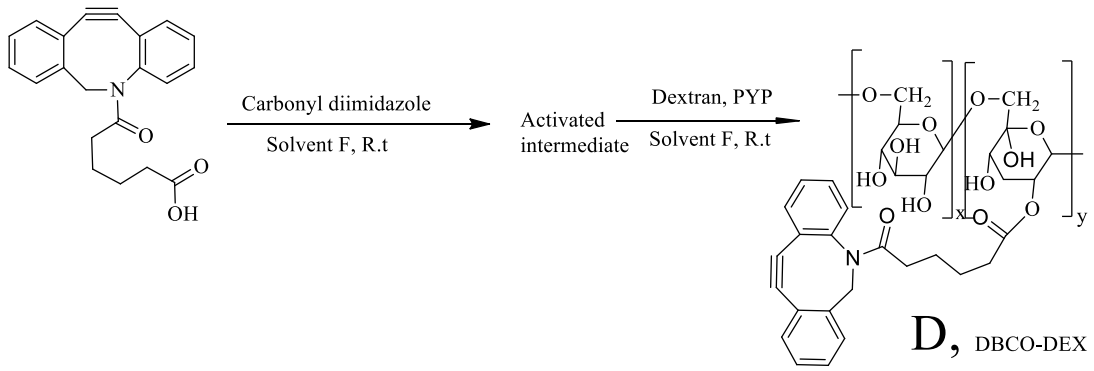

Scheme 2 Synthesis of DBCO-Dex. DBCO was activated with CDI in solvent F, and addition of dextran yielded DBCO-substituted dextran (DBCO-Dex).

Table 1 Hydrogels prepared with different DSs of alkynes (DBCO) using a 12% concentration of azide-Dex-PA (DS of azides is 11.7% and DS of NH2 groups of PLL is 40%).

Degree of substitution of alkyne in dextran per sugar unit (%)	**Water solubility**	**Hydrogel formation (azide-Dex-PA : DBCO-Dex (w/w))**
1.5	Soluble	No (1:1)
3	Soluble	Yes (2:1, 3:1)
4.8	Soluble	Yes (4:1, 6:1)
5.4	Soluble	Yes (4:1, 6:1)
14.3	Insoluble	No

The DS of DBCO per sugar unit was calculated from the ^{1}H-NMR results (Fig. 2-6) using the formula given below:

$$DS\ (\%) = ((\ I_{aromatic} / 8) / (I_{anomeric\ proton}) \times 1.04\ ) \times 100$$

Here, $I_{aromatic}$ protons and $I_{anomeric}$ proton are the integrals of the methylene peaks of the introduced DBCO acid located at around 7.5 ppm and of the anomeric proton of dextran at 4.9 ppm, respectively, and 1.04 is the correction factor for the average 4% of α-1,3 linkages in dextran (30, 31). Dextran with a higher DS of alkynes is water-insoluble, probably because of the increase in hydrophobicity.

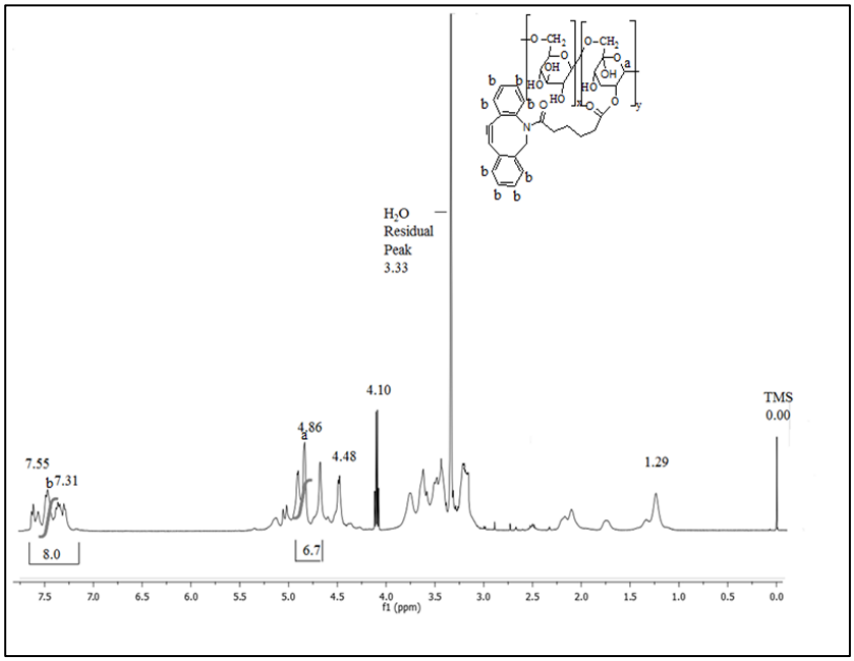

Figure 2-6 ^{1}H NMR spectrum of DBCO-Dextran (DS=14.3%).

2.3.3 Hydrogel formation via Cu-free click chemistry

Hydrogels were formed by reacting DBCO-Dex and azide-Dex PA (Scheme 3a) via strain-promoted azide–alkyne cycloaddition (SPAAC) click chemistry (47, 48). SPAAC has already been utilized for live-cell imaging (49) and in vivo metabolic labelling, as well as hydrogel formation; because of its significant advantages in terms of cytocompatibility and biocompatibility compared with Cu-catalysed click chemistry. This click-chemistry derived hydrogel also does not require any toxic Cross-linking agents. Hydrogel formation via SPAAC between DBCO-terminated polyethylene glycol (PEG) and azide-substituted PEG has been reported previously for tissue engineering applications (50). In this previous report, the viability of cells encapsulated in situ with the Cu-free SPAAC-derived hydrogel was significantly higher than that of the cells encapsulated by the

photocrosslinked PEG hydrogel because of the high cytocompatibility of SPAAC (48). Our purpose is to encapsulate cells in situ with a polyampholyte hydrogel in order to form a cell-cryoprotective scaffold; hence, bioorthogonal and cytocompatible reactions such as SPAAC will be useful.

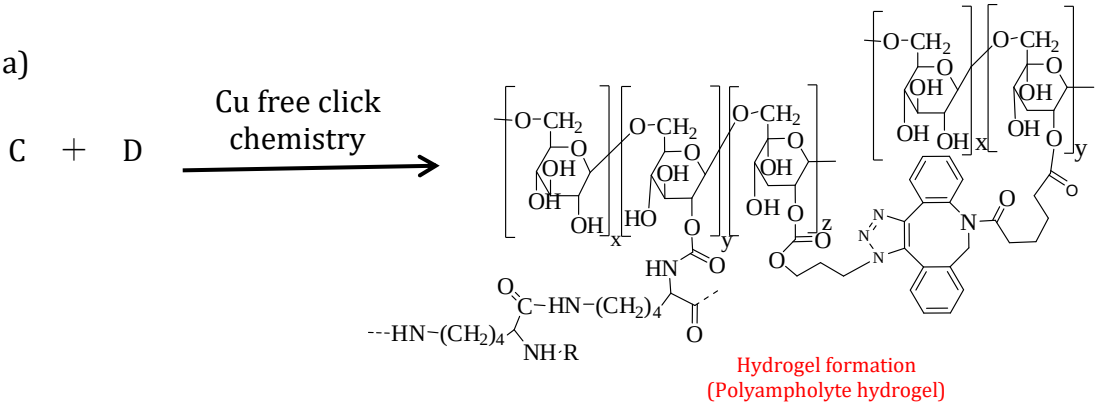

Scheme 3 Schematic representation of hydrogel formation using azide-Dex-PA and DBCO-Dex

2.3.4 Cryoprotective properties of the hydrogel

The cryoprotective properties of different hydrogels were checked using azide Dex-PA (DS of azide is 11.7%, and DS of NH_2 groups is 40%) and DBCO-Dex, which act as cross-linkers (DS of alkyne is 6.5%). L929 cells cryopreserved with these hydrogels (total polymer concentration was 10%) (Scheme 4a and b) showed a viability of more than 90% immediately after thawing (Fig. 2-7, Table 2). When the cells were cryopreserved without any cryoprotectants in a collagen hydrogel, which is widely used for tissue engineering applications, all cells were killed. Almost 0% viability was obtained when cells were cryopreserved within the hydrogel formed by azide-amino-Dex and azide-Dex without any succination. These results showed that the polyampholyte hydrogel was necessary to protect cells from freezing damage. Current cryopreservation techniques have mainly been devised and optimized for cell suspensions, and their application to adherent monolayers or thick biological samples is known to be less effective (51, 52). To cryopreserve larger volume cell-containing matrixes such as cell aggregates, tissue-engineered constructs, and cell sheets, a vitrification method is usually applied (13, 53). Vitrification is one of the most established methods for the cryopreservation of large cells like oocytes and embryos (54). Vitrification circumvents the problems associatedwith ice-crystal formation by inducing glass-

like solidification during rapid cooling in a high-concentration cryoprotectant solution. However, the high cytotoxicity from highly concentrated cryoprotectants is still a serious problem for maintaining tissue-like structures with high cell viability. As a substitute for a vitrification method, this study proposed a novel approach to cryopreservation of tissue-engineered constructs with a cryoprotective hydrogel.

a) b)

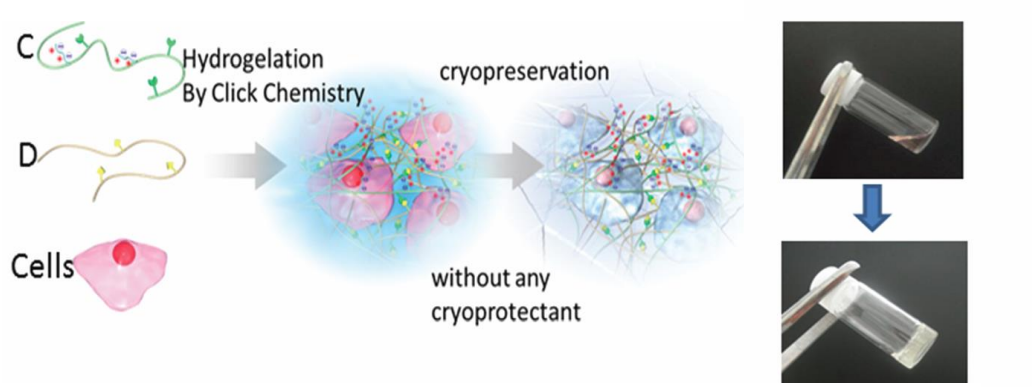

Scheme 4 a) Depiction of cell encapsulation and cryopreservation by in situ hydrogelation via SPAAC click chemistry. (b) Representative picture of cell-hydrogel construct (10% polymer concentration, azide-Dex-PA (0.69) (DS of azide 11.7%): DBCO-Dex (DS of DBCO 6.5%) ratio = 4: 1 (wt: wt), 570 mOsm, pH 7.4, cell density = 1 × 104 mL^{-1})

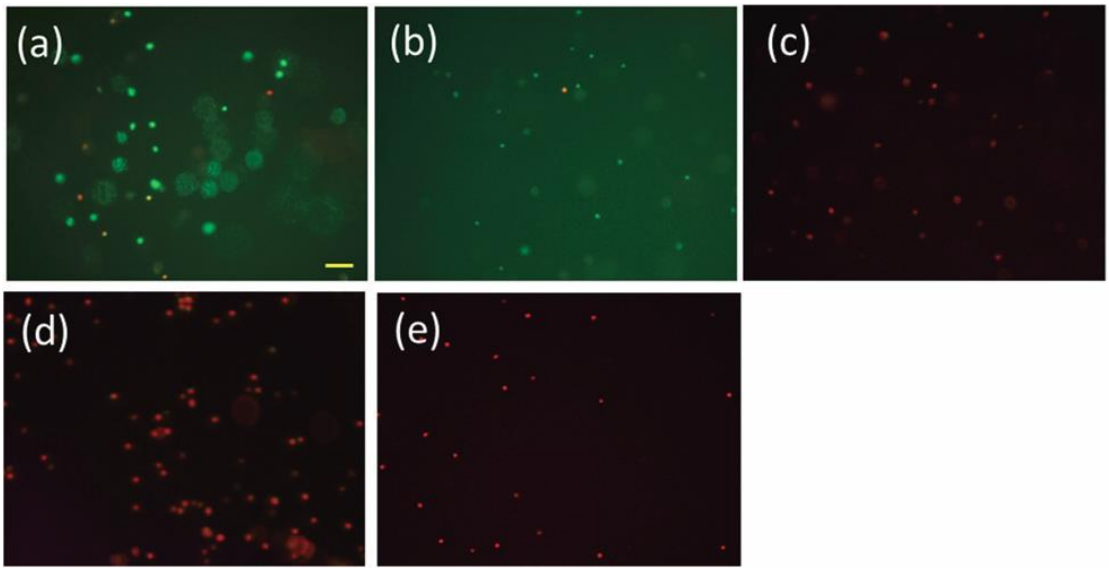

Figure 2-7 Cell viability after cryopreservation with two different types of hydrogels with different ratios of azide-Dex-PA (0.65) (DS of azide 11.7%) and Dex-alkyne (DS of DBCO 6.5%) and with a collagen hydrogel. Fluorescent microphotographs of cell encapsulated in (a) 4 : 1 azide- Dex-PA (0.69) : DBCO-Dex, (b) 6 : 1 azide-Dex-PA (0.69) : DBCO-Dex, (c) 4 : 1 azide-amino-Dex : DBCO-Dex, (d) 4 : 1 azide-Dex : DBCO-Dex, and (e) collagen hydrogel taken using a live–dead assay kit. The bar is 50 μm

Table 2 Viabilities of L929 cells cryopreserved in a hydrogel composed of azide-Dex-PA (DS 11.7%) and DBCO-Dex (DS 6.5%), in a hydrogel composed of azide-amino-Dex (without succination) and DBCO-Dex (DS 6.5%), in a hydrogel composed of azide-Dex (non-ionic) and DBCO-Dex (DS 6.5%), and in a collagen hydrogel, immediately after thawing.

Hydrogel component	Viability (%)
4 : 1(wt : wt) azide-Dex-PA(0.69) : DBCO-Dex[a]	93 ± 4.2
6 : 1 azide-Dex-PA(0.69) : DBCO-Dex[a]	94 ± 3.6
4 : 1 azide-amino-Dex : DBCO-Dex[a]	0 ± 0
4 : 1 azide-Dex : DBCO-Dex[a]	0 ± 0
1% collagen hydrogel	0 ± 0

[a] Total polymer concentration 10%, osmotic pressure 570 mOsm, pH 7.4.

Successful introduction of 0.041 mg mL^{-1} of the cell-attachment peptide RGDS into dextran in the present study, and found that cells could attach to and proliferate on the hydrogel (Fig. 2-8) during a culture over 7 days. This finding clearly demonstrates that we can introduce cell compatibility into a hydrogel formed in situ and that this system can be used to produce cell scaffolds with cryoprotective properties. Moreover, the hydrogel might be suitable as a tissue-engineering scaffold (55) because the triazole ring at the Cross-linking point is connected to dextran through carbonate esters (Scheme 3), and this structure is known to be hydrolysable under physiological conditions (25).

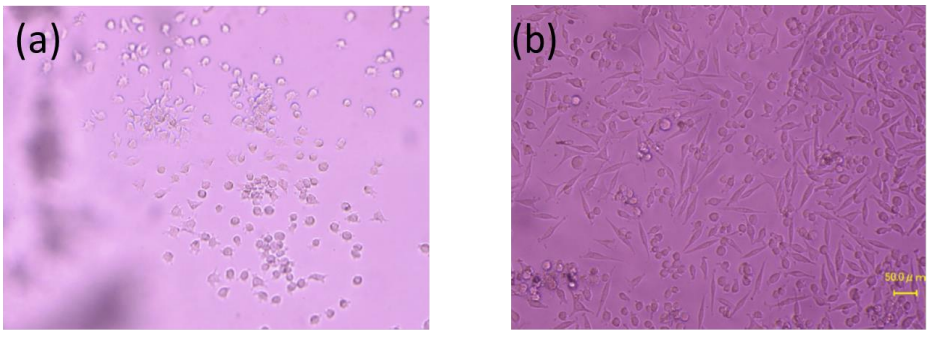

Figure 2-8 Microphotographs of L929 seeded on the RGD-substituted dextran hydrogel cultured for (a) 1 day and (b) 7 days. The bar is 50 μm

2.3.5 Rheological characterization of hydrogels

The strength of the hydrogels was investigated by performing rheological tests in order to establish the degree to which the variations in concentrations of DBCO-Dex and azide-Dex-PA influence Cross-linking. In Fig. 2-9, the dynamic mechanical properties of different hydrogels are shown. Different hydrogels were formed at different concentrations of DBCO-Dex and azide-Dex-PA, so the strength of the hydrogel can be tuned by varying the concentrations of the two reacting species. The storage modulus gradually increased with time because Cross-linking points were generated by the click chemistry reaction between the azides and alkynes. The gelation time and storage modulus 600 s after mixing of the two components are summarized in Table 3. The mechanical strength of the hydrogels can easily be varied from 6 Pa to 2.7 kPa. These values are consistent with the mechanical properties of tissue-engineered hydrogels and the extracellular matrix (56). When i mixed azide-Dex-PA and DBCO-Dex in weight ratios of 1 : 1 and 1 : 2.5, both the gelation time and storage modulus were observed to increase with the total polymer concentration.

Hydrogels formed with higher amounts of alkynes and lower amounts of azides are stronger than hydrogels formed with larger amounts of azides and lower amounts of alkynes. However, when the amounts of DBCO-Dex and azide-Dex-PA were similar, intermediate strengths were obtained. This is reasonable, because the DS of azide groups is higher than that of alkynes in dextran. Hence, when the amount of azide groups increases relative to the amount of alkynes, a substantial amount of azide groups will be unreacted during Cross-linking.

Furthermore, the gelation time for hydrogel formation can be tuned by varying the concentrations of azide groups and alkynes in the dextran. After some preliminary tuning, concentrations at which the hydrogel formation time is around 5–10 min were selected for cryopreservation purposes.

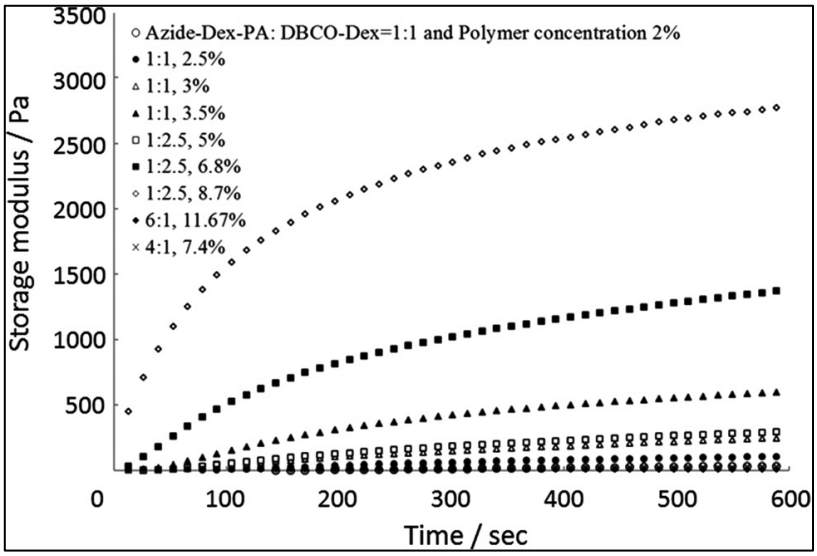

Figure 2-9 Storage moduli for different hydrogels with varying total polymer concentrations. Hydrogels composed of azide-Dex (DS of azide 11.7%) and DBCO-Dex (DS of DBCO 6.5%).

Table 3 Gelation time and storage modulus 600 s after mixing of different hydrogels prepared using different concentrations of DBCO-Dex (DS of alkynes is 6.5%) and azide-Dex-PA (DS of azides is 11.7%)

Azide-Dex- PA : DBCO-Dex (wt : wt)	**Total polymer concentration/%**	**Gelation time/s**	**Storage modulus at 600s after mixing/Pa**
1 : 1	2.0	560	53.6
1 : 1	2.5	480	134.1
1 : 1	3.0	120	243.8
1 : 1	3.5	60	595.9
1 : 2.5	5.0	120	308.0
1 : 2.5	6.8	60	915.8
1 : 2.5	8.6	50	2612.0
6 : 1	11.7	540	6.46
4 : 1	7.3	480	19.6

Scanning electron microscopy (SEM) was also performed to evaluate the physical and chemical nature of the crosslinked hydrogels. SEM images of the hydrogels

showed densely crosslinked networks with varying porosities and microstructures (Fig. 2-10). The pore size of the hydrogels was found to be approximately 50–150 μm, which is larger than the size of a cell. This observation suggests that during cryopreservation, the cells are inside the cavities of the hydrogel. This result suggests that an azide-conjugated polyampholyte cryoprotectant could be used with DBCO-Dex for biomedical therapeutic technologies such as an injectable hydrogel cell-delivery system (57) or orthopaedic applications (58). For example, stem cells cryopreserved with azide-Dex-PA can be mixed with DBCO-Dex immediately after thawing for injection into defect sites to form a scaffold for cell growth and tissue repair. This system does not require any pretreatment of the stem cells before injection, making cell maintenance, harvesting, and mixing with the hydrogel-forming media unnecessary. In our system, the stem cells could be preserved until just before usage, and the cells can be injected just after thawing without washing out the cryoprotectant.

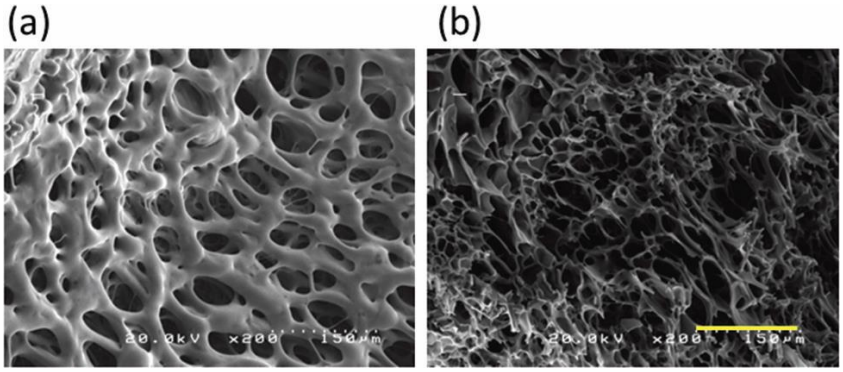

Figure 2-10 SEM image of lyophilized hydrogel composed of azide-Dex-PA (DS of azide 11.7%) (12 mg mL^{-1}) and DBCO-Dex (DS of DBCO 6.5%) (3 mg mL^{-1}) formed via Cu-free click chemistry in a DMEM medium without FBS. (a) Surface and (b) inside of the lyophilized hydrogel. The bar is 150 μm.

2.4 Conclusion

In this study, I developed polyampholyte cryoprotectants with azide groups that form in situ hydrogels that can encapsulate cells along with DBCO-Dex *via* Cu-free click chemistry. The system showed excellent cryoprotective properties without any additional cryoprotectants. This is the first challenge in the development of cryoprotective hydrogels by means of a combination of materials science and cryobiology. In the past few years, the potential to mould the shapes and sizes of

biologically relevant hydrogels has led to new directions in generating tissues. It has also provided opportunities to meet various challenges in tissue engineering such as vascularization, the formation of tissue architectures, and cell seeding. These methodologies are useful for engineering tissue architectures inside the cell-containing hydrogel. Overall, it appears that our dextran-based cryoprotective hydrogel has the potential to overcome many of the challenges that have troubled the field of tissue engineering.

2.5 References

1. Karow Jr. AM, Webb WR. Cryobiology, 1965, 4, 270– 273.
2. Brandl F, Sommer F, Goepferich A. Biomaterials, 2007, 28, 134–146.
3. Huaping T, Kacey GM. Materials, 2010, 3, 1746–1767.
4. Lee KY, Mooney DJ. Chem. Rev., 2001, 101, 1869–1879.
5. Drury JL, Mooney DJ. Biomaterials, 2003, 24, 4337–4351.
6. Tememoff JS, Mikos GM. Biomaterials, 2000, 21, 2405–2412.
7. Vrana NE, Matsumura K, Hyon SH, Geever LM, Kennedy JE, Lyons JG, Higginbotham CL, Cahill PA, Mc Guinness GB. J. Tissue Eng. Regen. Med., 2012, 6, 280–290.
8. Hyon SH, Cha W, Ikada Y. Polym. Bull., 1989, 22, 119–122.
9. Karow Jr. AM, Carrie Jr. O, Clower BR. J. Pharm. Pharmacol., 1968, 20, 297–301.
10. Fuller BJ. Cryoletters, 2004, 25, 375–388.
11. Lowenthal RM, Park DS, Goldman JM, Hill RS, Whyte G, Th'ng KH, Br. J. Haematol., 1976, 34, 105–117.
12. Douay L, Gorin NC, David R, Stachowiak J, Salmon C, Najman A, Duhamel G. Exp. Hematol., 1982, 10, 360–366.
13. Wu YN, Yu HR, Chang S, Magalhaes R, Kuleshova LL. Tissue Eng., 2007, 13, 649–658.
14. Fan WX, Ma XH, Liu TQ, Cui ZF. J. Biosci. Bioeng., 2008, 106, 610–613.
15. Chen FF, Zhang WJ, Wu W, Jin YQ, Cen L, Kretlow JD, Gao WC, Dai ZP, Wang JM, Zhou GD, Liu W, Cui L, Cao WL. Biomaterials, 2011, 32, 8426–8435.
16. Kito K, Kagami H, Kobayashi C, Ueda M, Terasaki H. Cornea, 2005, 24, 735–741.

17. Kotobuki N, Hirose M, Machida H, Katou Y, Muraki K, Takakura Y, Ohgushi H. Tissue Eng., 2005, 11, 663–673.
18. Petrenko YA, Jones DRE, Petrenko AY. Cryobiology, 2008, 57, 195–200.
19. Jiang GS, Bi KH, Tang TH, Wang JW, Zhang YK, Zhang W, Ren HQ, Wang YS. Int. Immunopharmacol., 2006, 6, 120413.
20. Matsumura K, Hyon SH. Biomaterials, 2009, 30, 4842–4849.
21. Matsumura K, Bae JY, Hyon SH. Cell Transplant., 2010, 19, 691–699.
22. Matsumura K, Bae JY, Kim HH, Hyon SH. Cryobiology, 2011, 63, 76–83.
23. Matsumura K, Hayashi F, Nagashima T, Hyon SH. J. Biomater. Sci. Polym. Ed., 2013, 24, 1484–1497.
24. Rajan R, Jain M, Matsumura K. J. Biomater. Sci. Polym. Ed., 2013, 24, 1767–1780.
25. De Geest BG, Van Camp W, Du Prez FE, De Smedt SC. J. Demeester and W. E. Hennink, Chem. Commun., 2008, 190–192.
26. Sun G, Shen YI, Ho CC, Kusuma S, Gerecht S. J. Biomed. Mater. Res. A, 2010, 93, 1080–1090.
27. Kudaibergenov SE. Advances in Polym. Sci.,1999, 144, 115-197.
28. Bekturova EA, Kudaibergenova SE, Rafikova SR. J. Macromol. Sci., Part C: Polym. Rev., 1990, 30, 233-303.
29. Laschewsky A. Polymers 2014, 6, 1544-1601.
30. Salamone JC, Rice WC. Polyampholytes. In Encyclopedia of Polymer Science and Technologie, 2nd ed., Wiley-Interscience: New York, NY, USA 11 (1988) 514-530.
31. Galin JC. Polyzwitterions. In Polymer Materials Encyclopedia, CRC Press: Boca Raton, FL, USA 9 (1996) 7189-7201.
32. Lowe AB, McCormick CL. Chem. Rev., 2002, 102, 4177–4189.
33. Kudaibergenov S, Jaeger W, Laschewsky A. Adv. Polym. Sci. 2006, 201, 157–224.
34. Pafiti KS, Philippou Z, Loizou E, Porcar L, Patrickios CS. Macromolecules 2011, 44, 5352.
35. An H, Lu C, Wang P, Li W, Tan Y, Xu K, Liu C. Polym Bull 2011, 67, 141.
36. Xiao H, Tao R, Cui W, Zhang S, Li RH. J. Appl. Polym. Sci. 2013, 127, 4052.
37. Zurick KM, Bernards M. J. Appl. Polym. Sci. 2014, 131, 4069.

38. Bamford CH, Middleton IP, Al-Lamee KG. Polymer, 1986, 27, 1981–1984.
39. Zhang J, Li C, Wang Y, Zhuo RX, Zhang XZ. Chem. Commun., 2011, 47, 4557–4559.
40. Habeeb AF. Anal. Biochem., 1966, 14, 328–336.
41. Lévesque SG, Lim RM, Shoichet SM. Biomaterials, 2005, 26, 7436–7446.
42. Van Dijk-Wolthuis WNE, Franssen O, Talsma H, Van Steenbergen MJ, Kettenes-van den Bosh WJ, Hennink WE. Macromolecules, 1995, 28, 6317–6322.
43. Mazur P. Cryobiology, 1997, 14, 251–272.
44. Mazur P, Pinn IL, Kleinhans FW. Cryobiology, 2007, 55, 158–166.
45. Matsumura K, Hayashi F, Nagashima T, Hyon SH. Cryobiol. Cryotechnol., 2013, 59, 23–28.
46. DeForest CA, Sims EA, Anseth KS. Chem. Mater., 2010, 22, 4783–4790.
47. Agard NJ, Prescher JA, Bertozzi CR. J. Am. Chem. Soc., 2004, 126, 15046–15047.
48. Xu J, Filion TM, Prifti F, Song J. Chem.–Asian J., 2011, 6, 2730–2737.
49. Beatty KE, Fisk JD, Smart BP, Lu YY, Szychowski J, Hangauer MJ, Baskin JM, Bertozzi CR, Tirrell DA. ChemBioChem, 2010, 11, 2092–2095.
50. DeForest CA, Polizzotti BD, Anseth KS. Nat. Mater., 2009, 8, 659–664.
51. Sotres-Vega A, Villalba-Caloca J, Jasso-Victoria R, Olmos-Zuniga JR, Gaxiola-Gaxiola M, Baltazares-Lipp M, Santibanez-Salgado A, Santillan-Doherty P. J. Invest. Surg., 2006, 19, 125–135.
52. Malpique R, Ehrhart F, Katsen-Globa A, Zimmermann H, Alves PM. Tissue Eng. C, 2009, 15, 373–386.
53. Magalhães R, Nugraha B, Pervaiz S, Yu H, Kuleshova LL. Biomaterials, 2012, 33, 829–836.
54. Rall WF, Fahy GM. Nature, 1985, 313, 573–575.
55. Scott EA, Nichols MD, Kuntz-Willits R, Elbert DL. Acta Biomater., 2010, 6, 29–38.
56. Even-Ram S, Artym V, Yamada KM. Cell, 2006, 126, 645–647.
57. Nagahama K, Ouchi T, Ohya Y. Adv. Funct. Mater., 2008, 18, 1220–1231.
58. Gyawali D, Nair P, Kim HK, Yang J. Biomater. Sci., 2013, 1, 52–64.

Chapter 3

Thixotropic injectable hydrogel using a polyampholyte and nanosilicate prepared directly after cryopreservation

3.1 Introduction

Structures existing in nature usually inspire for biomaterial construction. Designing of such biomaterials for tissue engineering applications requires a detailed understanding of polymers, cells, and nanostructures (1). To recapitulate these features, various nanoceramics, such as synthetic silicates (2), nano-hydroxyapatite (3-6) and bioactive glass (7-9), have been used. Additionally, various novel microscale technologies have been developed to create polymeric-based structures with nanofillers to provide architecture and materials similar to those in nature (10). Nanocomposite hydrogels have attractive features, such as highly hydrated 3D polymeric networks with nanoparticles and cytocompatiblity. The interaction of nanoparticles with polymers may be covalent (11-13) or physical (14-16) and may result in unique and useful combinations that provide features such as mechanical improvement, cell adhesiveness and degradation tuneability.

Various studies have shown that physical interaction of natural and synthetic polymers with synthetic silicates leads to the formation of physically cross-linked structures. Polyampholytes are special class of polymers in which cationic and anionic sites are randomly distributed along the polymer backbone (17, 18). In these polymers it may be possible that one charged species surmount the other or one of the charged species is dominant in narrow pH range. Typically polyampholyte carries net charge and this can be tuned with change in pH and ionic strength of the system under study. In this context they can behave either as polycationic or polyanionic species. In contrast polyzwitterions, which are special subclass of polyampholytes, bears same number of cationic and anionic groups within the same monomer unit that renders overall zero charge on them under neutral conditions (19). Due to this charge neutrality they exhibit different

properties from polyampholytes (20-23). Polyampholytes have various unique properties, such as antibiofouling, cryoprotection, and protein aggregation inhibition (24-33). Carboxylated poly-L-lysine (COOH-PLL) is a polyampholyte (34) with the appropriate ratio of amino to carboxyl groups and shows excellent cryopreservation ability without the addition of any other cryoprotective agents (CPAs) because COOH-PLL is itself a type of non-penetrating CPA. The application of low-temperature preservation has revolutionized biotechnology as both prokaryotic and eukaryotic cells can be cryopreserved at temperatures of -200°C. In a previous study, my collaborators developed a polyampholyte hydrogel having cryoprotective properties via click chemistry (35).

Synthetic nanoclays comprised of hectorites, such as laponite, have attracted much interest (36). Synthetic silicates have been used as osteogenic agents (37) in drug delivery systems (38), tissue-engineered products, (39) and commercial formulations, including paints, cosmetics, personal care products, household cleaners, and adhesives (40). Laponite has a disc-like shape, a diameter of about 25-30 nm, and a thickness of 1 nm (41-43), where the disc has an anisotropic distribution of charges. A negative charge particularly exists on the surface and the charge on the rim is pH-dependent, with a negative charge at high pH and positive charge at low pH (44, 45). This unusual charge distribution plays a critical role in determining the interactions of laponite with polymers, which are not simple and vary with the type (46), molecular weight (47), and charge of the polymer (48). One interesting property of laponite is cytocompatibility. A bioinert polyethylene oxide hydrogel was shown to acquire high cell adhesion through incorporation of laponite (15). These unique properties of laponite prompted us to use it as filler in the current study.

Synthetic nanoclays have very unusual flow properties when dispersed in water (49). These dispersed materials show high viscosity at a low shear rate and vice versa when subjected to continuous shear, thus displaying shear thinning or thixotropy (50, 51). Thixotropy allows injectable hydrogel formulations to be injected using fine needles. The development of injectable hydrogels (35) with tuneable properties, especially systems in which the biomaterial can flow with minimal pressure and where once injected the material can solidify to prevent loss to non-targeted areas, is desirable (15). The combined use of thixotropic (52,

53) and biocytocompatible gels can fulfill these requirements and may introduce a wide range of biomedical and biotechnological applications such as therapeutics, imaging and disease-related diagnostics (1).

In this study I attempted to formulate a unique injectable hydrogel for the purpose of cell delivery by using polyampholyte CPA (Fig. 3-1). This a unique system in which cells can be preserved until before usage and where after thawing, the cells in the hydrogel can be injected easily, without the need to wash out the CPA. Our results suggest that this thixotropic hydrogel can be used as a cell delivery system or have orthopedic applications.

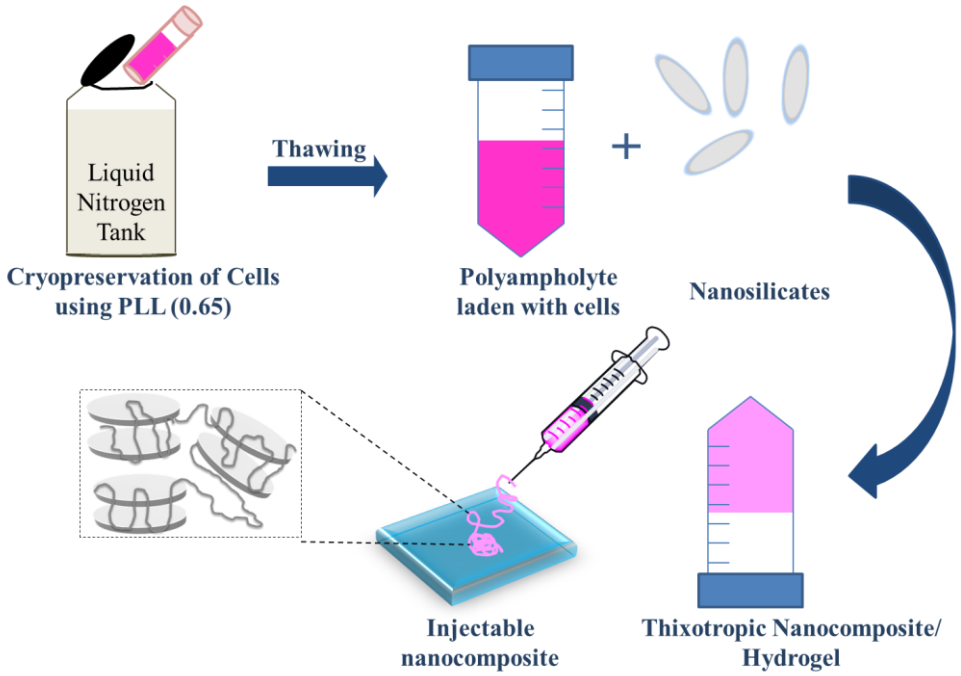

Figure 3-1 Schematic representation of thixotropic nanocomposite formation.

3.2 Nanocomposite synthesis

3.2.1 Polyampholyte preparation

COOH-PLL was prepared as reported previously in the literature (34). To synthesize COOH-PLL, 25% (w/w) ε-poly-L-lysine (PLL) aqueous solution was purchased from JNC Corp., (Tokyo, Japan) and mixed with succinic anhydride (SA) (Wako Pure Chem. Ind. Ltd., Osaka, Japan) at 0%–90% molar ratios (SA/PLL amino groups) and reacted at 50°C for 1 h to convert amino groups into carboxyl groups. Thus, carboxyl groups were introduced into PLL by treatment with SA, which reacts with amino groups as shown in Scheme 1. The ratio of carboxylation

was well controlled by reaction with SA (34). The succination ratio in this study was controlled to approximately 50, 65, and 90 mol%. The amount of amino groups in polyampholytes was determined by 1H-nuclear magnetic resonance (NMR) (Avance III 400, Bruker Biospin Inc., Switzerland) and the 2,4,6-trinitrobenzenesulfonate (TNBS) method (54). The ratio of carboxylation is shown in parentheses, e.g., PLL (0.65) indicates that 65% of the α-amino groups have been converted into carboxyl groups by SA addition.

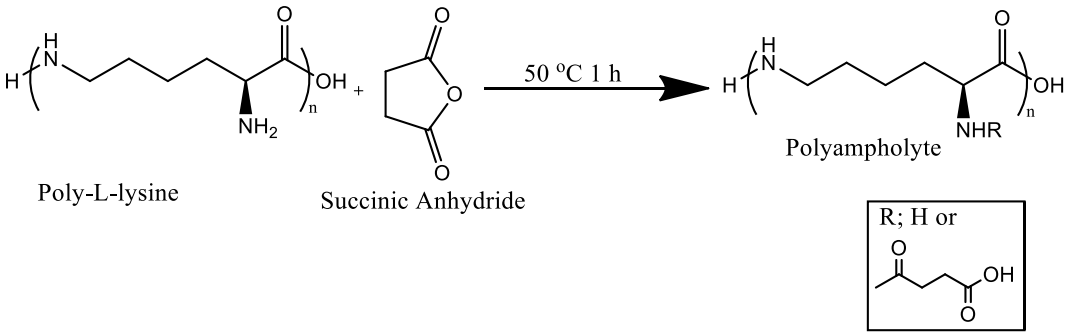

Scheme 1 Schematic representation of succination of PLL.

3.2.2 Zeta potential measurement

Zeta potentials of PLL (0.5), PLL (0.65), and PLL (0.9) were recorded using a Zetasizer 3000 (Malvern instruments, Worcestershire, UK) at various pH values. Solutions were prepared in water and the concentration for the measurement was 0.1%. The pH was adjusted using 1M HCl and NaOH solutions.

3.2.3 Nanocomposite formulation

Stock solutions with varying concentrations of COOH-PLL and laponite (XLG) with a chemical composition of $Na_{+0.7}((Mg_{5.5}Li_{0.3})Si_8O_{20}(OH)_4)_{-0.7}$ (BYK-Chemie GmbH, Wesel, Germany) were prepared in milli-Q water, which was used to retard gelation and allow complete dissolution of laponite particles prior to gelling. Nanocomposites were allowed to settle at room temperature until a clear gel was formed. Nanocomposite compositions were prepared by mixing the COOH-PLL and laponite stock and then stirring this mixture vigorously for 15 minutes to achieve the required polymer concentration and laponite loading. Prior to all analyses, all nanocomposites were allowed to settle for 30 minutes after preparation. Nanocomposites are coded as $N_xP(y)_z$ (where x, y, and z represent

the solid weight percentage of laponite, the succination percentage, and the solid weight percentage of the polymer, respectively).

3.2.4 X-ray diffraction (XRD) measurements

XRD measurements were performed using a Miniflex600 diffractometer (Rigaku, Japan) with Cu Kα radiation of 1.54 Å. Diffraction patterns were collected from 2Θ= 2° to 40° with increments of 0.01˚. All collected data were normalized to the same baseline for comparison of the final results. Samples were dried and stored in a desiccator before each measurement.

3.2.5 ATR-FTIR

The formation of nanocomposites was characterized by attenuated total reflectance Fourier transform infrared (ATR–FTIR). The lyophilized nanocomposite was mounted on ZnSe crystal on the single-reflection ATR accessory (JASCO ATR PRO450-S), and spectra were obtained using a JASCO FT/IR-4200 system.

3.2.6 Rheological analysis

Dynamic mechanical analysis was performed using the Rheosol-G5000 rheometer (UBM Co., Ltd., Kyoto, Japan). Moreover, a cone plate (39.99 mm diameter) with a gap height of 60 μm was used. All analyses were performed at 37°C, and mineral oil was placed around the circumference to prevent evaporation of water from the nanocomposite to minimize the effects of any shear associated with sample loading. All experiments were performed 10 minutes after loading. Frequency sweep experiments between 0.628 and 62.8 $rads^{-1}$ were performed at fixed strain amplitude of 0.967% to measure the storage modulus (G′) and loss modulus (G″). All experiments were performed in triplicate to check the reproducibility of the data.

To evaluate the thixotropy of the nanocomposites, a hysteresis loop experiment was performed by subjecting the hydrogel to a shear rate of 58 s^{-1} for 10 s.

3.2.7 Cryopreservation protocol and determination of cell survival

COOH-PLL cryopreservation solutions were prepared as follows: PLL (0.65) was dissolved in Dulbecco's modified Eagle medium (DMEM) without fetal bovine serum (FBS) at a concentration of 7.5%, 10%, or 20% (w/v) and the pH was

adjusted to 7.4 by HCl or NaOH. Osmotic pressure was adjusted by addition of 10 w% NaCl aqueous solutions to a physiological value of 300 mOsm/kg, determined using an Osmometer 5520 (Wescor, Inc., UT, USA). MC3T3-E1 cells were suspended in 1 mL of COOH-PLL cryopreservation solution at a density of 1×10^6 cells/mL in cryovials and stored in a -80˚C freezer for 24 hours. To evaluate cell viability, individual vials were immersed in a water bath at 37°C, and the thawed cells were diluted 10-fold in DMEM. After centrifugation, the supernatant was removed and the cells were resuspended in 5 mL of medium. All the cells were counted using a hemocytometer, and the trypan blue staining method (55, 56) was used to determine cell viability. The reported values are the ratios of living cells to total cells.

3.2.8 Cell adhesion and viability

Biomedical applicability of the nanocomposites was determined by seeding MC3T3-E1 mouse preosteoblasts on the nanocomposite surface. Cell adhesion was determined by seeding 2.0×10^5 cells on each nanocomposite. At 6 h post seeding, cells were fixed using 3.7% formaldehyde solution and the cell cytoskeleton was labeled with Alexa Flour 488 phalloidin fluorescent dye (Life Technologies, Carlsbad, CA, USA). Fluorescent images were obtained using a Biozero 800 system (Keyence, Osaka, Japan).

To evaluate encapsulated cell viability, MC3T3-E1 cells at a density of 4×10^6/mL of PLL (0.65) (10% w/v) were cryopreserved, and after thawing, the cells in COOH-PLL were mixed with laponite (8% w/v) to form the nanocomposite, $N_6P(65)_5$. This nanocomposite was spread as a thin film on a glass-bottom dish (Matsunami Glass IND., LTD., Osaka, Japan), and after 24 h of culture, cell viability was determined using a live-dead assay kit (Life Technologies Corp., NY, USA).

2.1.9 Statistical analysis

All data are expressed as the mean ± standard deviation (SD). All experiments were conducted in triplicate. A one-way ANOVA with post-hoc Fisher's protected least significant difference test was used for comparison among groups. Differences were considered statistically significant at a $P<0.05$.

3.3. Results and discussion

3.3.1 Preparation of polyampholytes and their cryoprotective properties

ε-PLL is a L-lysine homopolymer biosynthesized by Streptomyces species (57) and is used as a food additive because of its antimicrobial activities, which are ascribed to the cationic charge of its side-chain α-amino groups (58). According to our previous research, cytotoxicity decreases with the introduction of carboxyl groups into PLL. The polymer charge can be tuned by varying the level of succination, thus enabling the control of electrostatic interactions between the drugs and polymer. In the present study, the succination ratio was calculated by ^{1}H NMR (Fig. 3-2, 3-3, 3-4). Zeta potential measurement suggests that the charge on the polymer can be tuned by varying succination levels (Fig. 3-5) and pH. For example, PLL (0.65) was positively charged under acidic pH and it became negatively charged as the pH was increased because of the presence of both carboxyl and amino groups in the polymer.

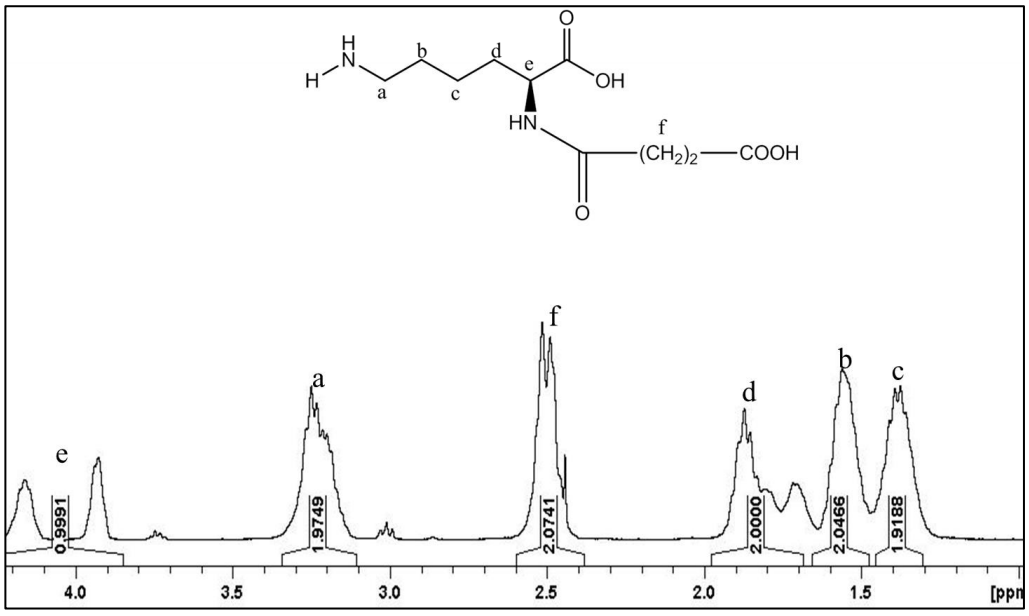

Figure 3-2 ^{1}H NMR of PLL (0.5) Degree of substitution is 50%

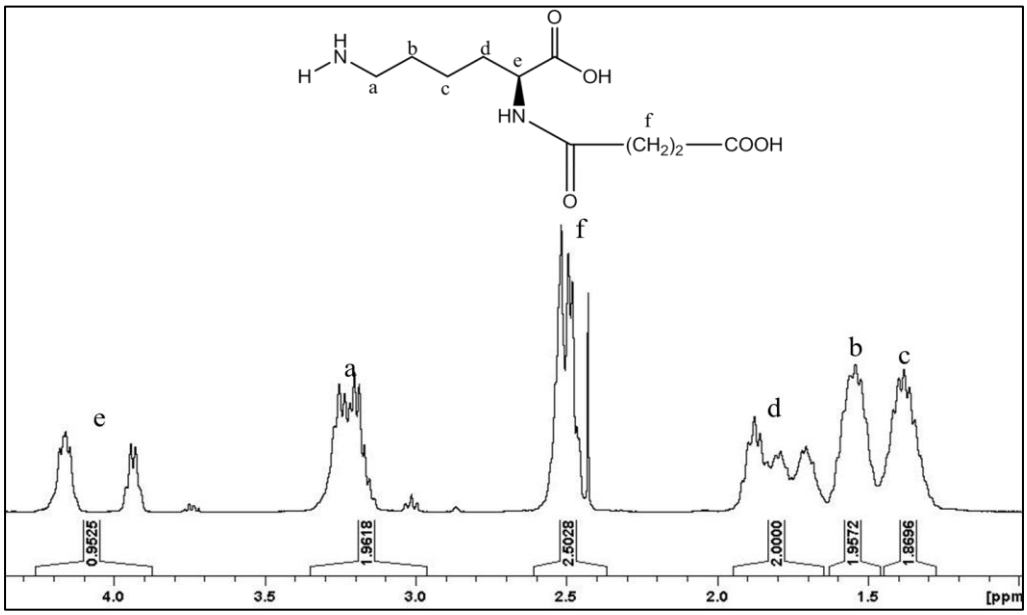

Figure 3-3 ^{1}H NMR of PLL (0.65) Degree of substitution is 63%

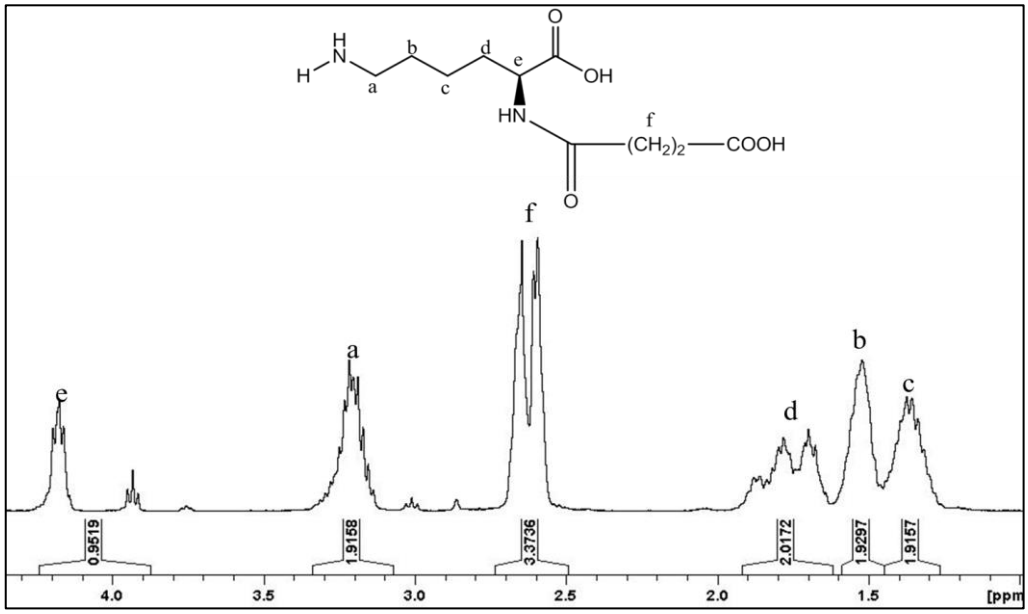

Figure 3-4 ^{1}H NMR of PLL (0.9) Degree of substitution is 85%

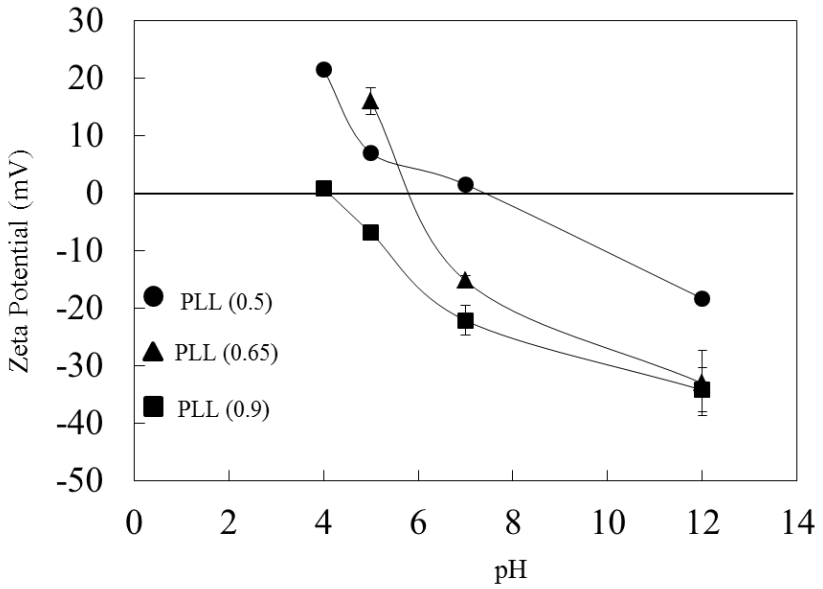

Figure 3-5 Zeta potential measurement of different polyampholyte at different pH

PLL (0.65) is a potent, non-penetrating CPA with low cytotoxicity. COOH-PLL has been shown to exhibit very high cryopreservation efficiency without the addition of any other CPA, and it has been used for the cryopreservation of various cell lines. Fig. 3-6 shows that PLL (0.65) at various concentrations had excellent post-thaw survival efficiency, higher than 90%. The result was in agreement with our previous report (34).

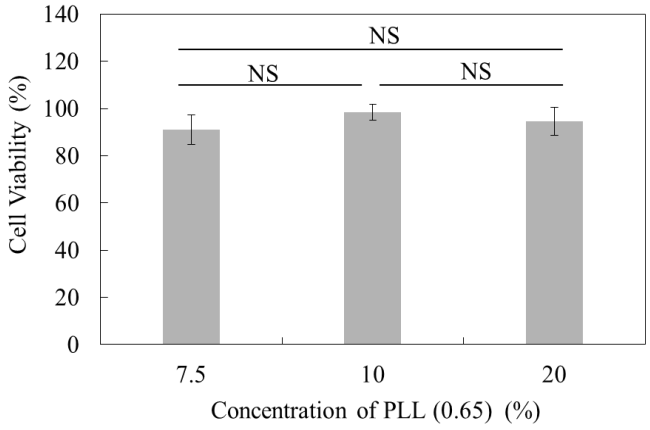

Figure 3-6 Cryoprotective property of PLL (0.65). The viability of MC3T3-E1 cells cryopreserved with various concentration of PLL (0.65) was measured immediately after thawing. The osmotic pressure was adjusted with 10% (w/w) NaCl aqueous solution. NS: not significant

3.3.2 Nanocomposite formulation

Formulation of nanocomposites involves the incorporation of laponite XLG. In the present study, PLL (0.5, 0.65, and 0.9) was used because it is a polyampholyte and its polymer chains were expected to be intercalated between the laponite discs via electrostatic interactions. Various nanocomposites were prepared by varying the polymer and laponite concentration (Table 1). Fig. 3-7 shows the possible structure of the nanocomposite $N_6P(65)_{1.5}$ at pH 7 that was formulated with PLL (0.65).

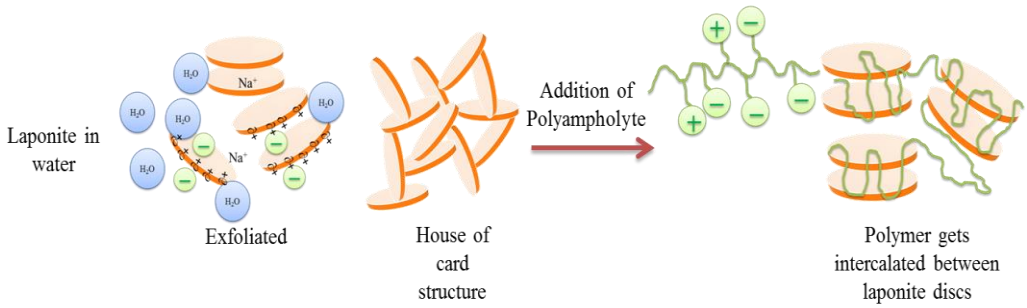

Figure 3-7 Illustration of nanocomposite formed by laponite and PLL (0.65)

Table 1 Various nanocomposites prepared by varying the polymer and laponite concentration

N_X (w/v)%	P_z (w/v)%, P: PLL (0.65)
3	1.5
5	1.5
6	1.5
6	2
6	3
6	5
6	6
6	1.5*
6	1.5**

3.3.3 Characterization of the nanocomposite

a) XRD measurement

X-ray diffraction patterns of dried gels are presented in Fig. 3-8. The X-ray reflections predominantly correspond to the COOH-PLL intercalated clay, suggesting the presence of polymer-clay stacks in the system (15). Intercalation of COOH-PLL chains between the clay platelets was deduced by comparing the d-spacing values from the XRD reflections of the layered pure laponite with d-spacing values from the XRD reflections of the layered nanocomposites. The intercalation peak for all the nanocomposites varied according to the pH and charge on the polymer. The difference in d-spacing (Table 2) between the polymer nanocomposite and pure laponite may be attributed to the presence of COOH-PLL chains between the clay platelets.

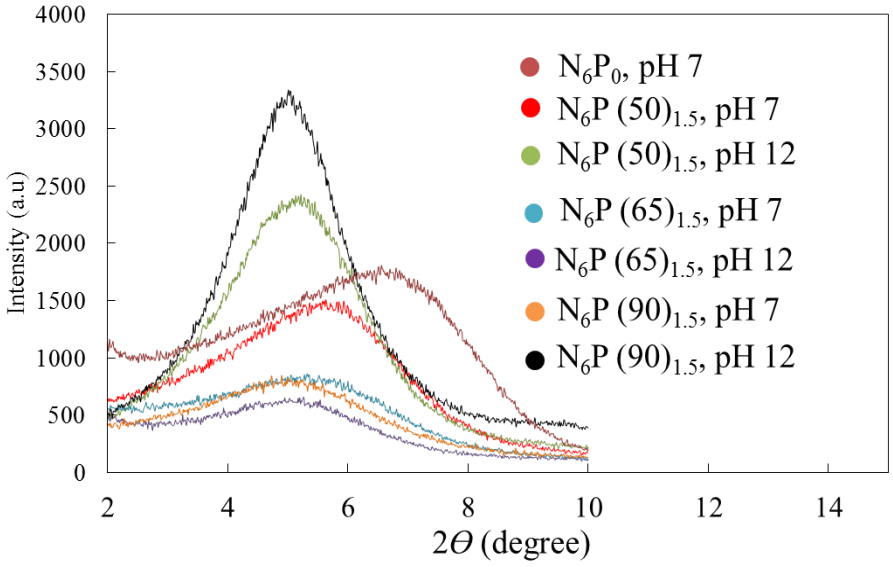

Figure 3-8 XRD patterns of nanocomposite of different polyampholyte with 6% laponite at various pH

Table 2 d-spacing of nanocomposite of different polyampholyte with 6% laponite at various pH

	pH	d (nm)
(Laponite) N_6P_o	7	1.3
$N_6P\ (65)_{1.5}$	7	1.7
	12	1.6
$N_6P\ (50)_{1.5}$	7	1.5
	12	1.7
$N_6P\ (90)_{1.5}$	7	1.9
	12	1.7

b) ATR-FTIR

In the lyophilized nanocomposite, peaks from both the polymer and laponite particles were observed. In Fig. 3-9, peaks around 3262 cm^{-1} (peptide proton mode of NH-CO of β sheet structure), 2944 cm^{-1} (CH_2 stretching), 1642 cm^{-1} (carbonyl of amide I), and 1529 cm^{-1} (NH bending of amide II) (59) indicate the presence of the polymer and those around 1640, 980, and 650 cm^{-1} (12) show the presence of laponite particles. This result verifies the presence of both PLL (0.65) and laponite moieties within the gels.

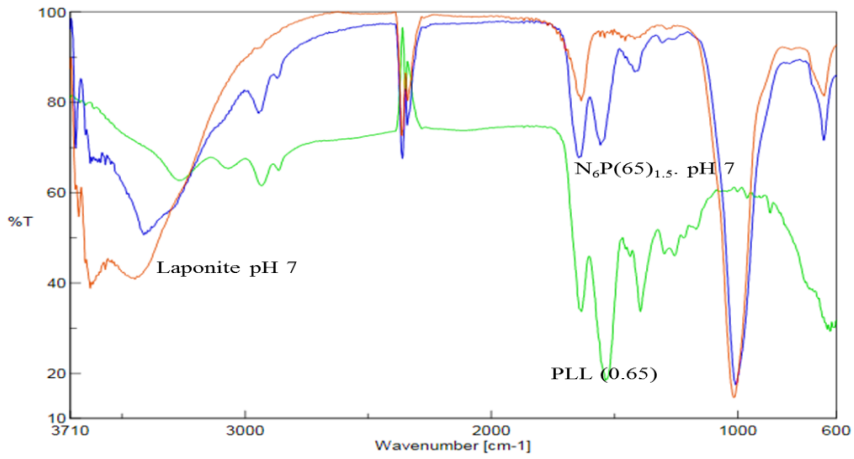

Figure 3-9 ATR-FTIR spectra of laponite; pH 7 (top), lyophilized nanocomposite $N_6P(65)_{1.5}$; pH 7 (middle) and PLL (0.65); pH 7 (bottom)

3.3.4 Dynamic mechanical analysis

Fig. 3-10 illustrates the dynamic mechanical analysis of laponite dispersions without polymer when the pH was varied from basic to neutral to acidic. In this system, the concentration of the laponite was fixed to 6% (w/v %). The results indicate the transition of the system from a strong gel to a very weak gel with pH variation. In salt-free water, laponite particles at a higher concentration are stabilized by repulsive interactions. When the interactions are screened by salt, the particles aggregate because of the formation of electrostatic bonds (45). Laponite dispersions in pure water are always found at pH 10 (60). When the pH of the laponite dispersion is varied, the concentration of ions in the system changes (61, 62). Thus interplay of ions and rim charge with different pH values of the laponite dispersion leads to different G′ and G″ values.

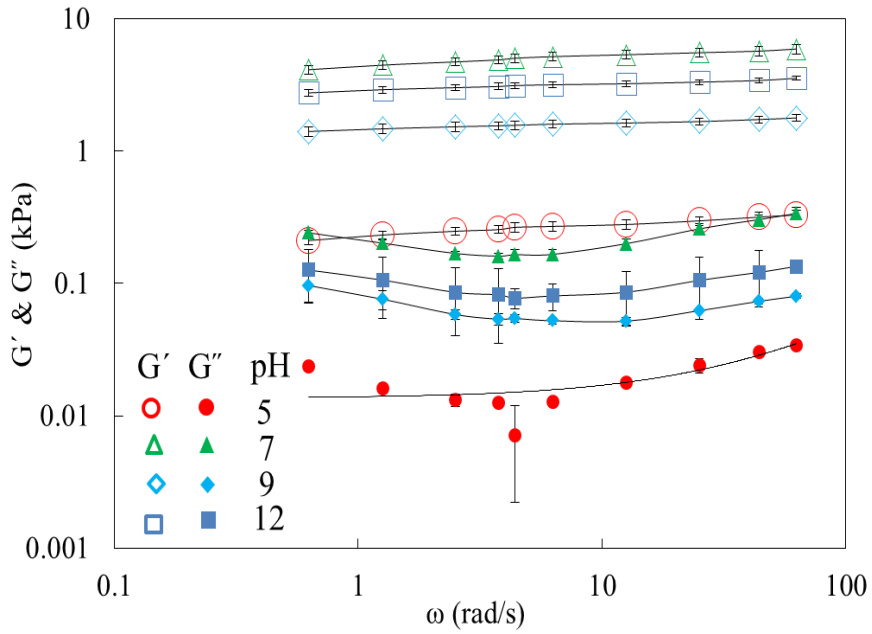

Figure 3-10 Shear and storage moduli of nanocomposites, 37°C laponite 6 wt% pH variation without polymer. Symbols represent the average for n= 3.

Fig. 3-11 depicts the change in mechanical strength of nanocomposite $N_6P(65)_{1.5}$ under various pH conditions. G′ was found to be higher than G″ in the experimental frequency region for all of the hydrogels. The maximum value of G′ was observed at pH 7 and the minimum value was observed for the nanocomposite prepared at acidic pH. The difference in the mechanical strength

of the nanocomposite under varying pH values can be attributed to the presence of COOH-PLL, as zeta potential measurements suggest that PLL (0.65) is negatively charged at pH 7 (Fig. 3-5). Additionally, it is well-known fact that polymers that are long enough to form inter-particle bridges generate a reversible polymer-clay network that dominates the rheological response of the system (46, 63, 64). The PLL (0.65) chain is expected to form bridges between nanosilicate discs, as supported by the XRD data (Fig. 3-8 and Table 2). This cross-linking in the laponite-PLL (0.65) system at pH 7 led to the formation of stronger polymer-clay networks. When the pH of this nanocomposite was increased, laponite and PLL (0.65) both were dominated by a high negative charge as previously indicated in the literature and by the present zeta potential measurements, respectively (36, 44). Under basic conditions it was previously reported that laponite particles are largely dominated by repulsive interactions and that a glassy phase is present. Upon the addition of the non-adsorbing polymer, the laponite glass melts and the formation of the arrested state is delayed (65). In the present study, at pH 12, PLL (0.65), which is highly negatively charged, acted as a non-adsorbing polymer that led to the lower G′ of the nanocomposite as compared to the value at pH 7. Fig. 3-11 shows that the system progressed from a strong gel to a very weak gel state when the pH was reduced. A likely explanation is that when the polymer and laponite are both positively charged, the face-rim bonds are no longer stable and the system undergoes irreversible change from a strong gel to mechanically weaker gel.

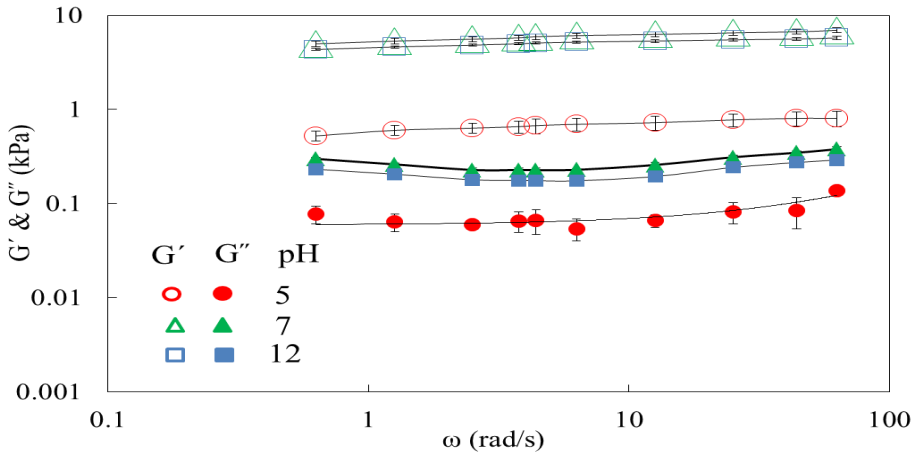

Figure 3-11 Shear and storage moduli of nanocomposites, 37°C $N_6P(65)_{1.5}$ pH variation; P: PLL (0.65). Symbols represent the average for n= 3

The polymer, which I have used in the current study, is a polyampholyte in which charge can be tuned by varying the succination ratio, so two other kinds of polymers were also synthesized, neutral PLL (0.5) and negative charged PLL (0.9). Similar trends were observed (Fig. 3-12 and Fig. 3-13).

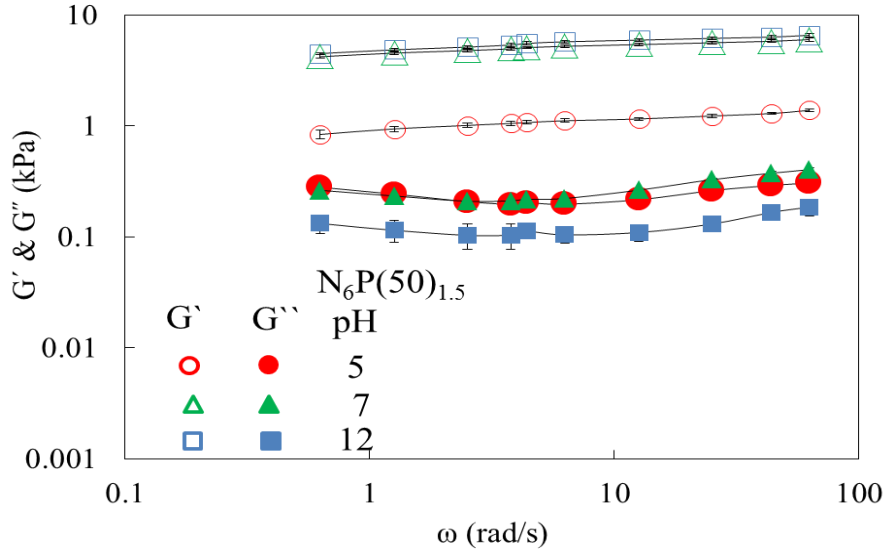

Figure 3-12 Shear and storage moduli of nanocomposite $N_6P(50)_{1.5}$ at various pH, 37°C composed of PLL (0.5). Symbols represent the average for n= 3

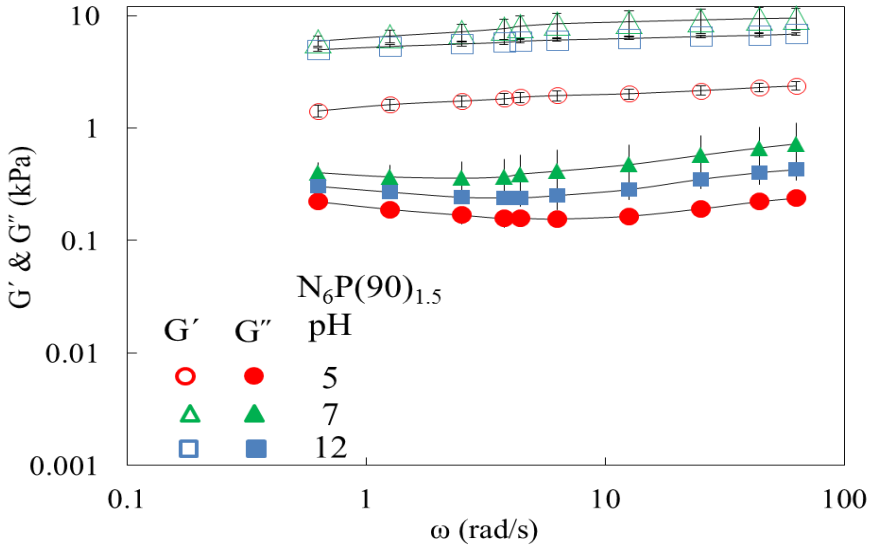

Figure 3-13 Shear and storage moduli of nanocomposite $N_6P(90)_{1.5}$ at various pH, 37°C composed of PLL (0.9). Symbols represent the average for n= 3

Fig. 3-14 illustrates the influence of the manipulation of PLL (0.65) concentration on the G′ and G″ of the nanocomposite for 6% laponite dispersions at pH 7. The mechanical strength increased with polymer concentration, but when the concentration of the polymer was almost the same as that of the laponite, the system changed from a strong gel to mechanically weaker gel, suggesting that as the amount of the polymer increased, the bridging or intercalation between the laponite discs and the polymer also increased, leading to a higher G'. However, when the polymer concentration was too high, then the rheological behavior of the nanocomposite was representative of a very weak gel, possibly because of increased steric hindrance of the adsorbed polymer that leads to unstable face-rim bonds and transformation to a lower mechanical strength (45).

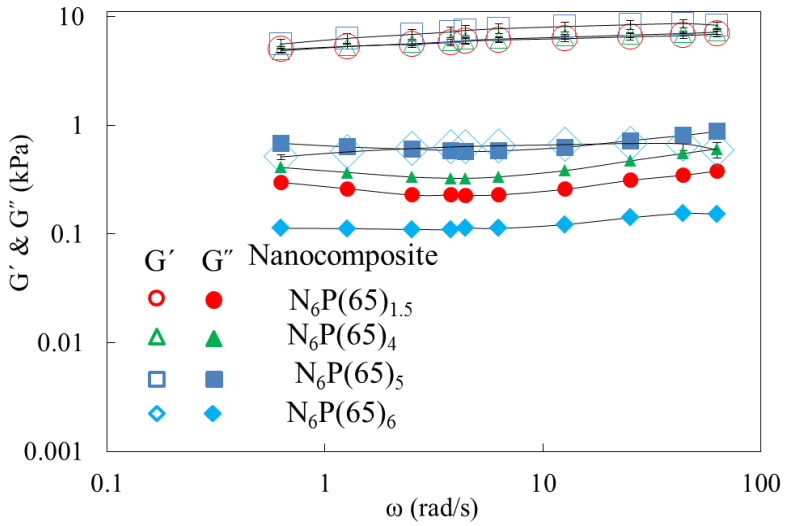

Figure 3-14 Shear and storage moduli of nanocomposites P: PLL (0.65) concentration variation, pH 7. Symbols represent the average for n= 3

Fig. 3-15 shows the effect of manipulating the laponite concentration on G′ and G″ when the PLL (0.65) concentration was fixed to 1.5%. The results indicate that the mechanical strength of the nanocomposite can be tuned by varying the laponite concentration. Mechanically stronger gels were obtained at higher laponite concentrations because of the presence of more Cross-linking points and relatively weaker gels were obtained at lower laponite concentrations because the Cross-linking density was reduced with a decrease in laponite concentration.

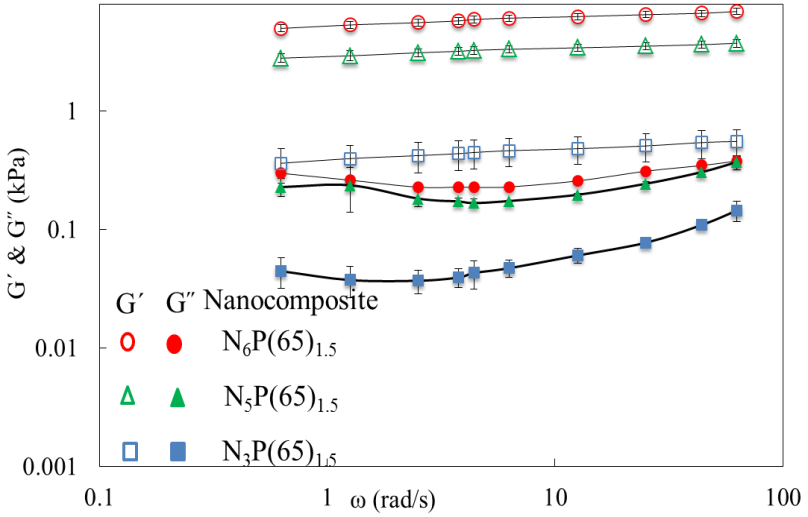

Figure 3-15 Shear and storage moduli of nanocomposites with laponite concentration variation with polymer; P: PLL (0.65), pH 7. Symbols represent the average for n= 3

Fig. 3-16 shows the tunable mechanical properties of the nanocomposite $N_6P_{1.5}$ at pH 7, formulated using PLL with various degrees of succination. This figure shows that the mechanical strength of the nanocomposite can be easily tuned from 4 to 10 kPa by varying the succination ratio in the polymer.

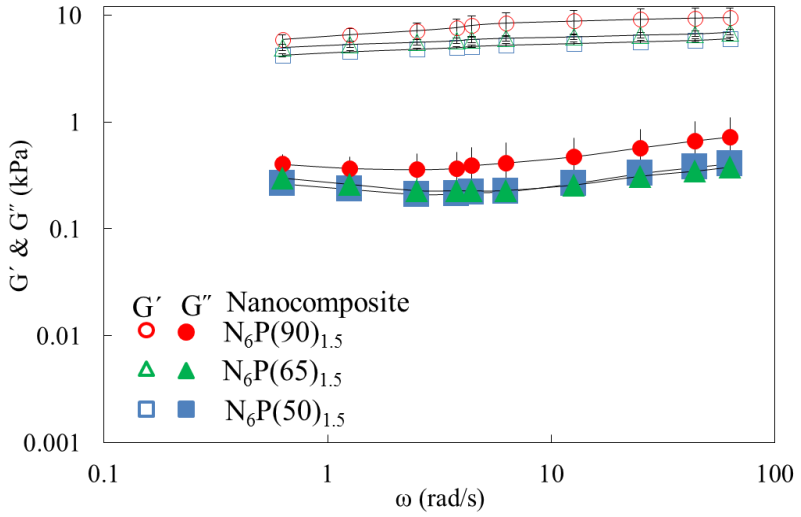

Figure 3-16 Comparison of shear and storage moduli of nanocomposites at pH 7, 37 ˚C composed of different succinated PLL. Symbols represent the average for n= 3

Thixotropic hydrogels are dynamic materials that behave as liquids when subjected to shear stress and then return to the liquid state when the stress is removed. This property is time-dependent, ranging from many minutes in the case of breakdown to many hours in the case of reconstruction (66). Therapeutics can be incorporated in these materials ex vivo, and then they can be injected in vivo by shear-induced flow (13). In my current study, I formulated nanocomposites that were loaded with cells. Structural changes and recovery in these hydrogels were estimated using a hysteresis loop (67). In these experiments, the shear rate was first increased to the maximum, value followed by a decrease to the initial start value. The area within the two curves is defined as the hysteresis loop and indicates the potential speed of the sol-gel transition. A larger area reflects a longer recovery time. The graph of the nanocomposite composed of $N_6P(65)_{1.5}$ at pH 7 shows structural recovery and suggests that the nanocomposite of this study can be return to its original shape after one hour (Fig. 3-17) and thus can be used for various biomedical purposes.

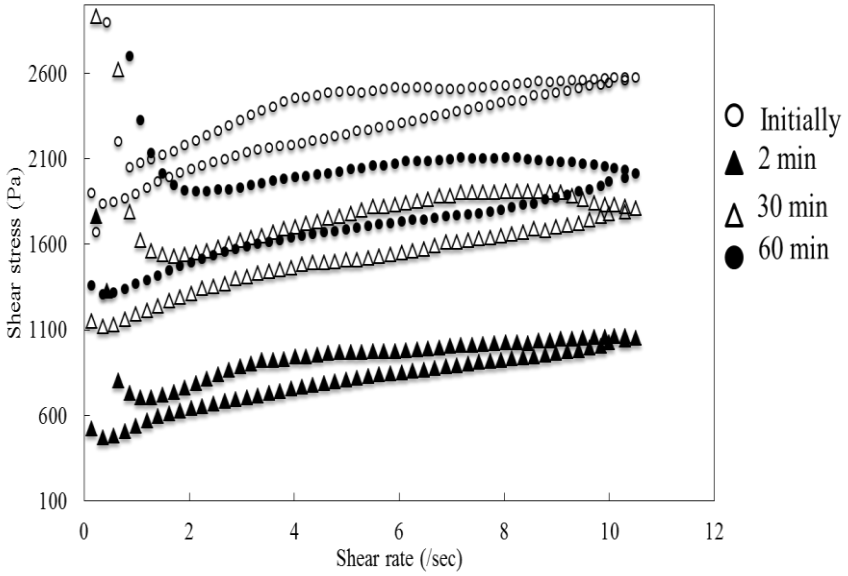

Figure 3-17 Hysteresis data of nanocomposite $N_6P(65)_{1.5}$. It shows the structural recovery of the nanocomposite

Fig. 3-18 (a) shows the behavior of the polymer-clay nanocomposite that we believe occurred during the hysteresis loop experiment. When the nanocomposite was loaded onto the rheometer plate before application of shear, the entire system was at rest. It is expected that the system consisted of a network between

randomly oriented laponite discs and polyampholyte chains that acted as cross-links between laponite discs. When shear was applied, polymer chains were desorbed from the rim and adopted various conformations such as trains and loops, thus imparting flow to the system and converting it from gel to sol. When the shear was removed, the system tried to regain its original structure (15). These materials can be injected through 20-25 gauge needles as shown in Fig. 3-18 (b).

a)

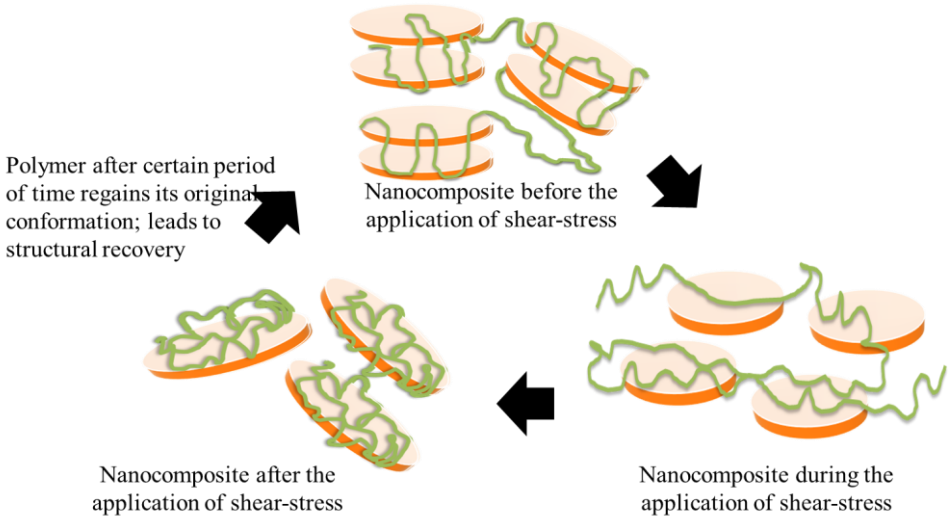

Figure 18 (a) Schematic representation of fate of nanocomposite N6P(65)1.5 during hysteresis loop test

b)

Figure 19 (b) Illustration of nanocomposite $N_6P(65)_{1.5}$ that can be injected through 22G needle

3.3.5 Cell adhesion and viability

Cell adhesion, in addition to tunable physical and chemical properties, is important for biomedical applications. Synthetic hydrogels are hydrophilic and are usually inert towards protein or cell adhesion. Adhesion was previously achieved by tethering of short oligopeptides, such as RGD or whole proteins, to the polymer (68). However, introduction of laponite to the polymer is a simple and efficient approach for achieving cell adhesion (69). Here, MC3T3-E1 cells were seeded onto the nanocomposites. Fig. 3-19 shows that varying the polymer and laponite concentrations can control cell adhesion. Moreover, because of the shape and surface charge of laponite discs, cells can easily internalize them via cadherin-mediated endocytosis (65). Thus, the presence of nanoparticles plays a key role in controlling cell adhesion. When internalization occurs, these nanoparticles upregulate osteoblast-related genes and proteins including osteocalcin and osteopontin, which leads to production of a mineralized extracellular matrix (70). These silicates are complex poly-ions that contain magnesium, which promotes cell adhesion, differentiation, spreading, and migration (71).

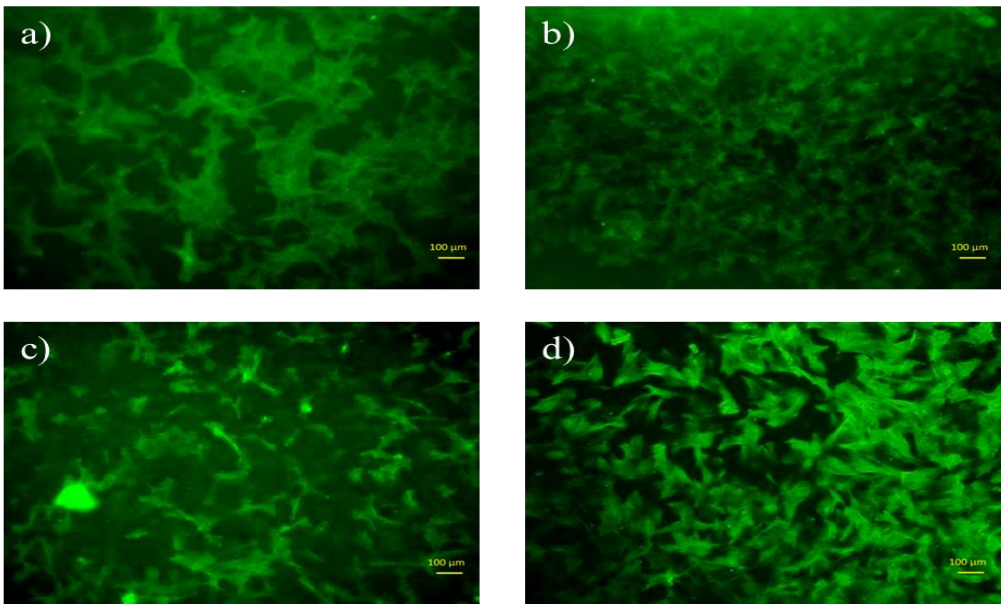

Figure 3-19 In vitro cell growth on PLL (0.65)-Laponite nanocomposite surfaces. MC3T3 E 1 subclone-4 mouse preosteoblast cells readily attach and spread on the nanocomposite surfaces: a) $N_3P(65)_{1.5}$ b) $N_6P(65)_{1.5}$ c) $N_6P(65)_5$ d) Tissue culture plate. Thus addition of laponite (6%) is responsible for the observed behaviour. Scale bars represent 100 µm.

Such nanocomposite properties of $N_6P(65)_{1.5}$ should enable it to be used as an injectable cell carrier. Cryopreserved MC3T3-E1 cells in 10% PLL (0.65) were easily encapsulated by simply mixing the PLL (0.65) after thawing with laponite, with no cell death in the nanocomposites Fig. 3-20. The nanocomposites were cytocompatible and the cells remained viable when cultured in the nanocomposite for 24 hours. The improved cell adhesion and cell viability in the nanocomposites after 24 hours demonstrates that this system can potentially be applied for cell delivery.

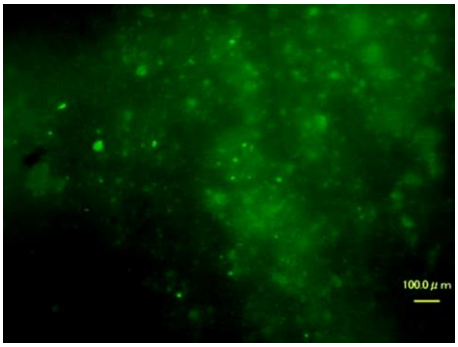

Figure 3-20 Cell viability of MC3T3-E1 cells after 24 hours in the nanocomposite $N_6P(65)_{1.5}$. Almost all cells are live. Scale bars represent 100 µm

In this study I formulated a thixotropic and injectable nanocomposite using a polyampholyte CPA and laponite. No previous study has emphasized the cryopreservation of cells until immediately before usage, where after thawing, they can be injected into the defect site without the need to wash out the CPA. In this study, mouse preosteoblast cells were cryopreserved with COOH-PLL, and after thawing, the CPA-laden cells were mixed with laponite in appropriate amounts to form smart hydrogels that showed thixotropicity, biocytocompatibility and tuneable mechanical properties, although in the present study, the hydrogel did not have a high storage modulus and it is thus applicable for soft materials only. To achieve high mechanical strength, chemical Cross-linking should be introduced in future research. Overall, our current findings suggest that this system can be employed for cell delivery applications.

3.4 Conclusion

Here, I constructed a novel system that has a range of potential biomedical and biotechnological applications. To our knowledge, this is the first study of the interaction between polyampholyte and laponite. The interplay of the charges on the two components of the nanocomposite enables good control over its mechanical properties. The system's switch ability from strong gel to very weak gel with a change in pH may open new avenues for cell delivery applications. This study overcomes the first developmental challenge for smart hydrogels by mixing cells immediately after thawing with laponite, which results in a gel form for the nanocomposite that can easily be injected by applying pressure. This system does not require any pretreatment of cells before injection, making cell maintenance after thawing unnecessary. In the pursuit of an injectable, thixotropic cell scaffold with modifiable mechanical properties, I have engineered a simple and effective nanocomposite that can be tailored to specific functionalities for various tissue-engineering applications.

3.5 References

1. Carrow JK, Gaharwar AK. Macromol. Chem. Phys., 2015, 216, 248-264.
2. Gaharwar AK, Peppas NA, Khademhosseini A. Biotechnol. Bioeng., 2014, 111, 441-453.
3. Thompson RC, Yaszemski MJ, Powers JM, Mikos AG. Biomaterials, 1998, 19, 1935–1943.
4. Zhang R, Ma PX. J. Biomed. Mater. Res., 1999, 44, 446–55.
5. Lu HH, El-Amin SF, Scott KD, Laurencin CT. J. Biomed. Mater. Res., 2003, 64A, 465–474.
6. Kim SS, Ahn KM, Park MS, Lee JH, Choi CY, Kim BS. J. Biomed. Mater. Res., 2007, 80A, 206–215.
7. Hench LL, Splinter RJ, Allen WC, Greenlee TK. J. Biomed. Mater. Res., 1971, 5, 117–141.
8. Hench LL. J. Am. Ceram. Soc., 1998, 81, 1705–1728.
9. Huang W, Day DE, Kittiratanapiboon K, Rahaman MN. J. Mater. Sci. Mater. Med., 2006, 17, 583–96.

10. Khademhosseini A, Langer R, Borenstein J, Vacanti J. Proc. Natl. Acad. Sci. U.S.A., 2006, 103, 2480-2487.
11. Gaharwar AK, Rivera CP, Wu CJ, Schmidt G. Acta Biomater., 2011, 7, 4139-4148.
12. Chang CW, Spreeuwel A, Zhang C, Varghese S. Soft Matter, 2010, 6, 5157–5164.
13. Lu HD, Soranno DE, Rodell CB, Kim IL, Burdick JA. Adv. Healthcare Mater., 2013, 2, 1028-1036.
14. Gaharwar AK, Schexnailder PJ, Kline BP, Schmidt G. Acta Biomater., 2011, 7, 568-577.
15. Stefanescu EA, Stefanescu C, Daly WH, Schmidt G, Negulescu LL. Polymer, 2008, 49, 3785-3794.
16. Haraguchi K, Li HJ, Matsuda K, Takehisa T, Elliott E. Macromolecules, 2005, 38, 3482-3490.
17. Kudaibergenov SE. Advances in Polym. Sci., 1999, 144, 115-197.
18. Bekturova EA, Kudaibergenova SE, Rafikova SR. J. Macromol. Sci., Part C: Polym. Rev., 1990, 30, 233-303.
19. Laschewsky A. Polymers, 2014, 6, 1544-1601.
20. Salamone JC, Rice WC. Polyampholytes. In Encyclopedia of Polymer Science and Technologie, 2nd ed., Wiley-Interscience: New York, NY, USA, 1998, 11, 514-530.
21. Galin JC. Polyzwitterions. In Polymer Materials Encyclopedia, CRC Press: Boca Raton, FL, USA, 1996, 9, 7189-7201.
22. Lowe AB, McCormick CL. Chem. Rev., 2002, 102, 4177–4189.
23. Kudaibergenov S, Jaeger W, Laschewsky A. Adv. Polym. Sci., 2006, 201, 157–224.
24. Rajan R, Jain M, Matsumura K. J. Biomater. Sci. Polym. Ed., 2013, 24, 1767-1780.
25. Rajan R, Matsumura K. Cryobiol. Cryotechnol., 2014, 60, 99-103.
26. Rajan R, Matsumura K. J. Mater. Chem. B, 2015, 3, 5683-5689.
27. Watanabe H, Kohaya N, Kamoshita M, Fujikawa K, Matsumura K, Hyon SH, Ito J, Kashiwazaki N. PLoS One, 2013, 8, e83613.

28. Maehara M, Sato M, Watanabe M, Matsunari H, Kokubo M, Kanai T, Sato M, Matsumura K, Hyon SH, Yokoyama M, Mochida J, Nagashima T. BMC Biotechnology, 2013, 13, 58.
29. Jin OS, Lee LH, Shin YC, Lee EJ, Lee JJ, Matsumura K, Hyon SH, Han DW. Cryo let., 2013, 34, 396-403.
30. Matsumura K, Hayashi F, Nagashima T, Hyon SH. J. Biomater. Sci. Polym. Ed., 2013, 24, 1484-1497.
31. Matsumura K, Bae JY, Kim HH, Hyon SH. Cryobiology, 2011, 63, 76-83.
32. Matsumura K, Bae JY, Hyon SH. Low Temperature Medicine 36 (2010) 65-68.
33. Matsumura K, Bae JY, Hyon SH. Cell Transplant., 2010, 19, 691-699.
34. Matsumura K, Hyon SH. Biomaterials, 2009, 30, 4842-4849.
35. Jain M, Rajan R, Hyon SH, Matsumura K. Biomater. Sci., 2014, 2, 308-317.
36. Jonsson B, Labbez C, Cabane B. Langmuir, 2008, 24, 11406-11413.
37. Mihaila SM, Gaharwar AK, Reis RL, Khademhosseini A, Marques AP, Gomes ME. Biomaterials, 2014, 35, 9087-9099.
38. Wang S, Wu Y, Guo R, Huang Y, Wen S, Shen M, Wang J, Shi X. Langmuir, 2013, 29, 5030-5036.
39. Xavier JR, Thakur T, Desai P, Jaiswal MK, Sears N, Hernandez EC, Kaunas R, Gaharwar AK. ACS Nano, 2015, 9, 3109–3118.
40. Baghdadi HA, Sardinha H, Bhatia SR. J. Polym. Sci. Pol. Phys., 2005, 43, 233-240.
41. Kroon M, Vos WL, Wegdam GH. Phys. Rev. E, 1998, 57, 1962-1970.
42. Morvan M, Espinat D, Lambard J, Zemb Th. Colloids Surf. A, 1994, 82, 193-203.
43. Laporte Industries Ltd., Laponite Technical Bulletin L104/90/A, 1990, p. 1
44. Tawari SL, Koch DL, Cohen C. J. colloid Interface Sci., 2001, 240, 54-66.
45. Martin C, Pignon F, Piau JM, Magnin A, Lindner P, Cabane B. Phys. Rev. E, 2002, 66, 021401.
46. Mongondry P, Nicolai T, Tassin JF. J. Colloid Interface Sci., 2004, 275, 191-196.
47. Labanda J, Sabat´e J, Llorens J. Colloids Surf. A, 2007, 301, 8–15.
48. Shen M, Li L, Sun Y, Xu J, Guo X, Prud'homme RK. Langmuir, 2014, 30, 1636−1642.
49. Ruzicka B, Zaccarelli E. Soft matter, 2011, 7, 1268-1286.
50. Pignon F, Magnin A, Piau JM. J. Rheol., 1996, 40, 573-587.

51. Martin C, Pignon F, Magnin A, Piau JM, Lindner P, Cabane B. Phys. Rev. E Stat. Nonlin. Soft Matter Phys., 2002, 66, 021401.
52. Nanda J, Biswas A, Banarjee A. Soft matter, 2013, 9, 4198-4208.
53. Barbucci R, Pasqui D, Favaloro R, Panariello G. Carbohydr. Res., 2008, 343, 3058-3065.
54. Haneeb AF. Anal. Biochem., 1996, 14, 328–36.
55. Ehrlich P. Br. Med. J., 1913, 2, 353–359.
56. Prull CR. Med. Hist, 47 (2003) 332-356.
57. Yamanaka Y, Maruyama C, Takagi H, Hamano Y. Nat. Chem. Biol., 2008, 4, 766–772.
58. Saimura M, Takehara M, Mizukami S, Kataoka K, Hirohara H. Biotechnol. Lett., 2008, 30, 377–85.
59. Rozenberg M, Shoham G. Biophys. Chem., 2007, 125, 166-171.
60. Cummins HZ. J. Non-Cryst. Solids, 2007, 353, 3891-3905.
61. Nicolai T, Cocard S. Eur. Phys. J. E, 2005, 5, 221-227.
62. Nicolai T, Cocard S. J. Colloid Interf. Sci., 2001, 244, 51-57.
63. Lal J, Auvray L. J. Appl. Crys., 2000, 33, 673-676.
64. Lal J, Auvray L. Mol. Cryst. Liq. Cryst., 2001, 356, 503-515.
65. Eckert T, Bratsch R. Phys. Rev. Lett., 2002, 89, 125701.
66. Barnes HA. J. Non-Newtonian Fluid Mech., 1997, 70, 1-33.
67. Ker RF. J. Exp. Biol., 1996, 199, 1501-1508.
68. M. Obara, M.S. Kang, K.M. Yamada, Cell, 1988, 53, 649-657.
69. Schexnailder P, Gaharwar AK, Bartlett R, Seal BL, Schmidt G. Tuning Macromol. Biosci., 2010, 10, 1416-1423.
70. Gaharwar AK, Mihaila SM, Swami A, Patel A, Sant S, Reis RL, Marques AP, Gomes ME, Khademhosseini A. Adv. Mater., 2013, 25, 3329-3336.
71. Mihaila SM, A.K. Gaharwar AK, Reis RL, Khademhosseini A, AP, Gomes ME. Biomaterials, 2014, 35, 9087-9099.

Chapter 4

Polyampholyte- and nanosilicate-based soft bio-nanocomposites with tailorable mechanical and cell adhesion properties

4.1 Introduction

One of the goals of tissue engineering is to develop methodologies that pave the way for the regeneration of living, healthy, functional tissues that can be utilized as tissue grafts or for organ replacement (1). The most common approach is to utilize three-dimensional (3D) scaffolds that can act as temporary support for cell growth and new tissue development. Designing such scaffolds can be carried out such that the scaffolds can serve as structural support by providing passive cues to the cells. Alternatively, certain biological cues can be introduced into the scaffolds to guide cell and tissue growth.

Hydrogels are attractive biomaterials and have been the focus of attention for many years. They are used in a wide range of biological applications owing to their biocompatibility and moisture-holding capacity, which mimics the natural water content of human tissue (2, 3). Hydrogels are hydrophilic polymer networks (4, 5) with a 3D configuration, making them promising candidates for implantable biomaterials applications. Injectable hydrogels can be implanted into various target sites in patients in a minimally invasive manner (6) with little prior knowledge of the defect site geometry. Thus, hydrogels are attractive biomaterials for clinical applications (7). Importantly, hydrogels may also represent effective and efficient treatment options for patients. For application of hydrogels, liquid hydrogel precursors are injected at the target site and can be crosslinked to solids by shifting the pH, temperature, and salt concentrations or by introduction of chemicals, enzymes, and photo-initiated free radicals (8-11). Successful delivery of therapeutics is highly dependent on gelation kinetics; slow gelation may lead to excessive cargo loss from the target site, whereas rapid gelation may result in premature polymerisation and delivery failure (12). Degradable hydrogels are desirable as tissue engineering scaffolds in a variety of applications (13). For

example, in cell-based therapies and protein delivery, hydrogel degradation can be used to control the release rate of the delivered components and allows for clearance of the device from the body when it is no longer needed (14). The design of such materials can be achieved by successful incorporation of biodegradable cross-linkers that facilitate controlled degradation (15-17). Despite these advantages, application of hydrogels as an ideal scaffold is limited due to their bio-inertness and poor mechanical properties. Moreover, owing to their inherently weak mechanical properties, application of hydrogels as functional substitutes for hard tissues and long-term drug delivery remains challenging (18, 19). In order to overcome these limitations, researchers have attempted to develop materials in which additional nanomaterials are integrated into the architecture, yielding combinatorial benefits such as bioactivity, adhesiveness, and mechanical improvement (20, 21).

Different strategies have been employed to create mechanically robust hydrogels. One such method involves the utilization of nanoclays as cross-linkers, leading to the formation of nanocomposites with enhanced mechanical properties (22, 23). Synthetic silicates are a novel class of nanomaterials with a high degree of anisotropy and functionality; these materials interact with biological entities in a manner that is entirely different from their respective 3D micro and macro counterparts because of their high surface to volume ratio (24, 25). Synthetic silicates strongly interact with polymeric networks, resulting in the formation of physically cross-linked networks and significantly increased mechanical stiffness (20, 21, 23). The exfoliated hydrogels containing silicate and polymer result in the formation of highly organized structures. Incorporation of the silicate nanoparticles within a polymer network yields strong bioactive characteristics, facilitating their potential use in a variety of musculoskeletal tissue engineering applications (26-28).

One of the most widely used hydrogels is based on polyethylene glycol (PEG). PEG hydrogels have been used for the development of scaffolds (14, 29, 30) and for drug delivery purposes (31-33). PEG by itself is not reactive, and use of PEG in hydrogels requires end group functionalization with Cross-linking groups (14). Various strategies have been employed to facilitate degradation in PEG-based hydrogels. In this work, i used 4-arm PEG with N-hydroxy succinimide ester (PEG-

NHS) to yield a fully hydrophilic hydrogel with rapid and highly specific Cross-linking chemistry. The polymer used herein (carboxylated poly-L-lysine [COOH-PLL]), forms degradable crosslinks with PEG-NHS and is a polyampholyte (34). Many reports have described the unique properties of polyampholytes, including their antibiofouling properties, suppression of protein aggregation, and cryoprotective properties (6, 35-44). The benefit of this polymer is that the charge can easily be varied, and thus, the electrostatic interaction between the drug and polymer can also be tuned, which is useful for drug delivery applications. The approach that I have developed herein rendered the scaffold degradable via hydrolysis without requiring the presence of specific biological compounds for degradation. Incorporation of synthetic silicate in this system provided scaffolds with good tunable mechanical properties, cell adhesiveness, and tailorable degradation times. This bio-inspired material, formulated to allow control of mechanical and degradation properties, could provide new directions for tissue engineering research and the application of polymeric hydrogels.

4.2 Hydrogel and nanocomposite synthesis

4.2.1 Materials

ε-Poly-L-lysine (PLL) aqueous solution was purchased from JNC Corp. (Tokyo, Japan), and succinic anhydride (SA) was purchased from Wako Pure Chemical Industries Ltd. (Osaka Japan). Four-arm PEG-NHS (ester linkage type [PTE 100 CS] and ether linkage type [PTE 100HS]; molecular weight [Mw] 10,000 Da) were purchased from NOF corporation (Tokyo, Japan). Laponite (XLG), which had a chemical composition of $Na_{+0.7}[(Mg_{5.5}Li_{0.3})Si_8O_{20}(OH)_4]_{-0.7}$, was obtained from BYK-Chemie GmbH, (Wesel, Germany) and used as received.

4.2.2 Polyampholyte synthesis

Carboxylated PLL (COOH-PLL) was prepared as previously described (34). To synthesize COOH-PLL, a 25% (w/w) PLL aqueous solution and SA at 65% mol ratio (SA/PLL amino groups) were mixed and reacted at 50˚C for 1 h to convert amino groups into carboxyl groups (Scheme 1). The amount of amino groups of polyampholytes was determined by the 2,4,6-trinitrobenzenesulfonate (TNBS)

method (45). In this study, I synthesized COOH-PLL with 65 mol% carboxyl groups and 35 mol% amino groups in one molecule because of the low cytotoxicity of this formulation owing to its negative zeta potential under neutral conditions (34). The ratio of carboxylation shown in parentheses, e.g., PLL (0.65), indicated that the given percentage of α-amino groups was converted into carboxyl groups by SA addition. In this study, I utilized amino groups for Cross-linking.

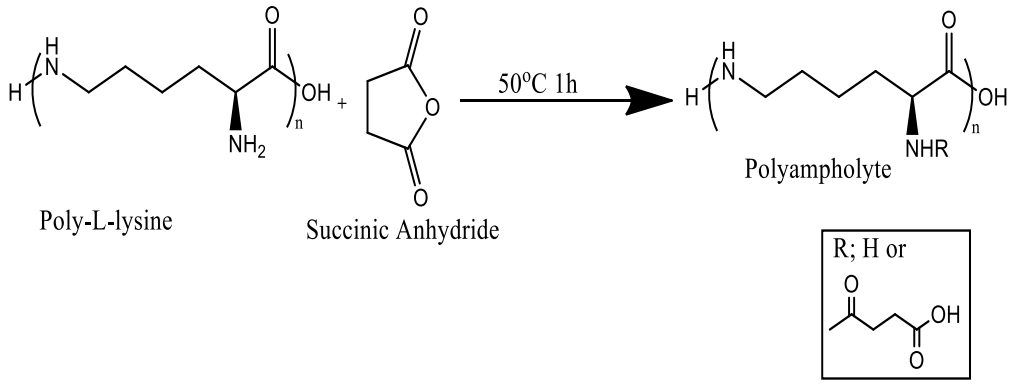

Scheme 1 Schematic representation of succination of PLL

4.2.3 Preparation of PEG-based hydrogel

Hydrogels were prepared by amide bond formation using degradable 4-arm PEG-ester-NHS (PDN) or non-degradable 4-arm PEG-ether-NHS (PMN) cross-linked onto PLL (0.65) and dissolved in Milli-Q water (Scheme 2). For the preparation of different hydrogels, the desired amounts of the cross-linker and polymer were dissolved in Milli-Q water. The hydrogel began to form after addition of the cross-linker 4-arm-PEG-NHS and PLL (0.65), with the success of hydrogel formation being dependent on the concentrations of the two reactants. Hydrogel formation was evaluated using the test tube-tilting method, where a test tube containing the gel was inverted, and by dynamic mechanical analysis.

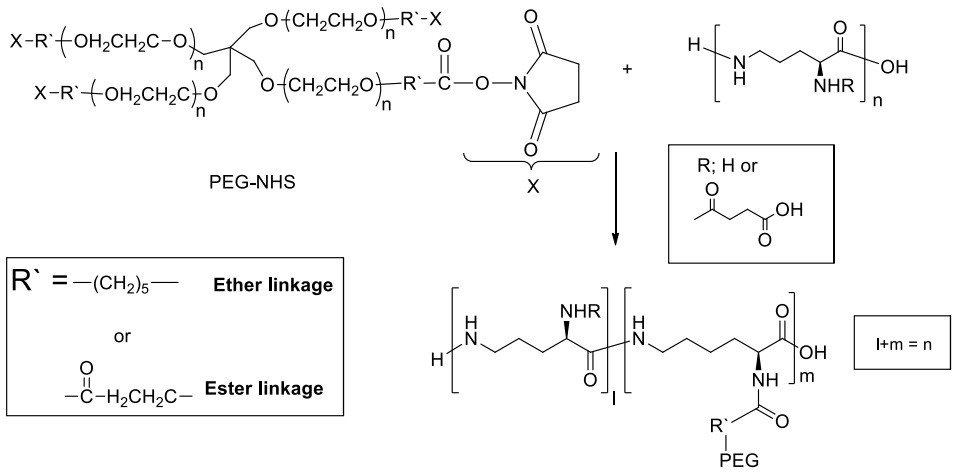

Scheme 2 Schematic representation of hydrogel preparation using PLL (0.65) and PEG-NHS

4.2.4 Nanocomposite formation

Nanocomposite hydrogels were fabricated with various concentrations of laponite XLG dissolved in Milli-Q water. Vigorous agitation was necessary to prevent clumping of the nanoclays. The desired amount of the cross-linker was then added. In this solution of laponite and PEG-NHS, the requisite amount of the polymer solution was added, and the resulting nanocomposite was termed $N_xC_yP_z$ (where x represents the solid weight percent of laponite, y is the solid weight percent of the cross-linker, and z represents the solid weight percent of the polymer). Initially, the laponite and PEG-NHS solution was a viscous liquid. However, once the polymer solution was added, the solution gelled within a few minutes.

4.2.5 Swelling and degradation studies

The hydrogel materials were swollen in aqueous phosphate buffered saline (PBS; pH 7.4) at 37°C. Two different cross-linkers (i.e., PDN and PMN) were used in this study. PDN was used at concentrations of 2, 4, 6, and 8 weight%, and PMN was used at a concentration of 4 weight%. Various hydrogels were cast using silicon moulds measuring 1 cm in diameter and were then allowed to air dry for 48 h before swelling studies were performed. Hydrogels were weighed (W_o) immediately after drying. Once dried, materials were placed in 3mL PBS at 37°C

and allowed to swell for 24 h. Readings were taken at regular intervals by removing the hydrogels from the immersion medium and weighing (Wt) after wiping away excess medium carefully. The swelling ratio was calculated using the following equation:

Degree of swelling (%) = $(W_t - W_o) / Wo \times 100$

After 24 h of swelling, the samples were monitored for degradation. For degradation studies, samples were removed at various times. Hydrogels were dried in an oven for 24 h and then weighed (W_{dt}). The remaining weight of the hydrogels was calculated using the following equation:

Remaining weight = W_{dt} / W_o

Fresh PBS, pre-equilibrated at 37°C, was replaced every 24 h at the time of measurement.

4.2.6 Rheology study

Dynamic mechanical analysis was carried out using a Rheosol-G5000 rheometer (UBM Co., Ltd., Kyoto, Japan). A cone plate with a diameter of 24.99 mm and a gap height of 50 μm was used. The frequency dependence of oscillatory shear modulus (e.g., G′ and G″) was evaluated. All analyses were carried out at 37°C, and mineral oil was placed around the circumference to prevent the evaporation of water from the nanocomposite for all tests. Nanocomposites were loaded immediately after mixing and were then left for 30 min on the rheometer plate before readings were collected.

4.2.7 Cell studies

To evaluate whether the hydrogels and nanocomposites allowed cell adhesion, MC3T3-E1 mouse pre-osteoblasts were seeded on hydrogels and nanocomposites. Briefly, cells were cultured in Dulbecco's modified Eagle medium (DMEM) supplemented with 10% foetal bovine serum (FBS). The cell culture was carried out at 37°C under 5% CO_2 in a humidified atmosphere. When the cells reached

80% confluence, they were detached from the plate using 0.25% (w/v) trypsin containing 0.02% (w/v) ethylenediaminetetraacetic acid in PBS without calcium and magnesium [PBS (−)]. Cells were then seeded on hydrogels and nanocomposite at a density of 5×10^4 cells/mL/sample. Cells were fixed at 6 h after seeding using 3.7% formaldehyde solution, and the cytoskeleton was labelled with Alexa Fluor 488 phalloidin fluorescent dye (Life Technologies, Carlsbad, CA, USA). Fluorescent images were acquired using a fluorescent microscope (Biozero 800; Keyence, Osaka, Japan). Representative images are shown.

4.3 Results and discussion

4.3.1 Preparation of the polyampholyte

ε-PLL is an L-lysine homopolymer biosynthesized by Streptomyces species. This compound is used as a food additive owing to its antimicrobial activities conferred by the cationic charge density of its side chain α-amino groups. According to our previous research, cytotoxicity decreases following introduction of carboxyl groups onto PLL. Therefore, carboxyl groups were introduced onto PLL by treatment with SA, which reacts with the amino groups as shown in Scheme 1. The ratio of carboxylation was well controlled by the reaction with SA. In this polymer, charge can be tuned by varying succination, allowing electrostatic interactions between the drug and polymer to be controlled. The introduction ratio in this study was controlled at around 65 mol%.

4.3.2 Hydrogel and nanocomposite preparation

Hydrogels prepared without the use of toxic cross-linkers have potential applications in tissue engineering. For example, they can be used in controlled drug delivery systems and 3D cell culture. Nanocomposites derived from laponite may provide insights into the formulation of bio-inspired materials.

Therefore, in this study, 4-arm PEG-NHS was crosslinked with PLL (0.65) at various concentrations. The time of gelation was determined by dynamic

mechanical analysis, as shown in Fig. 4-1. The gelation point could be estimated by the crossover point of G′ and G″. These data showed that gelation time decreased with the increase in cross-linker concentration, as summarised in Table 1. I fixed the polymer concentration at 4 w/v% throughout this study. Hydrogels formed by reacting 4-arm PEG-NHS and PLL (0.65) via amide bond formation (Scheme 2). This type of Cross-linking did not require any harmful radiation or toxic cross-linkers.

Formulation of nanocomposites involves the incorporation of laponite XLG. Several previous studies have described the interactions between PEG and laponite (46, 47). In the present study, I used PLL (0.65), a polyampholyte that was expected to be intercalated between the laponite discs. In this system, electrostatic and covalent interactions are present. Thus, I prepared various nanocomposites by changing the cross-linker and laponite concentrations (Table 2).

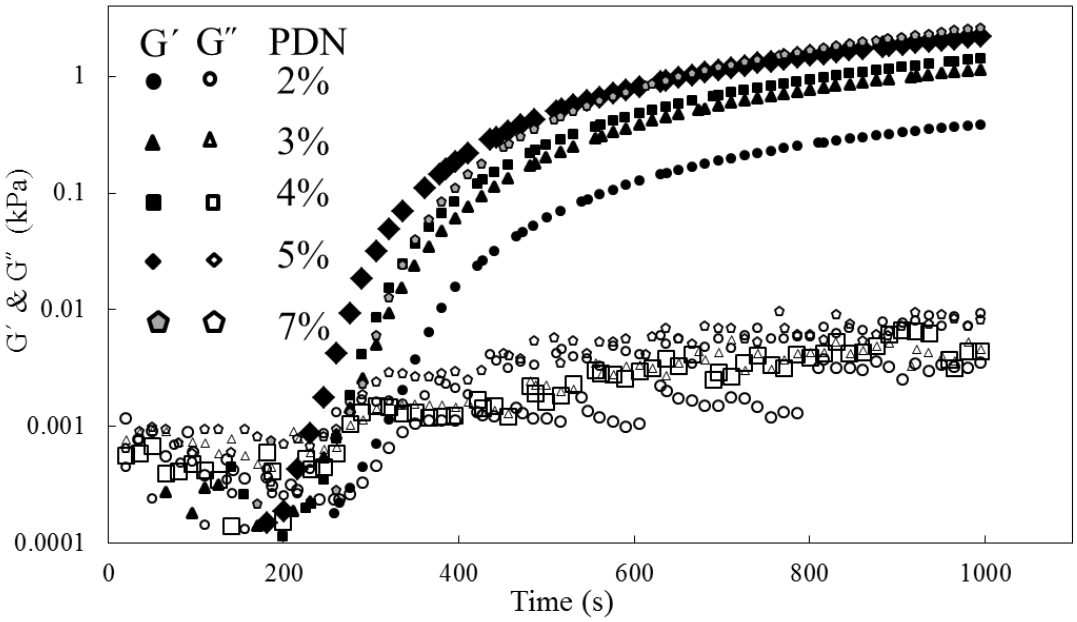

Figure 4-1 Shear and storage moduli for various hydrogels with varying cross-linker concentration (P: PLL (0.65) 7%).

Table 1 Different hydrogels were prepared using PLL (0.65) and PDN as cross-linker by varying concentration.

Polymer concentration (w/v)%	**Cross-linker concentration (w/v)%**	**Hydrogel formation**
7	4	Yes
7	3	Yes
7	2	Yes
7	1.5	No
4	8	Yes
4	6	Yes
4	4	Yes
4	2	Yes
4	1.5	No

Table 2 Various nanocomposites prepared by varying the cross-linker PDN and laponite concentration with PLL (0.65) 4%

N_X (w/v)%	**C_y (w/v)%**	**P_z (w/v)%**
1.5	2, 4, 8	4
3	2, 4, 8	4
6	2, 4, 8	4

4.3.3 Swelling and degradation study

The water absorbency and swelling behaviors of the dried hydrogels are shown in Fig. 4-2. The equilibrium swelling degree of the hydrogels decreased with increasing cross-linker concentrations. The increase in swelling could be attributed to the initial uptake of water molecule into the degrading matrix from

the surrounding buffer. The swelling ratio of the P4%:PDM8% hydrogel was higher than that of the P4%:PDN4%:PMN4% hydrogel. Thus, it is likely that the carboxyl oxygen of the ester is a strong H-bond acceptor, which may increase the water content in the hydrogel and result in higher swelling ratios (14). Higher Cross-linking density produced more Cross-linking points in the hydrogels, leading to reduced space for water in the matrix of the hydrogel and lower swelling rates when the hydrogel was brought into contact with the solvent.

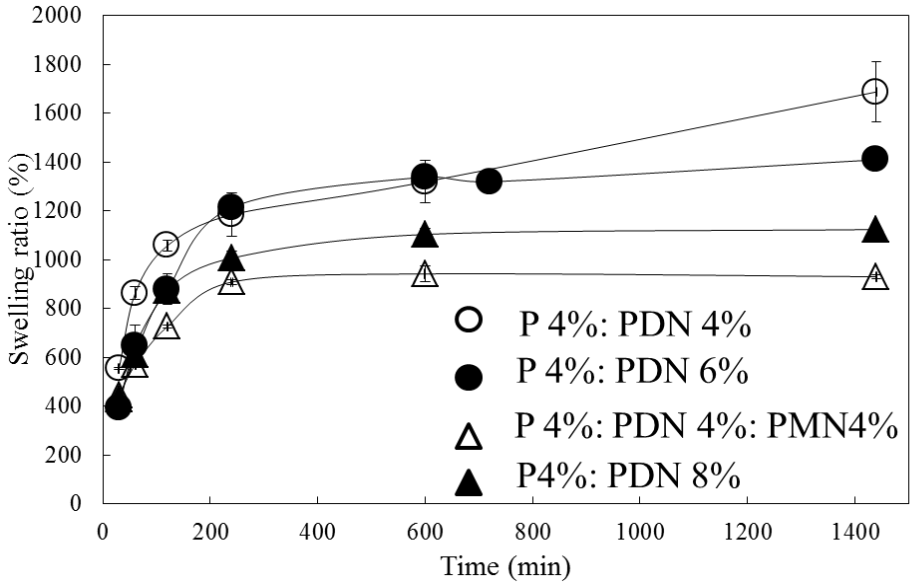

Figure 4-2 Swelling measurements of hydrogels: Swelling ratio is monitored as a function of varying cross-linker concentration. Symbols represent the average for n=3 samples.

In this study, I found that the degradation profile could be controlled by the concentration of the PDN cross-linker (ester-linkage type), as shown in Fig. 4-3. The ester represents a major cleavage site when the PDN cross-linker is used. Moreover, this ester linkage is acid labile and undergoes hydrolysis when exposed to water (48). In the presence of water, PDN chains are subjected to random scission at the ester bonds, and each ester bond has the same probability of being broken via hydrolysis. As the hydrogel degrades, water content increases, which further promotes the rate of hydrolysis. When the same cross-linker is used at different concentrations, the rate of hydrolysis should depend on the number of hydrolysable groups. The PDN cross-linker has one ester bond at the end of the chain separated by a long PEG chain. If the cross-linker concentration is low, then

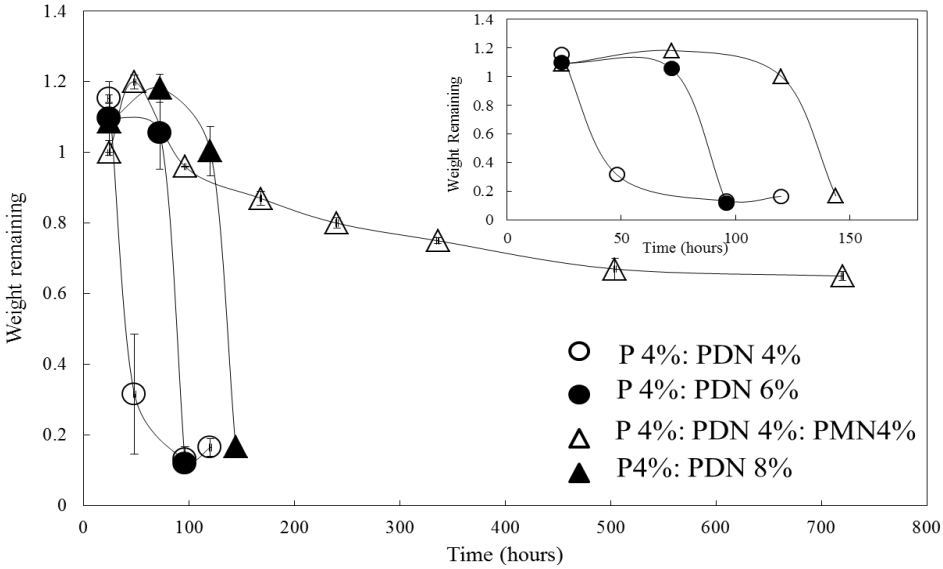

Figure 4-3 Degradation measurements of hydrogels: Degradation is monitored as a function of varying cross-linker concentration. Symbols represent the average for n=3 samples

the crosslink density will also be low; this would correspond to a lower concentration of ester bonds. Since fewer ester bonds are present in hydrogels prepared with lower concentrations of the cross-linker, these hydrogels will degrade faster in comparison to the hydrogels synthesized with higher cross-linker concentrations. By incorporation of the non-degradable cross-linker (PMN) along with the degradable cross-linker, the degradation time can be tuned from a few days to over 1 month. This can be explained by the fact that such a system will have higher Cross-linking density but the total number of ester linkages will have been decreased when compared to the hydrogel containing 8% degradable cross-linker. Thus, degradation was slower in the system developed with the combination of degradable and non-degradable cross-linkers.

4.3.4 Mechanical properties

In order to use a hydrogel scaffold as tissue matrix, it should be structurally stable to withstand in vivo mechanical stresses while providing support to ingrowing tissue (49). The mechanical properties of the hydrogels were determined using dynamic mechanical analysis. The mechanical strength of the hydrogel can be tailored by varying the concentration of the cross-linker. As the cross-linker concentration increases, the Cross-linking density in the hydrogel network increases, leading to the formation of a stronger hydrogel. Addition of silicate significantly influences the mechanical strength of the hydrogel. With increasing

concentrations of laponite in the system, the mechanical strength increases (47). As shown in Fig. 4-4, the mechanical properties of this system can be tuned from a few kPa to MPa. When the PLL (0.65) concentration was set at 4%, the G` of the hydrogel with 2% cross-linker changed from 1 to 40 kPa following the addition of laponite (Fig. 4-4a). Moreover, if the polymer concentration was increased to 4%, G` could be tuned from 1 to 140 kPa, and an addition increase to 8% polymer could increase G` to over 160 kPa following addition of 6% laponite (Fig. 4-4b, c). These mechanical behaviours could be attributed to the presence of both physically and covalently crosslinked structures within the same nanocomposite (20, 21, 50, 51).

a)

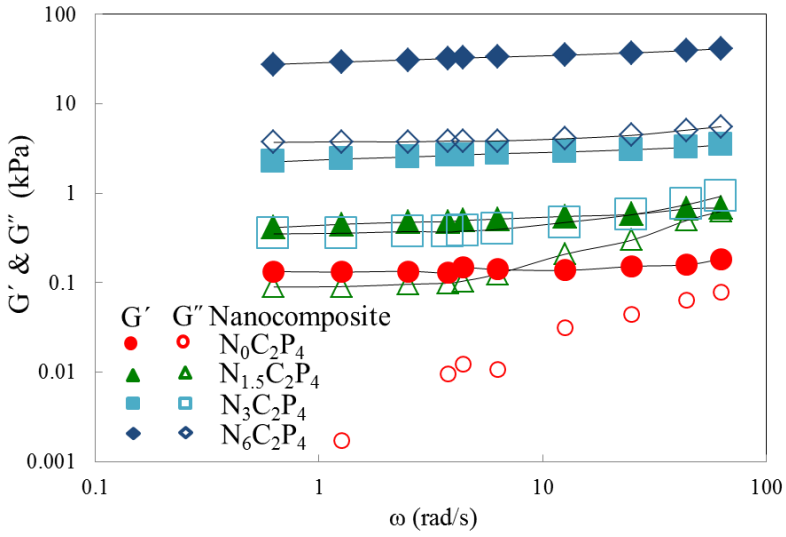

b)

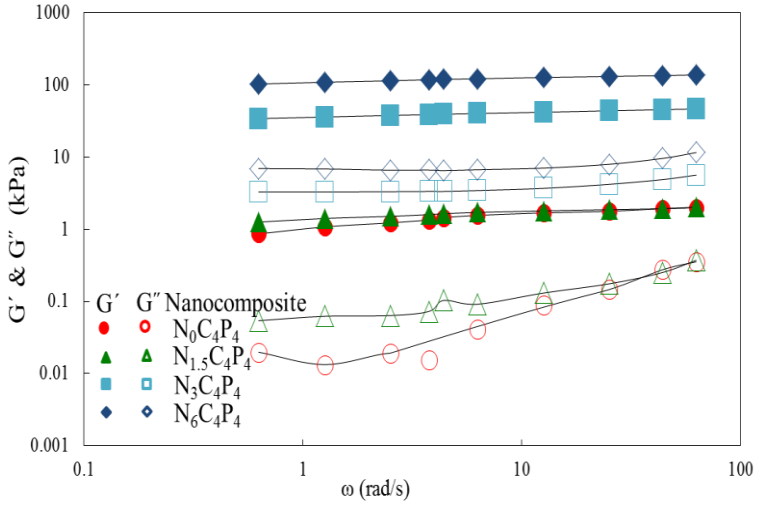

c)

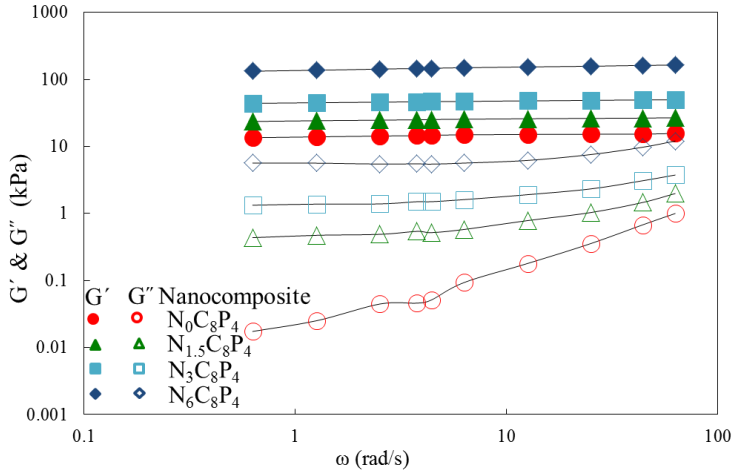

Figure 4-4 Shear and storage moduli of nanocomposites with varying laponite concentration: a) P: PLL (0.65) 4% and PDN 2% b) P: PLL (0.65) 4% and PDN 4% c) P: PLL (0.65) 4% and PDN 8%). Symbols represent the average for n= 3.

The PLL (0.65) compound used in this study is a polyampholyte; varying succination and the pH of the solution can alter the charge on this polymer. In this study, I focused only on PLL (0.65) at pH 7.4 with the goal of designing a technology for biomedical application. This compound contained both charges, and laponite had an anisotropic distribution of charges. Physical interactions between the polymer and laponite led to intercalation of the polymer chain between the laponite discs. PEG and PLL (0.65) could be adsorbed onto the charged silicate surface. This type of interaction resulted in the formation of viscoelastic network (52) within the covalently cross-linked PEG network. Thus, the enhanced mechanical properties could be attributed to the complex interactions between silicate nanoparticles and the polymer chains or the presence of both covalently and physically cross-linked structures. The broad range of mechanical properties of our nanocomposite hydrogels could be useful for application of these materials as cell scaffolds because different cell types may have different requirements for mechanical strength. For example, 1 kPa may be suitable for neuronal stem cells, whereas 10 kPa may be suitable for muscle cells and 100 kPa may be suitable for bone cells (53).

4.3.5 Cell culture study

A preliminary cell growth study suggested that osteoblasts adhered to the covalently cross-linked PEG-laponite-PLL (0.65) nanocomposites. In this study, MC3T3-E1 mouse pre-osteoblasts were seeded on the nanocomposites prepared with different concentrations of the cross-linker (0%, 4%, and 8%) with polymer PLL (0.65) (4%) and laponite (6%). These samples were then compared with hydrogel prepared with PDN as the cross-linker (8%) and PLL (0.65) (4%), as shown in Fig. 4-5. Interestingly, cells attached more easily to the hydrogel when the cross-linker concentration was lower. As expected, the PEG hydrogel did not support cell adhesion or spreading (no cells could be visualized; Fig. 4-5d). However, incorporation of laponite significantly enhanced cell attachment to the nanocomposite surface. Our present findings suggested that the covalently cross-linked nanocomposite induced a different type of cell bio-adhesion as compared to the physically cross-linked PLL (0.65)-laponite nanocomposite. This may be explained by the presence of two types of polymer chains (i.e., PLL (0.65) and PEG) in the covalently cross-linked system, which may hide some of the laponite surface from the attachment of serum proteins and cells, thus reducing cell adhesion. In contrast, in the physically cross-linked system, only one type of polymer chain is present; thus, silicate nanoparticles are more accessible to serum proteins, leading to improved cell attachment. Introduction of laponite leads to bio-cytocompatibility (54). Previous studies have shown that the disc shape and charge present on the laponite surface allows cells to easily internalize via cadherin-mediated endocytosis. When internalization occurs, these nanoparticles upregulate osteoblast-related genes and proteins, i.e., osteocalcin and osteopontin, promoting the production of mineralized extracellular matrix (55). Moreover, these silicates are complex polyions, and one of the components is magnesium, which is known to promote cell adhesion, differentiation, spreading, and migration (26, 56). By controlling the interactions between silicates and polymers, 3D polymeric scaffolds with bioactive properties in regenerative medicine can be fabricated.

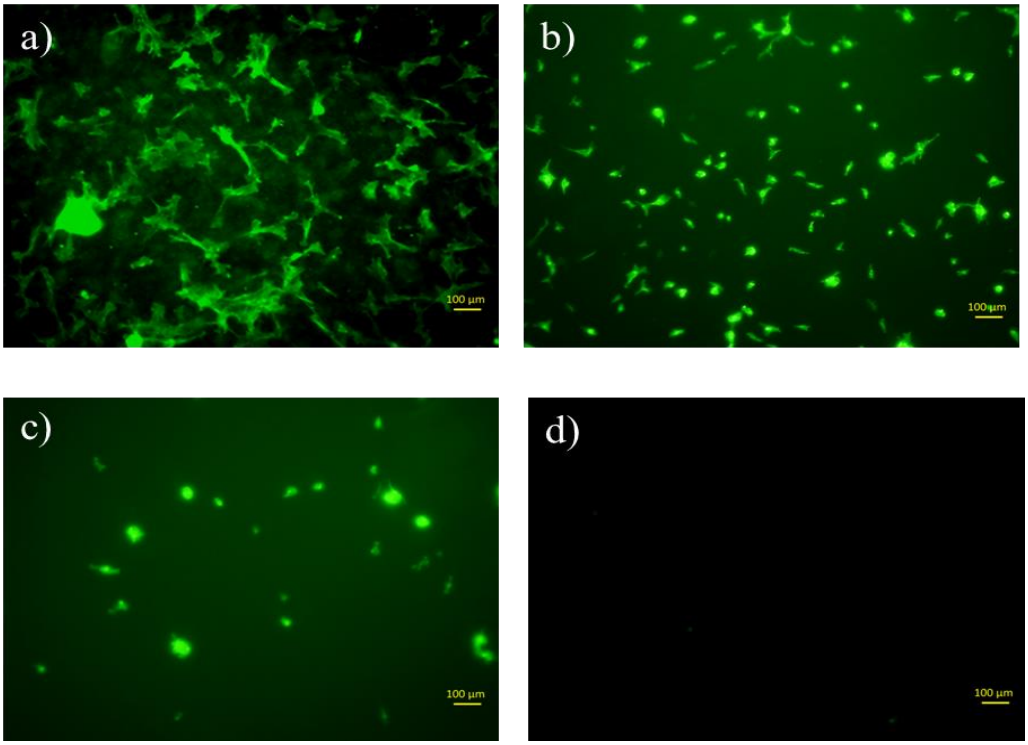

Figure 5-5 In vitro cell growth on COOH-PLL-PDN-Laponite nanocomposite surfaces. MC3T3 E 1 subclone-4 mouse preosteoblast cells readily attach and spread on the nanocomposite surfaces: a) PLL (0.65) 4%: PDN 0%: Laponite 6% b) PLL (0.65) 4%: PDN 4%: Laponite 6% c) PLL (0.65) 4%: PDN 8%: Laponite 6% d) Pure polymer hydrogel PLL (0.65) 4%: PDN 8% do not promote any cell adhesion or spreading. Thus addition of laponite (6%) is responsible for the observed behavior. Scale bars represent 100 µm.

4.4 Conclusion

In the current study, I developed a novel system with tailorable mechanical and degradation properties. I showed that it was possible to tune cell adhesion by controlling the hydrogel formulation. The methodology was simple and did not require the use of toxic cross-linkers. The variety of mechanical and degradation properties of our nanocomposite hydrogel made this material a suitable candidate for cell and drug delivery purposes. Although this study demonstrated the feasibility of applying nanocomposite hydrogels in various tissue engineering applications, this is only a model system, and further optimization of the physical and chemical properties of the system as well as in vivo studies are necessary in order to translate this research into clinical applications. Moreover, future studies may examine the potential application of synthetic polyampholytes with laponite.

This approach may yield new directions for studies of tissue engineering applications.

4.5 References

1. Nicodemus GD, Bryant SJ. Tissue Eng part B, 2008, 14, 140-165.
2. Lee LY, Mooney DJ. Chem. Rev., 2001, 101, 1869-1880.
3. Peppas NA, Hilt JZ, Khademhosseini A, Langer R. Adv. Matter., 2006, 18, 1345-1360.
4. Martens P, Metters AT, Anseth KS, Bowman CN. J. Phys. Chem. B, 2001, 105, 5131-5138.
5. Lutolf MP, Hubbell JA. Nat. Biotechnol., 2005, 23, 47-55.
6. Jain M, Rajan R, Hyon SH, Matsumura K. Biomater. Sci., 2014, 2, 308-317.
7. Nguyen MK, D.S. Lee DS. Macromol. Biosci., 2010, 10, 563-579.
8. Jeong B, Bae YH, Lee DS, Kim SW. Nature, 1997, 388, 860-862.
9. Mano F. Adv. Eng. Mater., 2008, 10, 515-527.
10. Petka WA, Hardin JL, Mcgrath KP, Wirtz D, Tirrell DA. Science, 1998, 281, 389-392.
11. Chung HJ, Park TG. Nano Today, 2009, 4, 429-437.
12. Lu HD, Soranno DE, Rodell CB, Kim IL, Burdick JA. Adv. Healthcare Mater., 2013, 2, 1028-1036.
13. Bryant SJ, Anseth KS. J. Biomed. Mater. Res., 2002, 59, 63–72.
14. Zustiak SP, Leach JB. Biomacromolecules, 2010, 10, 1348-1357.
15. Lu S, Anseth KS. Macromolecules, 2000, 33, 2509–2515.
16. Mason MN, Metters AT, Bowman CN, Anseth KS. Macromolecules, 2001, 34, 4630–4635.
17. Metters AT, Anseth KS, Bowman CN. Polymer, 2000, 41, 3993–4004.
18. Sun JY, Zhao X, Illeperuma WR, Chaudhuri O, Oh KH, Mooney DJ, Vlassak JJ, Suo Z. Nature, 2012, 489, 133-136.
19. Darnell MC, Sun JY, Mehta M, Johnson C, Arany PR, Suo Z, Mooney DJ. Biomaterials, 2013, 34, 8042-8048.
20. Gaharwar AK, Schexnailder PJ, Kline BP, Schmidt G. Acta Biomater., 2011, 7, 568-577.

21. Gaharwar AK, Rivera CP, Wu CJ, Schmidt G. Acta Biomater., 2011, 7, 4139-4148.
22. Haraguchi K, Curr. Opin. Solid State Mater. Sci., 2007, 11, 47-54.
23. Chang CW, Spreeuwel A, Zhang C, Varghese S. Soft Matter, 2010, 6, 5157–5164.
24. Xia Y. Nat. Mater., 2008, 7, 758-760 .
25. Cingolani R. Nat. Nanotechnol., 2013, 8, 792-793.
26. Zreiqat H, Howlett C, Zannettino A, Evans P, Tanzil GS, Knabe C, Shakibaei M. J. Biomed. Mater. Res. A, 2002, 62, 175-184.
27. Carrow JK, Gaharwar AK. Macromol. Chem. Phys., 2015, 216, 248-264.
28. Krsko P, Libera M. Materials Today 2005, 8, 36–44.
29. Lee SH, Miller JS, Moon JJ, West JL. Biotechnol Prog., 2005, 21, 1736–1741.
30. Mann BK, Gobin AS, Tsai AT, Schmedlen RH, West JL. Biomaterials, 2001, 22, 3045–3051.
31. Nie T, Baldwin A, Yamaguchi N, Kiick KL. J .Control Release 2007, 122, 287–296.
32. Leach JB, Schmidt CE. Biomaterials, 2005, 26, 125–135.
33. Bell CL, Peppas NA. Biomaterials, 1996, 17, 1203–1218.
34. Matsumura K, Hyon SH. Biomaterials, 2009, 30, 4842-4849.
35. Rajan R, Jain M, Matsumura K. J. Biomater. Sci., Polym. Ed., 24, 2013, 1767-1780.
36. Rajan R, Matsumura K. Cryobol. Cryotechnol., 2014, 60, 99-103.
37. Rajan R, Matsumura K. J. Mater. Chem. B, 2015, 3, 5683-5689.
38. Watanabe H, Kohaya N, Kamoshita M, Fujikawa K, Matsumura K, Hyon SH, Ito J, Kashiwazaki N. PLoS One, 2013, 8, e83613.
39. Maehara M, Sato M, Watanabe M, Matsunari H, Kokubo M, Kanai T, Sato M, Matsumura K, Hyon SH, Yokoyama M, Mochida J, Nagashima H. BMC Biotechnology, 2013, 13, 58.
40. Jin OS, Lee JH, Shin YC, Lee EJ, Lee JJ, Matsumura K, Hyon SH, Han DW. Cryoletters, 2013, 34, 396-403.
41. Matsumra K, Hayashi F, Nagashima T, Hyon SH. J. Biomater. Sci. Polym. Ed., 2013, 24, 1484-1497.
42. Matsumura K, Bae JY, Kim HH, Hyon SH. Cryobiology, 2011, 63, 76-83.

43. Matsumura K, Bae JY, Hyon SH. Low Temperature Medicine, 2010, 36(3), 65-68.
44. Matsumura K, Bae JY, Hyon SH. Cell Transplant, 2010, 19, 69-699.
45. Haneeb AF. Anal Biochem., 1966, 14, 328–36.
46. Mongondry P, Nicolai T, Tassin JF. J. Colloid Interface Sci., 2004, 275, 191-196.
47. Stefanescu EA, Stefanescu C, Daly WH, Schimdt G, Negulescu IN. Polymer, 2008, 49, 3785-3794.
48. Jo YS, Gantz J, Hubell JA, Lutolf MP. Soft Matter, 2009, 5, 440-446.
49. Ma PX. Mater. Today, 2004, 7, 30-40.
50. Atmuri AK, Bhatia SR. Langmuir, 2013, 29, 3179-3187.
51. Baghdadi HA, Sardinha H, Bhatia SR. J. Polym. Sci., Part B: Polym. Phys., 43, 233-240.
52. Haraguchi K, Li HJ, Matsuda K, Takehisa T, Elliott E. Macromolecules, 2005, 38, 3482-3490.
53. Ram SE, Artym V, Yamada M. Cell, 2006, 126, 645–647
54. Schexnailder PJ, Gharwar AK, Bartlett II RL, Seal BL, Schmidt G. Macromol. Biosci., 2010, 10, 1416-1423.
55. Gaharwar AK, Mihaila SM, Swami A, Patel A, Sant S, Reis RL, Marques AP, Gomes ME, Khademhosseini A. Adv. Mater., 2013, 25, 3329-3336.
56. Mihaila SM, Gaharwar AK, Reis RL, Khademhosseini A, Marques AP, Gomes MS. Biomaterials, 2014, 35, 9087-9099.

Chapter 5

Self-assembled nanogel incorporated Dextran and poly-L-lysine based hydrogels with controlled drug release properties

5.1 Introduction

Wound healing technically can be described as the loss of protective function of skin which is followed by the breakdown of continuity of epithelium but it may or may not be accompanied by the loss of functioning of the underlying connective tissue (1, 2). It is recognized in many ways by its anatomical location or whether the wound is acute or chronic and also by the type of tissue predominant in the wound bed.

Body has inbuilt natural mechanism to heal the wound. Wound healing can be by primary intention where wound heals by sutures, tissue adhesives, and staples or by combination of all of these. But when infection is present in the wound it is impossible to heal the wound by above-mentioned ways and it is left to repair by secondary intention (3, 4). Wound healing is actually a dynamic process, which is comprised of three phases Fig. 5-1.

Phases of wound healing includes:

- Inflammatory phase
- Proliferation phase
- Maturation phase

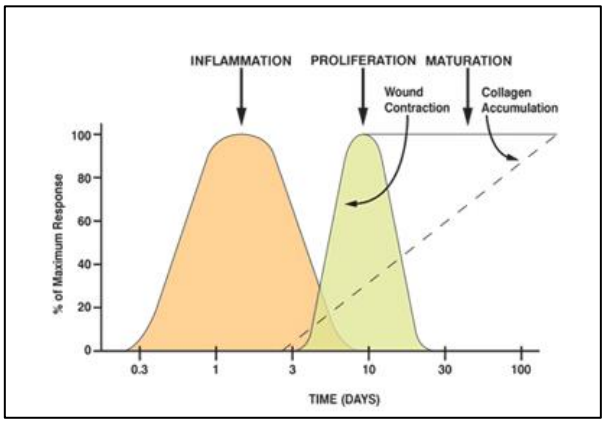

Figure 5-1 Phases of wound healing[3]

Inflammatory Phase

Body's first response to injury is inflammatory phase. When wounding occurs then contraction of blood vessels took place in the wound area and clot is formed. It is usually accompanied by the dilation of blood vessels leading to the release of cells, antibodies, white blood cells, growth factors and enzymes to reach the wounded area. This stage is usually recognized by inflammation; odema, heat, pain and functional disturbance. Phagocytic cells are dominant at this stage.

Proliferation Phase

This phase is marked by the development of new granulation tissue, which is composed of collagen and extracellular matrix. Within this, network of blood vessels developed that is angiogenesis occurred. Healthy granulation is controlled by the sufficient supply of oxygen and nutrients by the blood vessels to fibroblasts. Red/pink colour is an indication of good granulation. Dark granulation is usually the result of infection and poor perfusion of oxygen and nutrients.

Maturation Phase

It is the final phase and is response to the wound closure. In this remodeling of collagen from type 3 to type 1 occurs. In the wounded area the number of blood vessels and also cellular activity decreases.

During wound healing process, dressings play a crucial role for the regeneration and repair of dermal and epidermal tissue. Before 1960 wound dressings were not considered to play a major in healing process. But in 1962, Winter gave a concept, which described the importance of dressings in wound healing. This approach has paved the path for the development of functionally active dressing materials (5).

Wound dressings act as physical barrier to protect the injury from microorganisms and also permeable to moisture and oxygen. It expedites the healing process and provides better healing conditions (6). They are identified by peculiar properties such as protect the wound from secondary infections, absorb wound fluids and exudates, prevent the desiccation of wound, biocompatible,

non-antigenic, stimulate the growth factors, control odors, minimize pain etc. (7-9).

In order to improve the properties of wound dressing materials certain ingredients can be incorporated. For example wound dressings impregnated with antibacterial and antifungal drugs are useful for the formulation of topical dressings (10), for periwound skin protection inclusion of moisture barriers, sealants can be useful (11), odor-controlling dressings are favorable for the management of burn wounds in this case activate charcoal is highly recommended. For the treatment of diabetic foot ulcers, dressings incorporating honey is very useful because of the inherent antibacterial property of honey (12, 13).

Hydrogels can be good option for the development of wound dressings. Properties possessed by the hydrogels can easily meet the essential requirements of the wound dressing materials. These includes transparency of hydrogels which can allow easy follow up of the wound, providing moisture, releasing growth factors, barrier against microorganisms, easy to change and control over drug release (14). Rosiak et al. were the first who proposed the idea of using hydrogels as basic materials for the development of wound dressings (15). Since then many commercially available hydrogel based wound dressing materials under the trade name Vigilon, Kik gel, Hydron burn bandage, Aqua gel etc (16). Amongst hydrogels in-situ forming hydrogels are more preferred over preformed one as it allows taking the shape of wound without wrinkling or fluting (17). Although hydrogels meet most of the essential criteria of an ideal wound dressing material but their relatively low mechanical strength restricts their use (18).

Proteins and polysaccharides are usually the preferable materials for the regeneration of full thickness wounds due to their good biocompatibility (19, 20). However, these natural polysaccharides show relatively low mechanical strength so they need to be mixed with synthetic polymers or backbone modification is required. In pursuit of the development of better mechanical properties somehow their biocompatibility is affected. Optimally tailored polysaccharide based scaffold could provide controlled release of growth factors and drugs (21, 22).

Among the natural polymers suitable for such a purpose is dextran, a hydrophilic, biocompatible, and nontoxic polysaccharide composed of linear α-1,6-linked D-

glucopyranose residues. From a structural point of view, dextran has reactive hydroxyl groups that can be modified to and also introduction of functional groups is easy (23). Because dextran is naturally resistant to protein adsorption and cell adhesion, modification of its polymer backbone allows the development of a hydrogel with specific characteristics (24). It can easily be degraded in various organs of the body such as liver, colon, kidney and spleen by dextranases (25).

Dextran oxidation

Periodate oxidation of dextran is a simple catalysis-free reaction which gives purified product by dialysis. In this reaction periodate ion attacks on the vicinal diols particularly α-1,6 residues are attacked between carbons C_3-C_4 or C_3-C_2, breaking the C-C bond and yielding aldehyde groups Scheme 1 (26). This functionality has been used to conjugate N-nucleophiles. It is an easy, fast and almost complete reaction. This approach has been used widely to formulate hydrogels, as it does not involve any harmful initiators. Different aminated cross-linkers such as chitosan, gelation, 8-arm PEG has been used for such formulations (27).

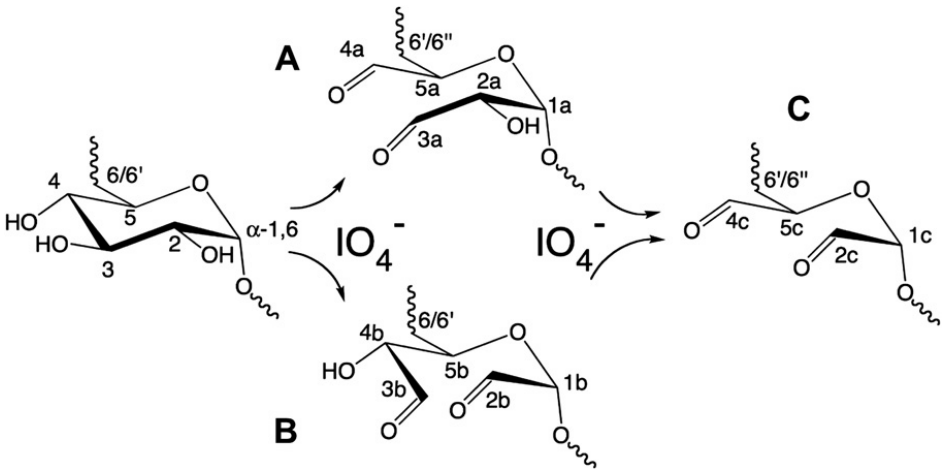

Scheme 1 Dextran's α-1,6 glucose residue possible periodate oxidations. (A) Periodate attack at C_3-C_4; (B) C_3-C_2 and (C) double oxidation [26]

Self-assembly of amphiphilic polysaccharides for drug delivery

Recently various approaches have been developed for controlled drug release purpose based on nanoparticles containing polysaccharides (28, 29). However, in

most cases it involves the use of harsh conditions such as organic solvents and highly acidic conditions which act as hindrance for its formulation (30). In order to combat this modification of polysaccharides backbone with hydrophobic moieties is a better approach. These amphiphilic polysaccharides can exhibit either inter or intramolecular hydrophobic interactions leading to the development of various kinds of drug delivery vehicles such as micelles, liposomes, microspheres, nanoparticles Fig. 5-2. Structure of these self-assemblies can easily be selected depending on the type of drug to be used and mode of administration (31- 34).

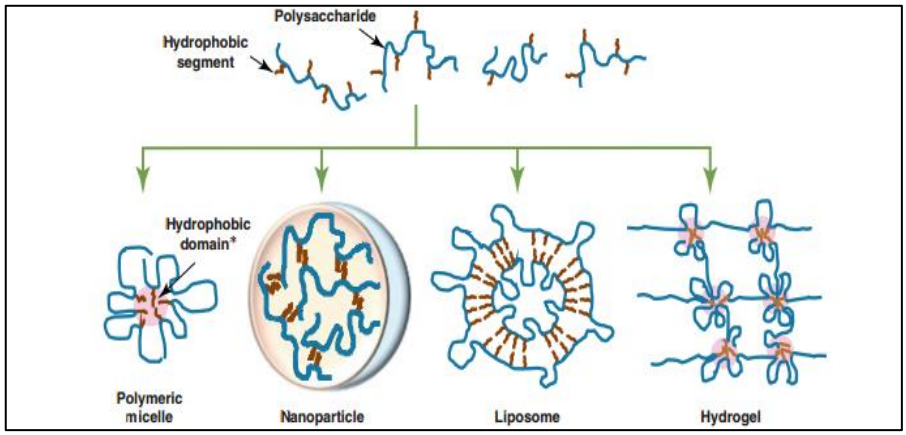

Figure 5-2 Schematic depiction of different drug delivery systems formed by self-association of amphiphilic polysaccharides in aqueous solution.*Hydrophobic domain due to the association of hydrophobic groups.

This hydrophobic core is used to solubilize drugs, which have low solubility in aqueous environment, and hydrophilic shell would absorb hydrophilic molecules through non-covalent interactions.

Amphotericin B (AmB)

AmB is a broad-spectrum antifungal drug. It is a macrocyclic Fig. 5-3 polyene antibiotic, which is majorly used for the treatment of deep-seated mycotic infections (35, 36). Water solubility of AmB is relatively poor and also it cannot be used at higher concentrations (37). This restricts the usability of the drug. It necessitates the development of newer systems, which can maintain the low toxicity, and good solubility of the drug (38).

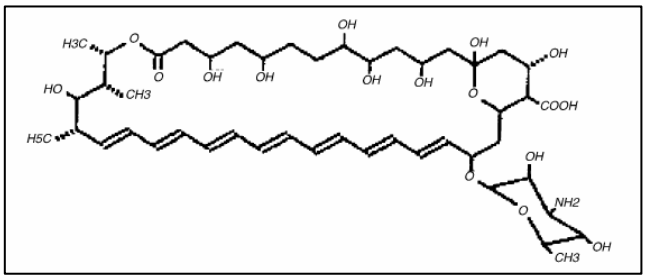

Figure 5-3 Chemical structure of antibiotic AmB[36]

Growth Factors

Growth factors can be described as soluble signaling polypeptides, which have the capacity to instruct specific cellular responses (39). These cellular responses can result into various cell actions such as differentiation or proliferation of cells. There are various components in the extracellular matrix that binds to the growth factors and modifies their function (40-42). Growth factors govern the cell behavior by binding to specific transmembrane receptors on target cells Fig. 5-4. In the given figure it is shown that The producer cell secretes soluble growth factors that bind to target cell receptors. The instructions are translated into the cell through complex signal transduction networks resulting in a specific biological cellular response. Insert illustrates how ECM can control growth factor presentation in a temporal and spatial fashion. Cell migration towards gradients of growth factors, bonded to ECM, can also be ECM . mediated, whereas cells will use integrin machinery to follow growth factor gradients. Upon degradation, ECM growth factors become available for cell binding via cell membrane growth factor receptors and will ultimately induce a specific biological cellular response (43).

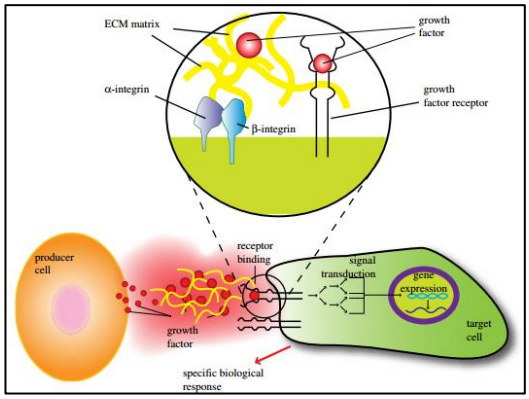

Figure 5-4 Cross talk between cells mediated by growth factors and ECM[43]

Growth factors can be introduced in the biomaterials using two strategies first is chemical immobilization and second is physical encapsulation (43).

In this work I have attempted to develop a system for wound healing applications. The system is based on dextran. Dextran backbone is firstly cleaved by sodium periodate and is converted to dextran aldehyde. These aldehyde groups were crosslinked by amine groups of ε poly-l-lysine. In order to control the gelation rate amine groups are modified by carboxylic anhydride. Mechanical property of these hydrogels can easily be controlled by the degree of oxidation of dextran and carboxylation. Dextran hydroxyl groups are also modified by hydrophobic alkyl chain in order to formulate self-assembled nano-assemblies. Nano-assembly formation can easily be tuned by varying the degree of substitution of hydrophobic alkyl chain. These assemblies have been employed to encapsulate the hydrophobic drug AmB. Amb shows burst release which is useful for wound healing application. In this chemically cross-linked system basic human fibroblast growth factor (bFGF) has been introduced physically. The system shows gradual release of the growth factor. This dual delivery of therapeutics can be useful for the development novel medical plasters in future.

5.2 Materials and Methods

5.2.1 Materials

Dextran with a molecular weight of 70 kDa was purchased from Meito Sangyo Co., Ltd. (Nagoya, japan). poly-L-lysine (PLL) (4 kDa, 25 wt% aqueous solution) was obtained from JNC Corp. (Tokyo, Japan). Pyridine and amphotericin B was purchased from (Wako Pure Chem. Ind. Ltd., Osaka, Japan); starch and sodium periodate was obtained from Nacalai Tesque, Inc. (Kyoto, Japan). 4-Dimethylaminopyridine (DMAP), Lithium chloride (LiCl), suucinic anhydride (SA) was obtained from TCI Corp. (Tokyo, Japan). All the chemicals were used without any purification.

5.2.2 Dextran aldehyde preparation using periodate oxidation

Aldehyde dextran was prepared by the method as reported in literature (44, 45). Dextran 20g was dissolved in 120 mL water and to it various amounts of sodium periodate (0-10) g was added. The reaction was carried out at 50˚C for 1 hour.

The reaction mixture was purified by dialysis using cellulose dialysis membrane (cut off molecular weight (MwCO) 14 kDa). The dialysis was carried out for 48 hours and water was changed regularly after every 2 hours. The product is obtained by drying in oven for 48 hours and then followed by vacuum drying at 25˚ C for 24 hours. The obtained film is mechanically crushed to obtain white powder and is stored at -20˚C.

Aldehyde introduced into dextran was determined by iodometry titration as reported (44). In this method firstly 10 mL of 1 w/v% aqueous solution of dextran aldehyde was pipetted into the 20 mL solution of I_2 (0.05 mol/L), to which 10 mL of NaOH (1 mol/L) was further added. This mixture was left for 15 minutes so that oxidation reaction can take place. After this 15 mL of H_2SO_4 (6.25 v/v%) was added. To determine the I_2 consumption in the reaction with aldehyde, titration with Na_2SO_3 (0.1 mol/L) was carried out using starch (20 w/w%) solution as an indicator. Readings were taken in the sets of 3.

5.2.3 Succination of ε-poly-L-lysine

Succinated poly-l-lysine (PLL-SA) was prepared as reported previously in the literature (46). To synthesize PLL-SA, 25% (w/w) PLL aqueous solution was mixed with SA at 0%–35% molar ratios (SA/PLL amino groups) and reacted at 50°C for 1 h to convert amino groups into carboxyl groups. Thus, carboxyl groups were introduced into PLL by treatment with SA, which reacts with amino groups as shown in Scheme 1. The ratio of succination was well controlled by reaction with SA (46). The succination ratio in this study was controlled to approximately 10, 20, and 35 mol%. The amount of remaining amino groups was determined by the 2,4,6-trinitrobenzenesulfonate (TNBS) method (47). The ratio of carboxylation is shown in parentheses, e.g., PLL (0.35) indicates that 35% of the α-amino groups have been converted into carboxyl groups by SA addition.

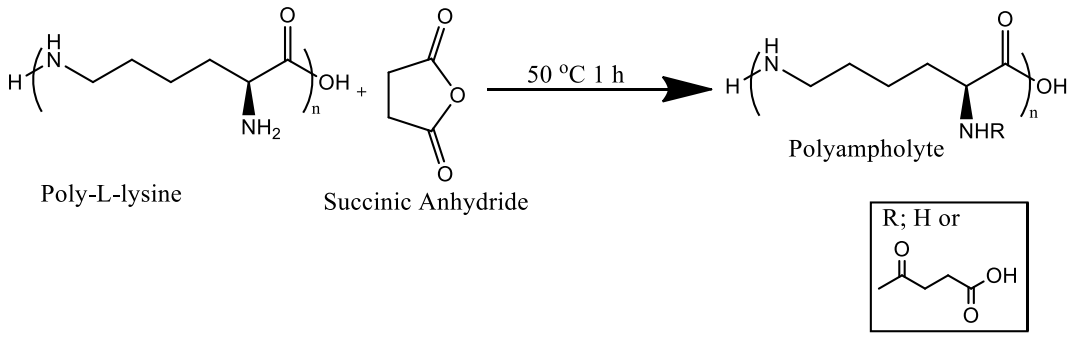

Scheme 1 Schematic representation of succination of PLL

5.2.4 Synthesis of alkyl chain grafted dextran

Using the strategy previously reported in the literature, grafting of alkyl chain in the dextran was done (48). Briefly 4 g of dextran was dissolved in 50 mL of DMF containing 1g of LiCl. To it 0.5 g of DMAP, 30 mg of pyridine was added and then various amounts of dodecyl succinic anhydride (DDSA) (0.2, 0.4, 0.8) was added to obtain various degree of substitution. The reaction was run for 3h at 80° C. The obtained product was precipitated using isopropyl alcohol and then precipitates were dissolved in water and subjected to dialysis using dialysis membrane of MwCO (14000) for 48h. Water of dialysis was changed after every 2h. The product is obtained by drying in oven for 48 hours and then followed by vacuum drying at 25˚ C for 24 hours and is named as Dex-DDSA. The obtained film is mechanically crushed to obtain white powder. Degree of substitution is defined by the percentage of glucose units substituted with alkyl chain and was determined using ^{1}H-NMR spectra in DMSO-d_6.

5.2.5 Preparation of self-assembled AmB loaded nanoparticles

Preparation of AmB loaded nanoparticles was done by dialysis method (49). 0.5g of Dex-DDSA and 0.05 g of AmB were dissolved in 20 mL of DMSO. This solution was stirred at room temperature for 1.5 h. The reaction was then subjected to dialysis for 24 h using dialysis membrane of MwCO (14000). Water was exchanged for every hour. The resulting solution was filtered using 0.22 μm filter and then lyophilized and is stored at -20°C. Empty nanoparticles were also prepared in the same manner except that AmB was not added.

Encapsulation efficiency (EE) and drug loading efficiency (LE) was determined using ultraviolet analysis (50). The procedure is drug loaded nanoparticles were dissolved in DMSO and then UV-visible spectrum was recorded at 416 nm on JASCO FP- 6500 using extinction coefficient $\varepsilon = 1.214 \times 10^5\ M^{-1}cm^{-1}$.

Encapsulation efficiency (EE) % = (amount of AmB in nanoparticles/total amount of added AmB) × 100

Drug loading efficiency (LE) % = (amount of AmB in nanoparticles/total amount of formulation components) × 100

The morphology of the nanoparticles was observed using transmission electron microscopy. Samples were prepared using 0.05% of the Dex-DDSA with various substitutions. 10µL of the samples was placed on a copper grid (NS-C15 Cu150P; Stem, Tokyo, Japan). Sample was then left to air dry for 10 minutes. TEM images were observed using Hitachi H-7100 system (Hitachi, Tokyo, Japan) with an accelerating voltage of 100 kV.

The mean size and zeta potential was measured using Zeta sizer 3000 (Malvern Instruments, Worcestershire, UK).

5.2.6 In vitro release study of AmB from Dex-DDSA nanoparticles

Release study was performed at 37°C using shaker (50). 3 mL of AmB loaded nanoparticles in dialysis bag of MwCO (14 kDa) was placed in container containing 30 mL of distilled water. This container was shaken at 100 rpm at 37°C. After regular intervals 3 mL of the distilled water was removed from external medium and was replaced with fresh one. This was diluted with equal amounts of DMSO and then subjected to UV-visible analysis. AmB concentration was determined based on the absorbance intensity at 410 nm according to the standard line obtained from a series of solutions with different AmB concentrations. AmB solution was prepared in 1:1 (water: DMSO) (49).

5.2.7 Preparation of Dex-ald/ PLL SA hydrogel

Aqueous solution of variously oxidized dextran and different succinated poly-L-lysine were mixed in different amounts to prepare the different hydrogels as shown in table 1. Firstly requisite amount of oxidized dextran was incubated for

10 minutes at 37 °C and then required amount of PLLSA was added. In all the cases pH of the mixture is around 7.

5.2.8 bFGF release from hydrogels

Hydrogels are prepared as described above but in order to carry out the release experiment of growth factor from them prior to gelation, 200 ng of bFGF was mixed with PLLSA. After gelation hydrogels were carefully removed from the molds and then placed in 100 mL of PBS and incubated at 37 °C on the shaker. After certain regular intervals 5 mL of PBS is removed from the surrounding medium and was replaced with the fresh one (51). These samples were stored at -80 °C before ELISA analysis was carried out. ELISA analysis was carried out as per the manufacturer's instructions.

$$\textbf{Cumulative release (\%)} = (M_t/M_0) \times 100$$

M_t is the amount of bFGF released at time t and M_0 is the initial amount of bFGF loaded in the hydrogel.

5.2.9 Rheological measurements of hydrogels

In order to evaluate the mechanical property of the hydrogels dynamic mechanical analysis was carried out using a strain-controlled rheometer (Rheosol G5000, UBM Co., Ltd., Kyoto, Japan). Cone-plate geometry with a cone diameter of 24.99 mm and an angle of 2° (truncation of 50 μm). Samples for rheological analysis was prepared as follows, aqueous solution of aldehyde dextran oxidized to various degrees using periodate mixed with different succinated PLL was loaded onto the rheometer plate. G′ dynamic storage modulus and G″ dynamic loss modulus was measured after 10 minutes of loading. Frequency sweep experiments between 0.628 and 62.8 $rads^{-1}$ were performed at fixed strain amplitude of 0.967%. All experiments were performed in triplicate to check the reproducibility of the data.

5.3 Results and discussion

5.3.1 Dextran aldehyde preparation using periodate oxidation

Oxidation of polysaccharides can easily be achieved by using periodate. In this reaction they open up their sugar units and polyaldehyde derivatives can be obtained as shown in Scheme 2. Introduction of aldehyde in the dextran was evaluated by iodometry. Degrees of oxidation in dextran increases almost linearly with the increase in the amounts of periodate which is in accordance with the result reported earlier (44, 52). A small amount of aldehyde dextran was detected even when no oxidation was carried out using periodate. As shown in Fig. 5-5 degree of oxidation in the dextran can easily be tuned by varying the amounts of periodate.

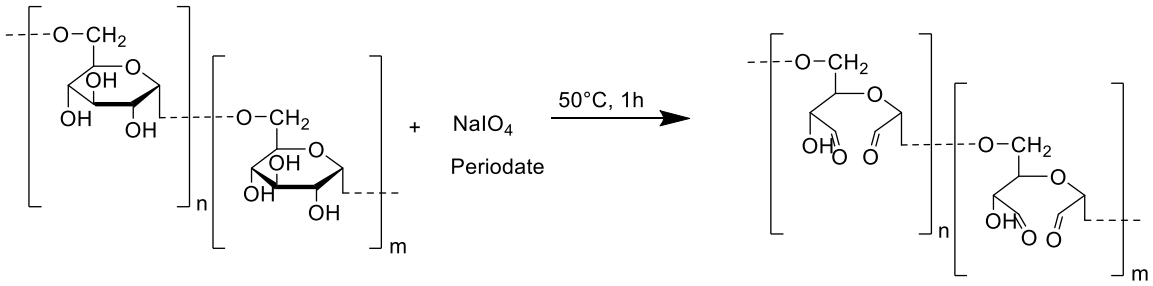

Scheme 3 Periodate oxidation of dextran to from Dex-ald.

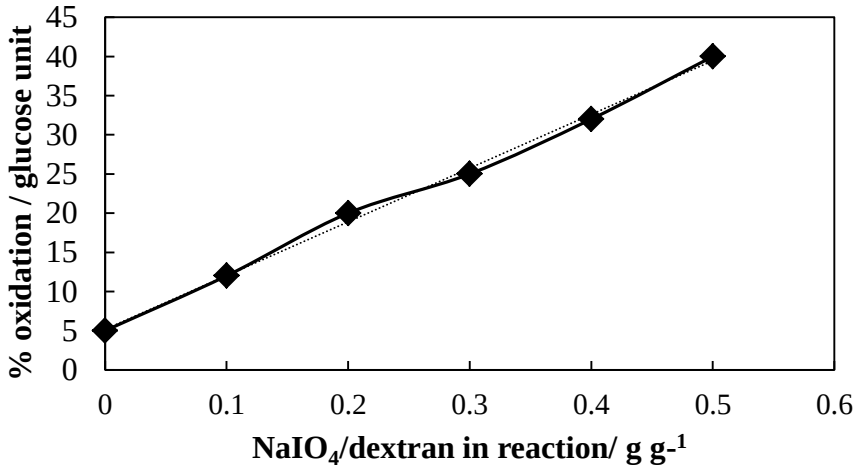

Figure 5-5 Effect of the varying the concentration of periodate on the oxidation of dextran.

5.3.2 Succination of ε-poly-L-lysine

ε-PLL is a L-lysine homopolymer biosynthesized by *Streptomyces* species and is used as a food additive because of its antimicrobial activities, which are ascribed to the cationic charge of its side-chain α-amino groups. According to our previous research, cytotoxicity decreases with the introduction of carboxyl groups into PLL (46). The polymer charge can be tuned by varying the level of succination, thus enabling the control of electrostatic interactions between the drugs and polymer. In the present study, the succination ratio was controlled to around 10- 35 mol%.

5.3.3 Synthesis of alkyl chain grafted dextran

Introduction of DDSA in dextran can successfully be achieved. Scheme 3 describes the grafting. Varying the amounts of DDSA can easily be control the substitution.

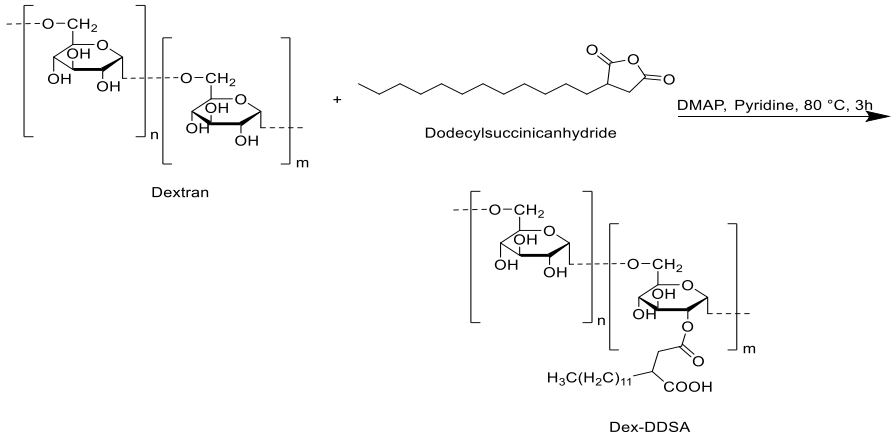

Scheme 4 Grafting of DDSA in the backbone of dextran.

The DS was calculated from the ^{1}H-NMR spectra (Fig. 5-6, 5-7 & 5-8) using the following formula:

$$DS\ (\%) = [(I_{methylene} / 20) / (I_{anomeric\ proton}) \times 1.04\ ] \times 100$$

Here, $I_{methylene}$ and $I_{anomeric\ proton}$ are the integrals of the methylene peaks of the introduced DDSA located at 1.23 ppm and of the anomeric proton of dextran located at 4.9 ppm, respectively, and 1.04 is the correction factor for the average 4% of α-1,3 linkages in dextran (53, 54).

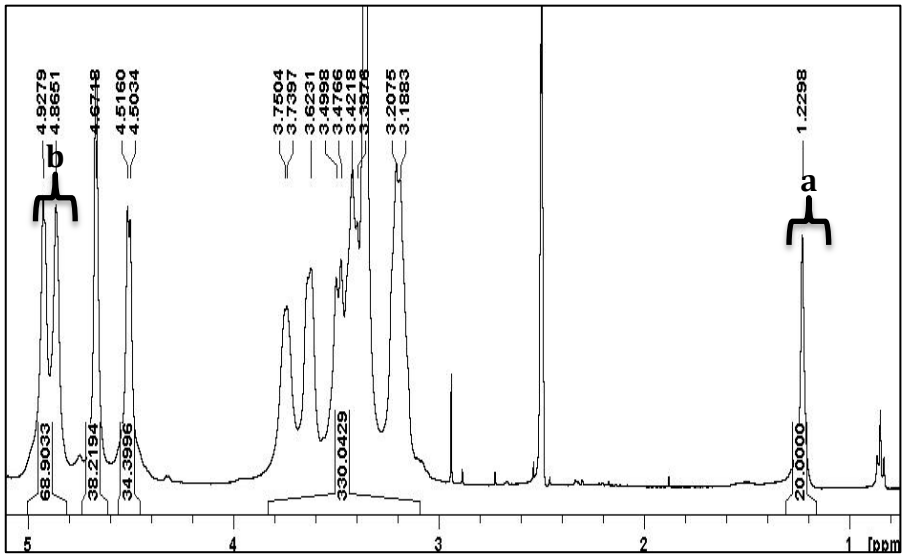

Figure 5-6 ^{1}H-NMR of Dex-DDSA. D.S. is 1.4%

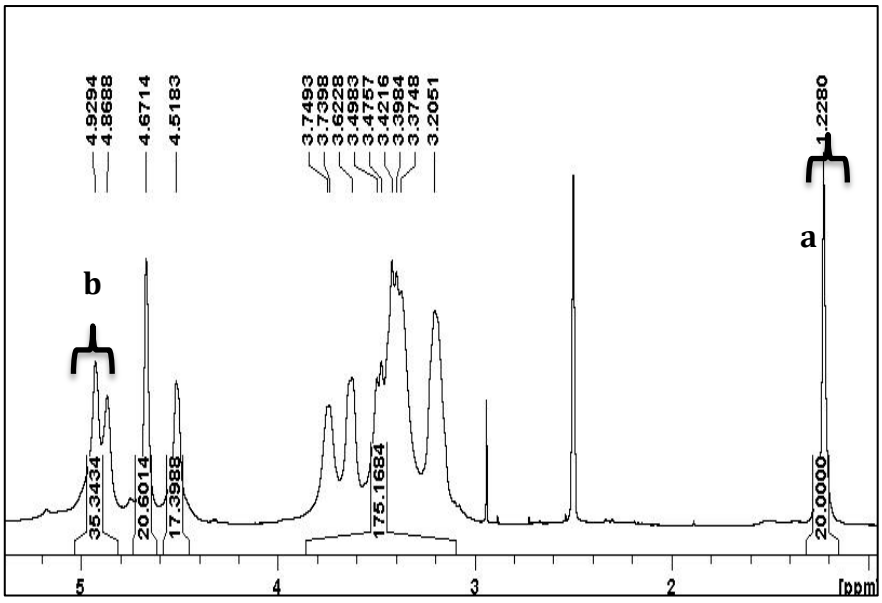

Figure 5-7 ^{1}H-NMR of Dex-DDSA. D.S. is 2.72%.

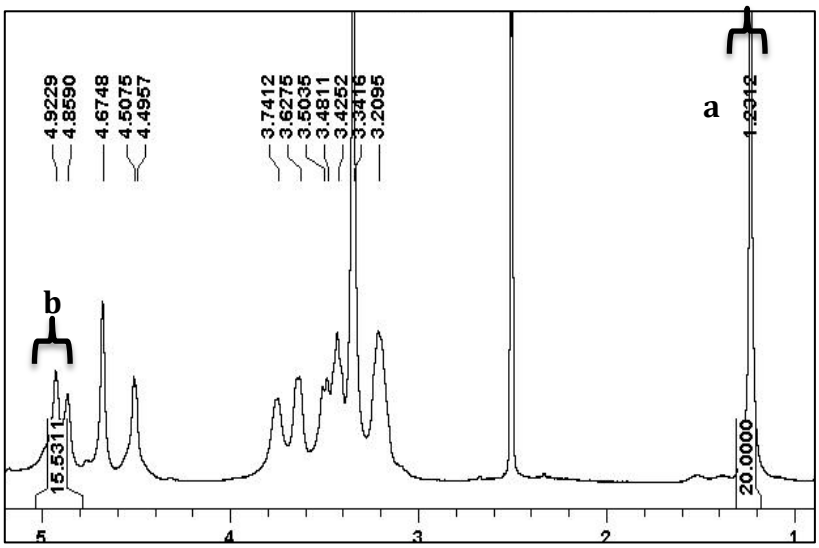

Figure 5-8 ^{1}H-NMR of Dex-DDSA. D.S. is 6.3%.

5.3.4 Preparation of self-assembled AmB loaded nanoparticles

DDSA substituted dextran form nanoparticles by self-assembly. Hydrodynamic radius of the nanoparticles can be tuned by varying the degree of substitution of DDSA in dextran as summarized in Table 1. The morphology of the nanoparticles formed by DDSA-Dex was also determined by TEM analysis as shown in Fig. 5-9. Size obtained from TEM micrographs is around 52±5 nm, 43.4±8 nm for a and b respectively. The morphology of nanoparticles is round.

From this data it can be seen that with increase in hydrophobicity size of the nanoparticles decreases. Hydrodynamic radius and TEM shows large difference in size, which can be attributed to dehydration of the nanoparticles due to the solvent evaporation during TEM experiment (55). Hydrodynamic radius is too high which is possible because steric hindrance caused by hydrophilic chain of dextran is expected to take larger volume due to its high molecular weight (56, 57). These large values can also be attributed to the formation secondary aggregates (58). However, zeta potential values do not change with increase in substitution of hydrophobic moiety.

Table 1 Characteristics of DDSA-dex nanoparticles with different degree of substitution of DDSA

Polymer	% Substitution	Particle size (nm)	Zeta potential (mV)	PI	% EE	%LE
A	1.4	533.8	-10.6	0.848	ND	ND
B	2.7	425.7	-13.4	0.637	42.35	3.8
C	6.3	282.8	-13.9	1	48.23	6.2

a) b)

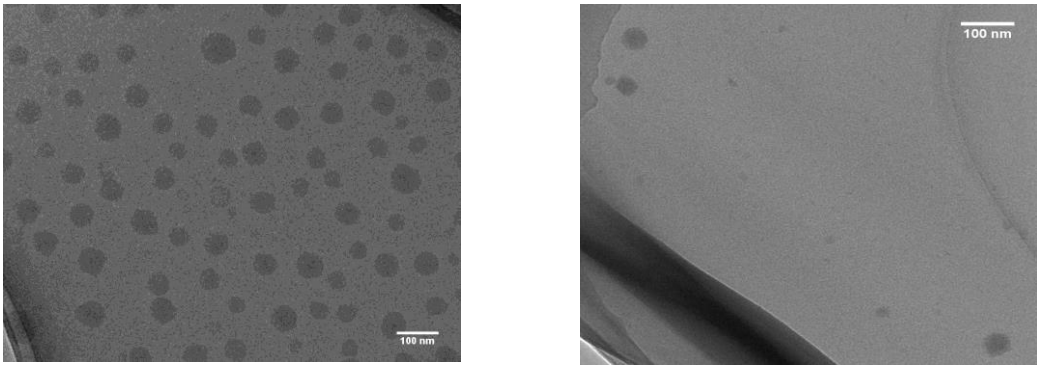

Figure 5-9 TEM micrograph of Dex-DDSA nanoparticle a) D.S. 2.7% b) D.S. 6.2%.

When drug Amb was loaded into the nanoparticles the morphology and size was not affected. Incorporation of Amb was successful in the hydrophobic core. This can be concluded on the grounds that empty polymer nanoparticles in UV-Vis spectroscopy at 416 nm shows no absorbance whereas Amb loaded nanoparticles are yellow in color and shows absorbance at this wavelength. This is possible only when AmB gets physically absorbed in the hydrophobic core Fig. 5-10.

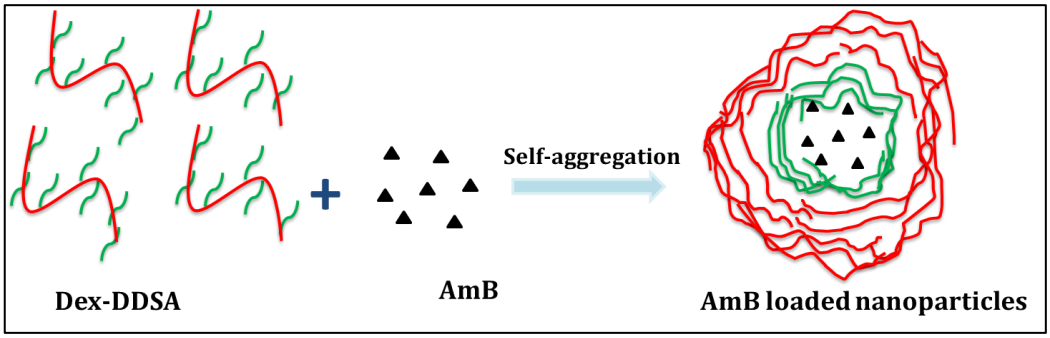

Figure 5-10 Schematic representation of self-assembled nanoparticles formed by Dex-DDSA in aqueous media.

5.3.5 In vitro release of AmB from Dex-DDSA nanoparticles

In vitro drug release from Dex-DDSA with D.S. 2.7% as shown in Fig. 5-11 shows a two-step release profile, ie, initially burst release of 30-40% followed by slow release of 85% upto 2 days. This fast release of antifungal drug is required for the formulation of hydrogels in wound healing applications as faster release will inhibit the further infection of the wounds from microorganisms.

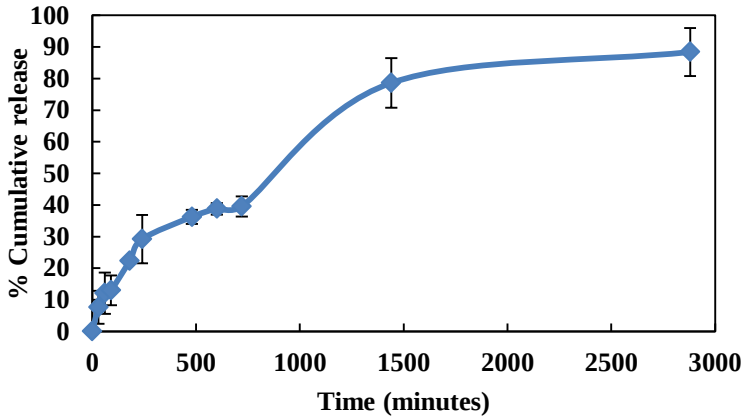

Figure 5-11 Cumulative release of AmB from hydrophobic core of Dex-DDSA with D.S. 2.7%.

5.3.6 Preparation of Dex-ald/ PLL SA hydrogel

Different hydrogels were prepared using fixed concentration of 10 w/w% of aldehyde dextran with different extents of oxidation. Gelation is very fast with poly-l-lysine without carboxylation. In order to tune the gelation time of the hydrogels aldehyde dextran was mixed with varying concentrations of succinated PLL as shown in Table 2. Gelation time can easily be tuned by varying the

concentration of the precursors and also on the extent of oxidation in dextran, which is in accordance with the previous report (44, 52).

Effect of degree of succination of PLL on gelation can also be observed. Gelation time can be delayed by increasing the succination in PLL. This is reasonable as increase in succination leads to decrease in the amino groups of PLL.

Table 2 Preparation of various hydrogels with variation in degree of oxidation of dextran and succination in PLL

Degree of oxidation	(w/w)% of Dex-ald	Succination of PLL (%)	(w/w)% of PLLSA	Hydrogel formation
14.2	10	10	5, 7.5, 10	Yes
		20	5, 7.5, 10	
		35	5, 7.5, 10	
22.6	10	10	5, 7.5, 10	Yes
		20	5, 7.5, 10	
		35	5, 7.5, 10	
25	10	10	5, 7.5, 10	Yes
		20	5, 7.5, 10	
		35	5, 7.5, 10	
40	10	10	5, 7.5, 10	Yes
		20	5, 7.5, 10	
		35	5, 7.5, 10	

5.3.8 bFGF release from hydrogels

Fig. 5-12 shows the release of growth factor from the hydrogels. From this it can be seen that the release of growth factor from the hydrogel is very fast. Although in order to formulate the hydrogel for wound healing application slow release is required so optimization of release from these hydrogels need to be done.

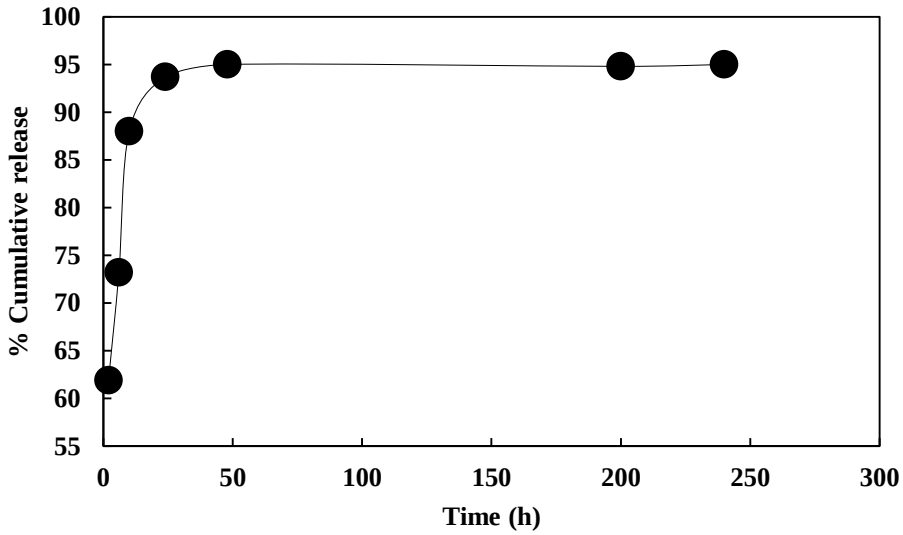

Figure 5-12 Shows the cumulative release of bFGF from hydrogel composed of 25% Dex-PLL (20) 10%.

5.3.8 Rheological measurements of hydrogels

Dynamic mechanical analysis of various hydrogels was carried out in order to determine their strengths. In this hydrogels are denoted by the abbreviation x%Dex-PLL (y) z% where x % represents the % oxidation of dextran, y represents the succination ratio and z represents the (w/w)% of PLLSA. Fig. 5-13 a, b and c represents the dynamic moduli of hydrogels 22.6% Dex with PLL (0.1), PLL (0.2) and PLL (0.35) at 10, 7.5 and 5 (w/w)% respectively. Storage moduli of the hydrogels can easily be tuned between 1 to 18 kPa. The amount of amino groups in PLL decreases with increase in the succination ratio. It leads to lower number of cross-linking points and thus decreases the storage moduli (52). Mechanically stronger hydrogels can be obtained with higher concentration of the cross-linker, which is reasonable as more is the concentration of the cross-linker higher will be the cross-linking points and stronger will be the hydrogels.

a)

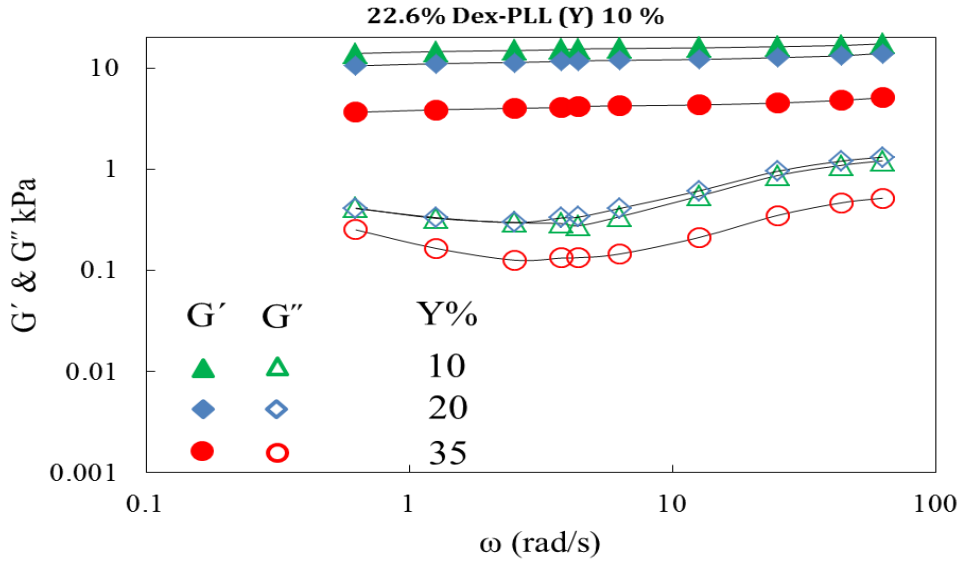
22.6% Dex-PLL (Y) 10 %
G´ & G˝ kPa
10
1
0.1
0.01
0.001
0.1
1
10
100
ω (rad/s)
G´ G˝ Y%
10
20
35

b)

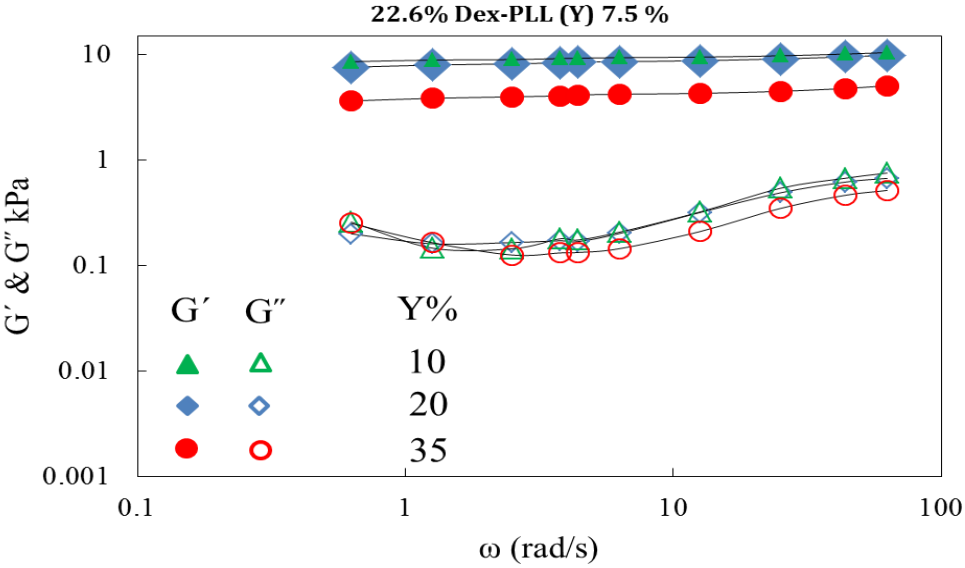
22.6% Dex-PLL (Y) 7.5 %
G´ & G˝ kPa
10
1
0.1
0.01
0.001
0.1
1
10
100
ω (rad/s)
G´ G˝ Y%
10
20
35

c)

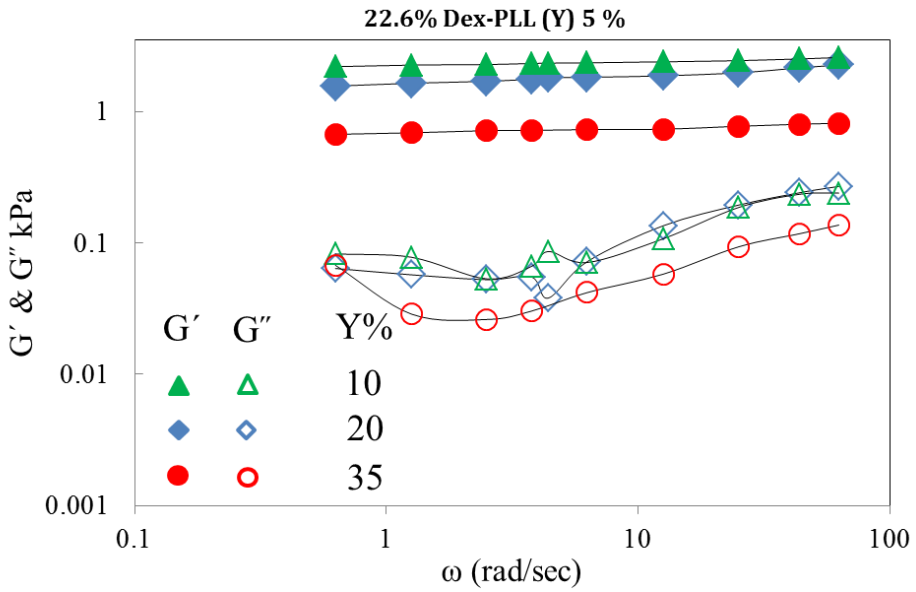

Figure 5-13 Dynamic moduli of 22.6% OxDex with different succinated PLL at different concentrations a) 10% b) 7.5% c) 5%. All readings were taken in triplicate.

Similar observations can be made from Fig. 5-14 a and b. From these figures it can be observed that when oxidation of dextran was increased from 22.6% to 40% storage moduli of the gels can be tuned from 2 to 35 kPa. Higher concentrations and lower degree of succination gives mechanically stronger hydrogels (52).

a)

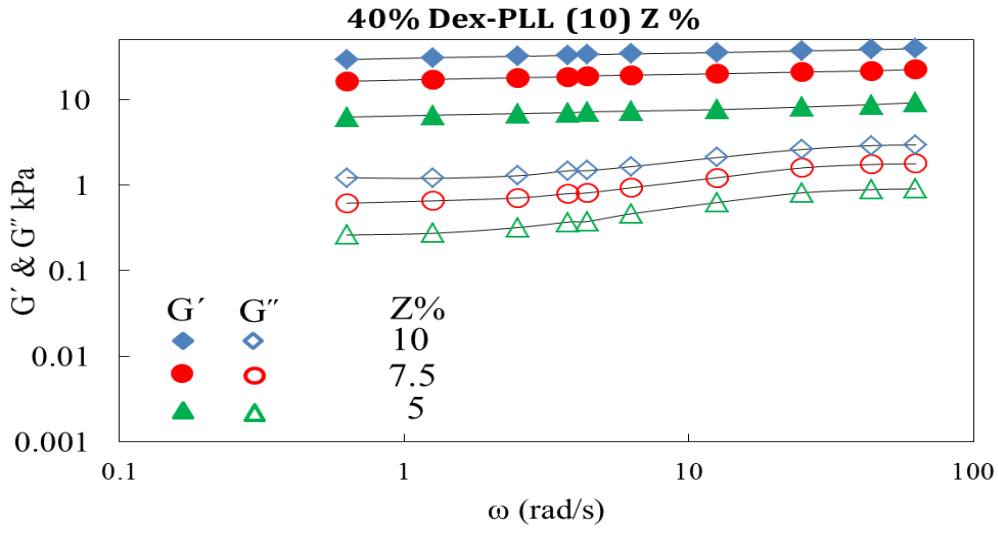

b)

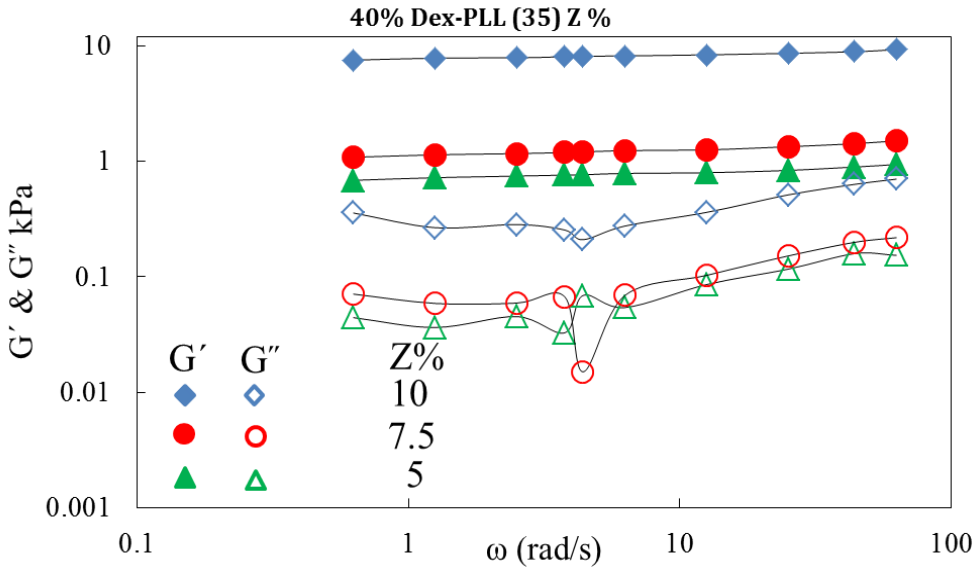

Figure 5-14 Dynamic moduli of 40% OxDex with different succinated PLL at different concentrations a) PLL SA (10) b) PLL SA (35). All readings were taken in triplicate.

Fig. 5-15 represents the effect of dextran oxidation on the mechanical property of the hydrogel. It can be seen from the graph as the degree of oxidation in the dextran increases storage moduli as the number of cross-linking point increases. Storage moduli can be controlled between 10 kPa to 40 kPa. These rheological results are consistent with the previous reports (52).

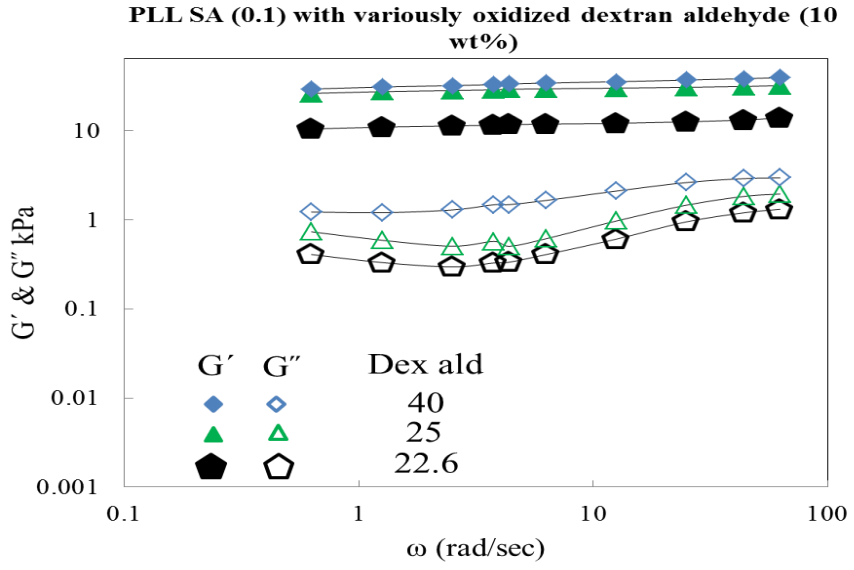

Figure 5-15 Dynamic moduli of various oxidized Dex with different PLL SA (10) each with 10% concentration. All readings were taken in triplicate

5.4 Conclusion

In the current study, I was successful in the development of novel nanoparticle incorporated dextran based hydrogels. In these hydrogels mechanical property can easily be tuned by varying the oxidation in dextran and also by controlling the succination in the cross-linker. Self-assembled nanoparticles incorporated with in the chemically cross-linked hydrogel makes it a suitable system for hydrophobic drug delivery. Size of these self-assembled nanoparticles can easily be tailored by varying the substitution of DDSA in dextran. Drug release from these nanoparticles shows a two-step process, which is highly suitable for the development of hydrogels for topical wound dressing materials. However, growth factor from this material shows burst release. This needs to be optimized. Ideally growth factor should show a slow release for over a period of 30 days. This can be achieved by the incorporation of laponite in the hydrogels. It is expected that growth factor can bind through electrostatic interactions with laponite and thus release can be controlled. In the pursuit of development of hydrogel as topical wound dressing material, I have formulated a system that enables differential release of drug, which will reduce the possibility of bacterial infection at wound site and accelerates wound healing.

5.5 References

1. Enoch S and Price P. Cellular, molecular and biochemical differences in the pathophysiology of healing between acute wounds, chronic wounds and wounds in the aged. Worldwidewounds, 2004.
2. Leaper DJ and Harding KG. Wounds: Biology and Management. Oxford University Press, 1998.
3. Cooper P. A systematic approach to advanced wound healing and management. Cromwell Press, UK, 2005.
4. Hutchinson J. The Wound Programme. Centre for Medical Education: Dundee 1992.
5. Winter GD. Nature, 1962, 93, 293–294.
6. Adamian AA, Dobysh SV, Kilimchuk LE, Shandurenko IN, Chekmareva IA. Khirurgiia (Mosk), 2004, 12, 10–14.

7. Seaman S. J. Am. Podiatr. Med. Assoc., 2002, 92, 24–33.
8. Sawant SV, Sankpal SV, Jadhav KR, Kadam VJ. Res. J. Pharm. Technol., 2012, 5, 561–569.
9. Boateng JS, Matthews KH, Stevens HN, Eccleston GM. J. Pharm. Sci., 2008, 97, 2892–2923.
10. Zilberman M, Elsner JJ. J. Control Rel., 2008, 130, 202–215.
11. Yudanova TN, Reshetov IV. Pharm. Chem. J., 2006, 40, 85–92.
12. Kerihuel JC. J. Wound Care, 2010, 19, 208-215.
13. Moura LI, Dias AM, Carvalho E, de Sousa HC. Acta Biomater., 2013, 9, 7093–7114.
14. Higa OZ, Rogero SO, Machado LDB, Mathor MB, Lugao AB. Radiat Phys Chem., 1999, 55, 705–707.
15. Rosiak JM, Rucinska-Rybus A, Pekala W. Method of manufacturing of hydrogel dressings, 1989, Patent USA, No. 4, 871, 490.
16. Razzak MT, Darwis D, Sukirno Z Radiat Phys Chem., 2001, 62, 107–113.
17. Balakrishnan B, Mohanty M, Umashakar PR and Jayakrishnan A. Biomaterials, 2005, 26, 6335-6342.
18. Yoshii F, Zhanshan Y, Isobe K, Shiozaki K, Makunchi K. Radiat Phys Chem., 1999, 55, 133–138.
19. Malafaya PB, Silva GA, Reis RL. Adv. Drug Deliv. Rev., 2007, 59, 207–233.
20. Wiegand C, Hipler UC. Macromol. Symp., 2010, 294, 1–13.
21. Zahedi P, Rezaeian I, Ranaei-Siadat SO, Jafari SH, Supaphol P. Polym. Adv. Technol., 2010, 21, 77–95.
22. Zhong W, Xing MM, Maibach HI. Cutan. Ocul. Toxicol., 2010, 29, 143–152.
23. De Geest BG, Camp WV, Du Prez FE, De Smedt SC, Demeester J, Hennink WE. Chem. Commun., 2008, 190–192.
24. Sun G, Shen YI, Ho CC, Kusuma S, Gerecht S. J. Biomed. Mater. Res. A, 2010, 93, 1080–1090.
25. Mehvar R. J Controlled Release 2000, 69, 1-25.
26. Guthrie R. Adv Carbohydr Chem 1961, 16, 105.
27. Suvorova OB, Iozep AA, Passet BV. Rus J App Chem., 2001, 74, 1016-1020.
28. Coviello T. et al. J. Control. Rel., 2007, 119, 5–24
29. Vauthier C and Bouchemal K. Pharm. Res., 2009, 26, 1025–1058.

30. Hassani LN, Hendra F and Bouchemal K. drug discovery Today, 2012, 17, 11/12.
31. Mi FL. et al. Carbohydr. Polym., 2005, 60, 219–227.
32. Wang, W. et al. Langmuir, 2001, 17, 631–636.
33. Liang, G. et al. J. Pharm. Pharmacol., 2007, 59, 661–667.
34. Dufes, C. et al. Pharm. Res., 2000, 17, 1250–1258.
35. Graybill JR. Ann. Intern. Med., 1996, 124, 921–923.
36. Vandermeulen G, Rouxhet L, Arien A, Brewster ME, Pre´at V. International Journal of Pharmaceutics, 2006, 309, 234–240.
37. Legrand P, Romero E, Devissaguet JP, Eleazar Cohen B, Bolard J. Antimicrob. Agents Chemother., 1992, 36, 2518–2522.
38. Brajtburg J, Bolard J. Clin. Microbiol. Rev., 1996, 9, 512–531.
39. Cross M, Dexter TM. Cell, 1991, 64, 271 –280.
40. Cao L, Arany PR, Wang YS, Mooney DJ. Biomaterials, 2009, 30, 4085–4093.
41. Discher DE, Janmey P, Wang YL. Science, 2005, 310, 1139–1143.
42. Ramirez F, Rifkin DB. Matrix Biol., 2003, 22, 101–107.
43. Lee K, Silva EA and Mooney DJ. J. R. Soc. Interface, 2011, 8, 153–170.
44. Hyon S-H, Nakajima N, Sugai H, Matsumura K. J Biomed Mater Res Part A 2014, 102, 2511–2520.
45. Mo X, Iwata H, Matsuda S, Ikada Y. J Biomater Sci Polym Edn, 2000, 11, 345–351
46. K. Matsumura and Hyon SH. Biomaterials, 2009, 30, 4842-4849.
47. A.F. Haneeb, Anal Biochem 1966, 14, 328–36.
48. R. Gref R, Amiel C, Molinard K, Daoud-Mahammed S, Sebille B, Gillet B, Beloeil JC, Ringard C, Rosilio V, Poupaert J, Couvreur P. J. Control. Release, 2006, 111, 316.
49. Zhang X, Zhu X, Ke F. Polymer, 2009, 50, 4343–4351.
50. Zhou W, Wang Y, Jian J, song S. International Journal of Nanomedicine 2013, 8, 3715-3728.
51. Sun G, Shen YI , Kusuma S, Talbot KF, Steenbergen CJ, Gerecht S. Biomaterials, 2011, 32, 95-106.

52. Matsumuraa K, Nakajima N, Sugai H, Hyon SH. Carbohydrate Polymers, 2014, 113, 32–38
53. Salamone JC, Rice WC. In Encyclopedia of Polymer Science and Technologie, 2nd ed., Wiley-Interscience, 1988, 11, 514-530.
54. Galin JC. In Polymer Materials Encyclopedia, CRC Press: Boca Raton, FL, USA, 1996, 9, 7189-7201.
55. Li Y, Liu R, Liu W, Kang H, Wu M, Huang Y. Journal of Polymer Science: Part A: Polymer Chemistry, 2008, 46, 6907-6915.
56. Maksimenko AV, Schechilina YV, Tischenko EG. Biochemistry (Mosc), 2001, 66, 456 – 463.
57. Baldwin AL, Chien S. Arteriosclerosis, 1988, 8, 140 – 146.
58. Jones MC, Leroux JC. Eur. J. Pharm. Biopharm., 1999, 48, 101-111.

Chapter 6

Conclusion

In this study of my doctoral thesis, my aim was to develop different systems that can be used for tissue engineering and biomedical applications based on polyampholyte by the interplay of chemistry and biology. The main focus was to develop different scaffold using different strategies. Each hydrogel so developed have unique application. They can have potent applications in the field of tissue engineering and regenerative medicine.

In chapter 2, I have developed cryoprotective hydrogels *via* Cu-free click chemistry, which was based on Dextran polyampholyte, and first of its kind. In this study, dextran based polyampholyte with azide groups can form *in situ* hydrogels with DBCO-Dex *via* Cu-free click chemistry. The system showed excellent cryoprotective properties without any additional cryoprotectant. Cells encapsulated with such *in situ* hydrogels can be cryopreserved well without the addition of any cryoprotectant. This is the first challenge in the development of cryoprotective hydrogels by means of a combination of materials science and cryobiology. It has also provided opportunities to meet various challenges in tissue engineering such as vascularization, the formation of tissue architectures, and cell seeding. These methodologies are useful for engineering tissue architectures inside the cell-containing hydrogel. Thus, these hydrogels can serve as scaffolds with cryoprotective properties that also provide structural integrity to tissue constructs.

In chapter 3, I formulated thixotropic hydrogels based on polyampholyte and laponite. It is a novel system, which for the first time describes the interaction of polyampholyte with laponite that renders tuneability in mechanical property of the nanocomposite. In this system therapeutics can be encapsulated by changing system from gel to sol by the application of pressure and then it reverts back to its original structure in definite span of time. The system's switch ability from strong gel to very weak gel with a change in pH may open new avenues for cell delivery applications. This study overcomes the first developmental challenge for smart hydrogels by mixing cells immediately after thawing with laponite, which results

in a gel form for the nanocomposite that can easily be injected by applying pressure. This system does not require any pretreatment of cells before injection, making cell maintenance after thawing unnecessary. In the pursuit of an injectable, thixotropic cell scaffold with modifiable mechanical properties, I have engineered a simple and effective nanocomposite that can be tailored to specific functionalities for various tissue-engineering applications.

In chapter 4, I tried to develop a system in which chemical cross-linking was introduced in the physically cross-linked gels. This leads to the formation of a system in which degradation and mechanical property can be tailored. In this system it is possible to tune cell adhesion by controlling the hydrogel formulation. The methodology is simple and does not require the use of toxic cross-linkers. The variety of mechanical and degradation properties of our nanocomposite hydrogel made this material a suitable candidate for cell and drug delivery purposes.

In chapter 5, I developed system for wound healing application, which is capable of codelivery of dual therapeutics in controlled fashion. Incorporation of antifungal drug in the hydrophobic core of the nano-assemblies makes it a suitable candidate for wound healing application. In this system there is a good control over the release of antifungal drug from nano-assemblies and growth factor from the hydrogel. Release of the therapeutics and mechanical properties of the system can easily be tuned. The rational design of hydrogels enables differential release of drug, which will reduce the possibility of bacterial infection at wound site and accelerates wound healing.

I believe I was able to successfully fabricate different hydrogels with various unique applications using polyampholytes. Besides their cryoprotective property, in my study I was able to utilize their behavior of charge tuneability for the development of hydrogels by the incorporation of laponite as a cross-linker. Due to the presence of charge on both the components, numerous combinations were obtained. To my knowledge, no such work has been reported before which describes the interaction of polyampholyte with laponite. The beautiful interaction of the two by changing various parameters has opened up new avenues in the field of tissue engineering. These systems can be potentially useful

in the fields of stem cell based therapies (where substrate stiffness plays crucial role in cell differentiation), pH-triggered cell delivery, drug delivery applications, etc.

Although these hydrogels have broad range of applications that covers different areas of tissue engineering, but these are model systems only. It is a fundamental study which describes the different methodologies to develop hydrogels for tissue engineering applications. In order to use them for clinical applications, in-vivo study need to be carried out. I believe my study has broadened the basic understanding of the hydrogels. This has covered some pit-holes in the research field. I expect my study will assist in the development of better systems in the future.

Achievements

Main Publications

1. Minkle Jain, Robin Rajan, Suong-Hyu Hyon and Kazuaki Matsumura, "Hydrogelation of dextran-based polyampholytes with cryoprotective properties via click chemistry" Biomaterials Science, Royal Society of Chemistry, 2 (3), 2014, 308-317. (Selected as journal cover)
2. Minkle Jain and Kazuaki Matsumura "Thixotropic injectable hydrogel using a polyampholyte and nanosilicate prepared directly after cryopreservation". (Submitted)
3. Minkle Jain and Kazuaki Matsumura "Polyampholyte and nanosilicate based soft bio-nanocomposites with tailorable mechanical and cell adhesion properties" (Submitted).
4. Minkle Jain and Kazuaki Matsumura "Self-assembled nanogel incorporated Dextran based hydrogels with controlled drug release properties" (in preparation).

Related publication

5. Robin Rajan, Minkle Jain and Kazuaki Matsumura "Cryoprotective properties of completely synthetic polyampholytes via reversible addition-fragmentation chain transfer (RAFT) polymerization and the effects of hydrophobicity", Journal of Biomaterials Science, Polymer Edition, Taylor & Francis Group,24, 2013, 1767-1780. (Top 10 most read article of all time).
6. Kazuaki Matsumura, Minkle Jain and Robin Rajan, Cell and Materials Interface in Cryobiology and Cryoprotection in Cell and Material Interface: Advances in Tissue Engineering, Biosensor, Implant, and Imaging Technologies, Edited by Nihal Engin Vrana, CRC Press, Taylor & Francis Group, 2015. **(Book Chapter)**
7. Minkle Jain and Kazuaki Matsumura, "Dextran Based Polyampholyte Having Cryoprotective Properties", MRS Proceedings, Cambridge University Press, 2013. **(Conference Proceeding).**

Acknowledgement

Firstly I would like to pay sincere thanks and gratitude to my advisor Associate Prof. Dr. Kazuaki Matsumura for his continuous guidance, immense support, motivation and always believing in me. His teachings helped me a lot in pursuing my research and writing of the thesis. He has helped me to develop a positive outlook for research and patience for failures. I could not have imagined a better advisor than him.

Besides my supervisor I would also like to thank my sub supervisor Prof. Dr. Noriyoshi Matsumi and minor research supervisor Prof. Dr. Kohki Ebitani for their guidance. I would also like to thank my external research supervisor Associate Prof. Dr. Satoshi Fujita (University of Fukui) and for giving me opportunity to work in his laboratory and guiding me. I am also thankful to my other two referees Prof. Dr. Masayuki Yamaguchi and Associate Prof. Dr. Tatsuo Kaneko for their critical comments and suggestions.

I am also thankful to my friend Robin Rajan for supporting me throughout my research, stimulating discussion, giving me new ideas for my work, for the sleepless nights we worked together in lab before deadlines and always a healthy competitor and last for all the fun we had in the lab in the last four years.

I am also thankful to my fellow Japanese lab mates for helping me in all the official works and always supporting me in my research.

Lastly, I would like to dedicate my PhD thesis to my mother Sunita Jain who was always very supportive in my research and in my life in general. She always motivated me to achieve more and always guided me ethics of work. I think I was able to pursue my PhD only because of her. I am also thankful to my father, brother and other family members for keeping my spirits high throughout my life and in my PhD.